REPORT DOCUMENTATION PAGE

Form Approved OMB No. 0704-0188

1. AGENCY USE ONLY (Leave blank)	2. REPORT DATE	3. REPORT TYPE AND DATES COVERED
	3 June 2000	Conference Proceedings

4. TITLE AND SUBTITLE

Thermochemical Processes In Plasma Aerodynamics

5. FUNDING NUMBERS

F61775-00-WF023

6. AUTHOR(S)

Conference Committee

7. PERFORMING ORGANIZATION NAME(S) AND ADDRESS(ES)

Leninetz Holding Company, NIPGS
Hypersonic System Research Institute - 212 Moskovsky Prospekt
St. Petersburg 196066
Russia

8. PERFORMING ORGANIZATION REPORT NUMBER

N/A

9. SPONSORING/MONITORING AGENCY NAME(S) AND ADDRESS(ES)

EOARD
PSC 802 BOX 14
FPO 09499-0200

10. SPONSORING/MONITORING AGENCY REPORT NUMBER

CSP 00-5023

11. SUPPLEMENTARY NOTES

Report is in four sections, all electronic (Word documents)

12a. DISTRIBUTION/AVAILABILITY STATEMENT

Approved for public release; distribution is unlimited.

12b. DISTRIBUTION CODE

A

13. ABSTRACT (Maximum 200 words)

The Final Proceedings for Thermochemical processes in plasma aerodynamics, 30 May 2000 - 3 June 2000

This is an interdisciplinary conference. Topics to be covered include: Thermochemical conversion of a fuel; Plasma chemistry; Thermochemical and plasma-chemistry processes influence on flows; Active thermal protection on the basis of endothermic reactions; Problem of catalysis at conversion of a hydrocarbon fuel; Burning of a modified hydrocarbon fuel; Non-equilibrium kinetics with participation of hydrocarbon components, etc.

14. SUBJECT TERMS

EOARD, Magnetohydrodynamic (MHD), Hypersonics, Plasma Aerodynamic

15. NUMBER OF PAGES

94

16. PRICE CODE

N/A

17. SECURITY CLASSIFICATION OF REPORT	18. SECURITY CLASSIFICATION OF THIS PAGE	19. SECURITY CLASSIFICATION OF ABSTRACT	20. LIMITATION OF ABSTRACT
UNCLASSIFIED	UNCLASSIFIED	UNCLASSIFIED	UL

Workshop

Thermochemical processes in plasma aerodynamics

Saint-Petersburg
May 30 - June 3, 2000

Hypersonic System Research Institute
of Holding company "LENINETZ"
212 Moskovsky pr., St. Petersburg, 196066, Russia

Organized:

Hypersonic System Research Institute

In co-operation and sponsorship by:

HC "LENINETZ"
EOARD
AFOSR
USAFRL
ULHT SPSU and HC "LENINETZ"

CONTENTS

CHEMICAL HEAT REGENERATION AND FUEL TRANSFORMATION IN ENERGETIC PLANTS

Korabelnikov A.V., Kuranov A.L., Malkov Yu.P., Rotinian M.A.

212 Moskovsky prospekt, St. Petersburg, 196066, Russia.
Hypersonic System Research Institute
Tel./ Fax:(812) 291-82-94, E-mail:ajax@comset.net

Now in many industrially developed countries the intensive work is conducted in the field of hypersonic technologies development to create aerospace transport systems and hypersonic airplanes of different purposes. The hypersonic technologies by virtue of novelty, science capacity and multifunctionality fulfill a role of motive power of technological progress in a broad spectrum of areas bound not only by aviation. Their assimilation will allow countries to remain among the advanced states of a world that are capable to create a technique of XXI century.

In Russia the research and experimental work "Oryol" is devoted to the problem of development and creation of reusable space transport systems and hypersonic airplanes [1]. Among the foreign programs it is necessary to mark the program of US Air force on hypersonic technologies (HyTech), supposed to be realized in 1995-2003 with financing of 15-20 million $ annually. The purpose of this program is development of demonstration sample of a hypersonic air-breathing engine (HABE) on hydrocarbonaceous fuels for Mach numbers of flight M=4 - 8 [2]. The nearest object of application is winged rocket of long range (> 1500 km) of the "air - ground" class. Though this program is focussed on making of one-use systems with flight time no more than 12 min, it is called to make a scientific, technical and technological basis for development of hypersonic vehicles on endothermic hydrocarbon fuels of a broad spectrum of application: reusable rockets, airplanes, trans-atmospheric means. By results of ground tests in 2003 under requirements simulated the flight at M=8 it is supposed to accept a next program of demonstration flights. The HyTech program for Mach numbers $M \leq 12$ is intimately coordinated with activity of NASA in the field of hypersonic technologies of liquid hydrogen air-breathing engine for high Mach numbers of flight.

The problems of application of hydrocarbon fuels for hypersonic flight vehicles (HFV) are periodically considered in literature. The first works in this direction are referred to 60-s years [3-4]. Then the attention of the aviation specialists was for a long time switched to the designs connected with use of liquid hydrogen as a fuel. However now interest to hydrocarbon endothermic fuels again has increased. Today many experts are convinced, that for HFV of restricted size or small mass of hydrocarbonaceous fuels are, apparently, unique possibility for providing of high speeds of flight [5].

The designs of hypersonic airplanes with use of heat-absorbing reactions for cooling of separate parts of vehicles were surveyed in [6,7]. However the most energetically integral the concept "Ajax" is seemed [8,9], developed by the "Leninets" Holding Company.

Energy features of the "Ajax" project. As it was already indicated in [9], the philosophy of HFV development under the "Ajax" concept is based on the active energy interaction with an air flow circulating it.

It means, that the part of a kinetic energy of this flow, earlier irrevocablely losing, is converted by separate onboard systems to other kinds of useful used energy. So, for example, during deceleration of highly ionized airflow in MHD system its kinetic energy is transformed partially in electrical energy, reaching tens of megawatt. The received electric power can be applied in turn in a plasma system of flow control to increase the lift-to-drag ratio of a flight vehicle.

Another channel of energy exchange is the system of active thermal protection. It is a combination of recuperative heat exchangers, which are placed in the most heat-stressed parts of airframe and engine. Various physical and chemical processes, from elementary heating of coolant to endothermic catalytic reactions, proceed there. The hydrocarbon fuel (aviation kerosene) is coolant and reactant, and utilized heat from aerodynamic heating and power plant is energy source for realization of physicochemical transformations. Thus, from the point of view of energetics, in difference from other designs "AJAX" flight vehicle utilizes fuller the primary energy, which is reserved aboard as chemical energy of fuel. It helps to increase the efficiency of thermodynamic cycle of the engine. The considered heat-protection system executes not only usual function, providing temperature conditions of the airframe, but also serves simultaneously as the system of preparation of new modified fuel containing molecular hydrogen.

It became possible due to application on board of HFV a method of chemical heat recovery (CHR).

CHR-method. The chemical way should be highlighted among various ways of the heat regeneration as the versatile one. The analysis of the functioning of numerous power devices shows that the efficiency of an organic fuel usage is still low and does not exceed 40%. For existing heat devices this situation may be explained thus: the fuel energy conversion is accompanied by large heat losses to the environment with the exhaust gases, the heat transfer through walls of devices, and the considerable irreversible losses during the process of the fuel burning. These losses could be considerably decreased by the utilization of previously lost heat in the special catalytic reactors (heat exchangers). In the process of the utilization, the initial organic fuel is converted into the new kind of the fuel, so-called synthetic gas (mixture of H_2 and CO). The comparative thermodynamic analysis of the process of the combustion of the initial and the converted fuels shows, that the quantity of irreversible losses is also lower in the last case than in the previous one. Therefore, the chemical heat utilization and the combustion of the converted fuel lead to the increase of the power plants efficiency and to the fuel save. Moreover, the synthetic gas combustion leads to the decrease of the pollutants emission into the atmosphere. That is why the process of the chemical heat regeneration is an example of the new energy-saving and environmentally friendly technology.

While in traditional devices the energy of the fuel is converted into the heat in one stage by means of its direct combustion, in CHR-devices the process of the fuel energy conversion is divided into two stages. The first stage is the heat removal from the heated surface and realization of endothermic reaction of conversion of the initial fuel. The second one is the combustion of the reaction products (converted fuel) which have larger calorific value in comparison with the initial reactants.

It should be pointed out that the first stage has a fundamental interest as the method of the cooling (heat protection) of the heat-stressed structural elements. The heat protection is ensured not only by means of convection and radiation, but by means of the heat absorption at the phase transitions and chemical transformations also. At the same

time, the latter do not have destructive character as in the case of ablative heat shield materials, but they are methods of generation of new fuel.

Development of thermochemical methods of raise of fuel efficiency with simultaneous utilization of thermal losses requires a solution of a number of scientific and applied problems. Their range basically is contoured in a fig.1. Three interdependent blocks of problems are clearly seen: 1) selection of fuel and endothermic processes, development of catalysts for a realization of chemical reactions; 2) making of heat-exchange instrumentation, in particular, thermochemical reactor (TCR) as structural devices of the system of heat protection and transformation of fuel; 3) organization of combustion process and selection of the scheme of combustion chamber for modified fuel.

Steam reforming. Amongst the existing endothermic reactions we consider the steam reforming. The choice was based on such reaction criteria as heat, temperature level, rate, grow of calorific value, amount of received hydrogen and some others.

Reaction heat exerts considerable influence on the heat quantity absorbed in the thermochemical reactor. Consider as an example the reaction of steam reforming of methane at stoichiometric relation between the components (CH_4-0,47 kg, H_2O-0,53 kg).

$$CH_4 + H_2O = 3H_2 + CO - 207 \text{ kJ}$$

The change of enthalpy of initial reagents during the preparation stage (so-called physical cooling resource) is the result of heating, evaporation and superheating of methane-water mixture. This change is $\Delta H_{phys} = 3{,}3$ MJ/kg of mixture in the range from $t = 0$ °C to $t = 727$ °C. Chemical cooling resource, is equal to the reaction heat, $\Delta H_{chem} \approx 6{,}6$ MJ/kg of mixture. Thus, the total cooling resource $\Delta H_{\Sigma} = \Delta H_{phys} + \Delta H_{chem} = 9{,}9$ MJ/kg of mixture.

The cooling capacity of liquid hydrocarbons/water mixture falls insignificantly when amount of carbon atoms in molecule grows. By and large it is possible to consider that methane and its liquid homologes mixed with water are capable to provide cooling capacity up to 8-10 MJ/kg of mixture. For comparison, the change of enthalpy of liquid hydrogen heated to temperature of autoignition ($t = 577$ °C, $\Delta t = 830$ °C) is equal to $\Delta H_{phys} = 12$ MJ/kg. Thus, hydrocarbon/water composition comes nearer to the case of cooling by liquid hydrocarbon on available cooling capacity, and outperforms that case on relative cooling capacity $\Delta H/H_u$ (H_u is the heat of combustion). This circumstance and also high potential (exergy) of received gaseous fuel allow to view application of hydrocarbon fuels with thermochemical conversion for realization of cycles, which will outperform the Brighton's cycle used traditionally in air-breathing engines [13].

It is necessary to note that the catalytic steam reforming of hydrocarbons exceeds by thermal effect and amount of received hydrogen in some times the non-catalytic endothermic processes such as pyrolysis, cracking and depolymerization of hydrocarbon. The complexity is in making the developed heat-exchange catalytic surface and maintenance of its properties during all time of work.

Concrete form for reaction of steam reforming depends on the process conditions (temperature, pressure, relation between water and hydrocarbon, and others). Therefore, at high temperatures ($t > 1000$ deg C) the reactions go until the formation of H_2 and CO (high-temperature reforming):

$$aC_nH_m + bH_2O \rightarrow fH_2 + gCO \qquad (1)$$

At low temperatures ($t < 400$ °C) the reaction output is strongly shifted to the formation of CH_4 and CO_2 and the resulting reaction of gasification can be written as (low-temperature reforming):

$$aC_nH_m + bH_2O \rightarrow dCH_4 + eCO_2 \qquad (2)$$

Generally, reactions (1) and (2) are accompanied by two additional independent reversible reactions, which determine equilibrium composition of converted gas:

$$CH_4 + H_2O \leftrightarrow CO + 3H_2 \qquad (3)$$

$$CO + H_2O \leftrightarrow CO_2 + H_2 \qquad (4)$$

Unfortunately, the process of hydrocarbon decomposition is complicated by undesirable reactions of free carbon (coke) formation that leads to the coking of catalysts. The coke, depositing on the catalyst surface, deactivates the catalyst blocking its active centers. In addition, the coke, clogging the pores, causes the destruction of catalyst at the expense of difference in coefficients of expansion. We considered in detail the following ways to decrease the coking:

a) appropriate choice of initial fuel;

b) promotion of catalysts;

c) exceeding of stoichiometric relation H_2O/C;

d) efforts on rational organization of the process (for example, two-stage scheme of decomposition, optimal shape of catalysts, elimination of local temperature inhomogeneities etc.);

e) use of special fuel additives;

f) regeneration of catalyst.

It is known that the rate of coke deposition on surfaces of nickel-containing catalysts reduces in the order ethylene > benzol > heptane > hexane > butane > methane. And the ratio of C/H in the methane molecule is minimum. Thus if the raw material is methane, carbon deposit formation is not a critical problem. From this comes the conclusion that it is necessary to organize the process of dissociation of the initial liquid hydrocarbon (kerosene) in such a manner that in the most crucial, largest surface area, and most inaccessible places of heat-shielding construction, the conversion would involve gaseous methane. Such arrangement is possible at using a two-stage system for the steam reforming of liquid hydrocarbons (Fig. 2). In such system, the process occurs in two steps. First, liquid hydrocarbons are gasified at low temperature (t = 300-450 °C) via the reaction (2). In the second step, the products of gasification are transformed according to the reactions (3), (4) in a high temperature (t = 700-900 °C) conversion step. This scheme of the working process has several advantages compared to a single-step scheme. For high-temperature conversion we use the gas mixture consisting of methane that is stable to coke formation, carbon dioxide and small amount of hydrogen, damping the cracking reactions. As a result the danger of cooking the catalyst is substantially reduced. This scheme also gives possibility to reduce the excess of water vapor in the conversion process and to approach stoichiometry relation between the initial components.

The scheme of two-stages process given at Fig.2 is simplified, becoming one-stage scheme at the following conditions: (i) the initial fuel is methane; (ii) the working time is not large and then the coke formation is negligible. In both cases the immediate high-temperature steam reforming is efficient.

Application in aviation of liquefied natural gas consisting for 90 % and more of methane, is considered now as perspective. At ANTK A.N.Tupolev the particular practical experience in this direction is already accumulated [14], therefore version of use of liquid methane as starting hydrocarbon fuel with the subsequent thermochemical transformation finds a real base.

Catalysts and heat-exchange. As is generally known, the process of steam reforming of hydrocarbons is a basic industrial method to produce technical hydrogen. It is carried out in tube furnaces, which are heated on the outside and filled with granular catalytic packing. The bulk catalyst has very large contact surface; however this surface works ineffectively because along its way from the heating wall, which is essentially non catalytic, to the surface, where catalysis takes place, the "chemical" component of the heat flux has to overcome a series of thermal resistances: from the heating wall to the gas, from the gas to the granule surface with gas flowing over it, from the surface to the pores that are located inside the granules.

Thus, in this case, convective and diffusive head transfer do not occur in parallel (this is favorable for resultant enhancement of heat transfer); on the contrary, these processes take place sequentially, that is, from convective to diffusive heat transfer. As a result, the temperature at the granule surface,

which determines the chemical reaction on the average, appears to be considerably lower than that for the heating wall; that is, the effect of the chemical reaction on the intensity of heat transfer at the heating wall is much less then it could be.

Besides, practically all reactors with fixed granular layer have the following defects: significant radial gradients of temperatures and concentrations; a low degree of using catalyst volume; high hydraulic resistance of granule layer; irregularity on altitude of mechanical loading on catalyst.

The use of granulated catalysts aboard flight vehicle is undesirable generally, as at mobility of reactionary space the granule propensity to migration and repacking will only grow, that will cause to intense friction and crumbling of granules. Therefore it is necessary to have new approach to creation both catalysts, and units of conversion in whole to increase intensity of catalytic processes in industry, and also develop new CHR technology for heat machines of various purposes.

Besides the traditional requirements imposed on the activity, selectivity and life time, the on-board catalysts should satisfy several specific conditions, such as: (i) they should be integrated with the heat transfer surface; (ii) they should have high thermoconductivity, and thermocyclic, shock, vibration, and chemical-heat resistance; (iii) they should operate under the action of time-dependent and large magnitude heat flows. A number of catalysts, in particular, catalytic covers (planar catalysts) put directly on a heated wall satisfy these requirements.The advantages of TCR with catalyst put directly on a heating surface before packed-bed reactor is confirmed by the comparative analysis [15].

The problem of thermal resistance and activity of catalytic coats is surveyed in details in [16]. Model of the heated wall of small thickness with a microporous coat by thickness of L_{Π}, porosity Π and diameter of pores d_{Π}, and also plan of heat interchange process in such system are shown in a fig.3a. Here q_c - heat flow on a radiopaque wall, q_x and q_k - chemical and convective component of a heat flow on a surface of porous coat, T, P, c_1- temperature, pressure and concentration of methane, accordingly. The analysis was conducted by solving the equation of heat conductivity in the porous structure:

$$\lambda_{\Pi}(1-\Pi)\frac{d^2T}{dy^2} = q_v,$$

and the methane diffusion equation:

$$\rho D_1 \Pi \frac{d^2 c_1}{dy^2} = j_{1v},$$

where λ_{Π} is the effective coefficient of thermal conductivity of the porous coating material; q_v is the volumetric density of the internal heat sinks due to the chemical reaction; j_{1v} is the volumetric rate of the chemical reaction; ρD_1 is the effective coefficient of methane diffusion in the pores of the coating.

Figures 3b-3d show the main results of the calculation- the effectiveness of the microporous catalytic coating ; here, the local heat flow rates at the wall with a coating are presented. The coatings had the same porosity of Π=50% and a variable thickness and pore diameter. The date is given for p=0.3MPa, T_w=1200K, T_f= 800K; α_c=1150W/(m^{2}K), and c_{lo}=0.376.

As it is seen from figure, the coats with pores of a rather big size (d_{Π} > 0.1 microns) are ineffective; the optimal interval is 0.1-0.001 microns. The increasing of thickness and, accordingly, available area of catalytic surface of coats is reasonable in restricted limits. For the low thermal conducting coats with λ_{Π}=0.2 W/(m·K) the optimum is around of thickness of L_{Π}=10 microns. In a fig.4 the values of temperature overfall in a coat with d_{Π}=0.01 microns depending on thickness and thermal conduction under the same requirements, as in a fig.3 b-d, except for α_k=2100 W/(m^2·K). Both figures display, that as from a point of view of catalytic effectiveness, and adhesion strength of coats a principal technological

problem is security of their thermal conduction at a level of λ_{Π}=1-5 W/(m·K). The possibility of use as the carrier of catalyst of low thermal conduction coats on the basis of $\alpha - Al_2O_3$ with $\lambda_{\Pi} \cong 0.2$ W/(m·K) at q_c=1 MW/m^2 and more is problematic even at their minimum thickness. Apparently, the solution permitting to make a wall catalyticly active without drawing of an intermediate catalyst carrier loosening its thin surface layer for increasing of active area of interaction would be perfect.

Experimental installation. Study of the process of transformation of hydrocarbon fuel was made in TCR of different configuration. One of TCR fragments is shown in a fig.5. Reactor was a cavity formed by two coaxial cylinders with length of L ~500 mm and a breadth of a clearance of d=2,0 mm between them.

Internal surface of this cavity was covered with Ni-Cr planar catalyst. Methane was selected as one of reactants in the considered reaction of steam reforming. This choice is not random; it is dictated by technological features of offered system of heat protection. As already noted, heat protection reactors are fed by gas mixture based on methane. The gas mixture is the production of gasification of aviation liquid fuel (for example, kerosene) in the auxiliary device. We get hydrogen from methane and water. Steam reforming of methane has maximal heat-absorbing effect and minimal tendency to the coking.

The schematic diagram of experimental set-up for steam reforming of methane is shown in Fig. 6. The water heated and evaporated in the evaporator (1). The heating of steam and methane from a gas cylinder was implemented by electric heaters (2 and 3, accordingly). Then the reactants mixed and fed in THR (5) at temperature about 550°C, where endothermic reaction runs. The heat input Q to methane/steam mixture is realised through the reactor internal wall from plasmatron (4). The temperature of THR internal wall was measured by thermocouples (6). The samples for analysis of reaction product composition were taken with the help of special sample containers (7). The analysis of gas samples taken during the experiments was performed on mass-spectrometric installation.

The experimental set-up is supplied with process instrumentation to provide the measurement and control such parameters of the steam, methane, nitrogen as temperature, pressure, flow rate and others. The correspondent transducers are connected to the computer installation to provide automatic measurement and processing of the experimental data according to the developed software.

Results of experiment. Experiments on steam methane reforming were conducted under the following conditions: temperature of a steam methane mixture on an inlet of reactor ~820 K, speed of a mixture varied in a range of 5-15 m\s, maximal temperature of a reactor wall did not exceed 1200 K. The experimental data were fixed at reaching of a quasistationary regime of experimental bench under condition of invariance of the basic parameters of the process. At turn on of installation this time was not less than half-hour at passage from one temperature to other - 10 min.

In a fig.7 the typical profile of temperature allocation of a reactor wall is shown. The initial segment of the curve corresponds, basically, to convective warm-up of a mixture up to reaction temperature. Then the gradual deceleration of the wall temperature propagation and its collapse caused by intensive takeoff of heat on heat-absorbing reaction of steam conversion begins. At feeding in reactor of neutral gas of nitrogen of similar effect is not observed, and there is a convective warm -up of a mixture (dashed line) during all length of reactor.

The distributions of methane and hydrogen concentrations along the reactor length are shown in Fig. 8. They give a picture of chemical reaction inside the reactor.

The relations between the degree of methane conversion X and the heat flux

density averaged along the length of the reactor q_{av} and the velocity of steam/methane mixture at the reactor input are shown in Fig.9, 10. Their analysis allows to make some conclusions:

1. At decreasing velocity the degree of conversion grows. It is explained by increase of a residence time of reacting substance in the reactor.

2. Averaged density of a heat flow grows with the increase of velocity. This effect can be caused by the increase of probability of an event of the chemical reaction at relative decrease of quantity of the reagent, and also by redistribution of roles between "chemical" and convective components of adsorbed heat flow. Separation of these effects requires setting up special experiments and further studying.

3. The increase of wall temperature at a fixed ratio H_2O/CH_4 influences positively both on degree of conversion and on absorbed heat flux.

4. For obtaining of maximal heat absorption effects at and producing of molecular hydrogen it is necessary to have a system of different TCR (size, type of catalyst, parameters of operation), optimal on object functions.

Conclusion Generalizing the results of industrial use of methane steam reforming and the laboratory researches of this process at non-limited heat input, it is possible to make a conclusion about a possibility of thermochemical conversion of an initial fuel in a system of reactors with various degrees of conversion (10-100%) at heat utilization in a broad range of heat loads (0,05-1 MW/m^2).

In closing it may be said that the successful development of the considered technology is impossible without a close "feed-back" with its "consumers". The products of conversion of hydrocarbons include such combustible components as H_2, CH_4, CO; their contents can vary within wide range of limits depending upon the working mode of reactor. The fuel properties in turn determine the scheme, workability, and efficiency of a power plant in many respects. Therefore, in experiments on combustion of hydrocarbon fuels with the additives of conversion products, it is very important to determine the requirements to their optimal composition in reactor output and reactor productivity. The feedback can seriously affect technological development of reactors and catalysts. It is necessary to continue the works on this direction.

The technology of chemical heat regeneration can find application in various industries, where hydrocarbon fuel is used, such as:

1. transport energetics (internal-combustion, gas-turbine and air-breathing engines);
2. stationary gas-turbine plants on thermal power stations and heat-engineering facilities (furnaces, dryers etc.);
3. devices for conversion and accumulation of solar energy and heat from the nuclear power plants;
4. chemical energetic engineering.

References

1. Анфимов Н.А. Российская программа «Орел». Исследования концепции перспективной многоразовой космической транспортной системы. Космонавтика и ракетостроение, 1996, №8
2. R.A.Mercier. Air force hypersonic technology program. Rept. at the 9th International space planes and hypersonic systems and technologies conference. 1-4 Nov. 1999, Norfolk
3. M. Yaffee. Fuel may cool manned flights at Mach 4. Aviation week, March 14, 1960
4. H. Lander, A.C.Nixon. Endothermic fuels for hypersonic vehicles AAIA 68-997
5. Шихман Ю.М., Яновский Л.С. Анализ проблем использования углеводородных топлив для гиперзвуковых полетов. Научно-технический отчет №12216, ЦИАМ, Москва, 1995

6. D.H. Petley. Thermal management for Mach 5 cruise aircraft using endothermic fuel. AAIA 90-284-CP
7. R.M. Zubrin. The methane-acetylene cycle aerospace plane: a promising candidate for Earth to orbit transportation. AAIA 92-0688
8. Фрайштадт В.Л., Тимофеев Г.А., Исаков В.Н. и др. Патент РФ №2046203, МПК 6 F 02 K 11/00, 7/16, 3/08, 1981г.
9. Турчак А.А., Фрайштадт В.Л., Куранов А.Л. «Новые гиперзвуковые технологии по концепции «Аякс» Полет, №9, 1999
10. Корабельников А.В., Куранов А.Л., Метальников В.М.и др. Расчет элементов тепловой защиты гиперзвукового летательного аппарата. Прикладная физика, 1997, №4
11. A.V. Korabelnikov, A.L. Kuranov. Thermochemical conversion of hydrocarbon fuel for the "AJAX" concept. AIAA 99-3537
12. Носач В.Г. Энергия топлива. Киев: Наукова думка, 1989
13. Фаворский О.Н., Курзинер Р.И. Развитие воздушно-реактивных двигателей для авиации высоких скоростей полета. ТВТ, 1990, т.28, №4
14. Малышев В.В. О перспективе криогенной авиации. ТВФ, 1997, №6
15. Сафонов М.С., Борисов С.А., Бельнов В.К. Сопоставление структур размещения катализаторов в пластинчатом реакторе-теплообменнике. ТОХТ, 1989, т.23, №1
16. Курганов В.А., Зейгарник Ю.А., Корабельников А.В., Маслакова И.В. Термохимический принцип охлаждения на основе реакции паровой конверсии метана. Теплоэнергетика, 1996, №3

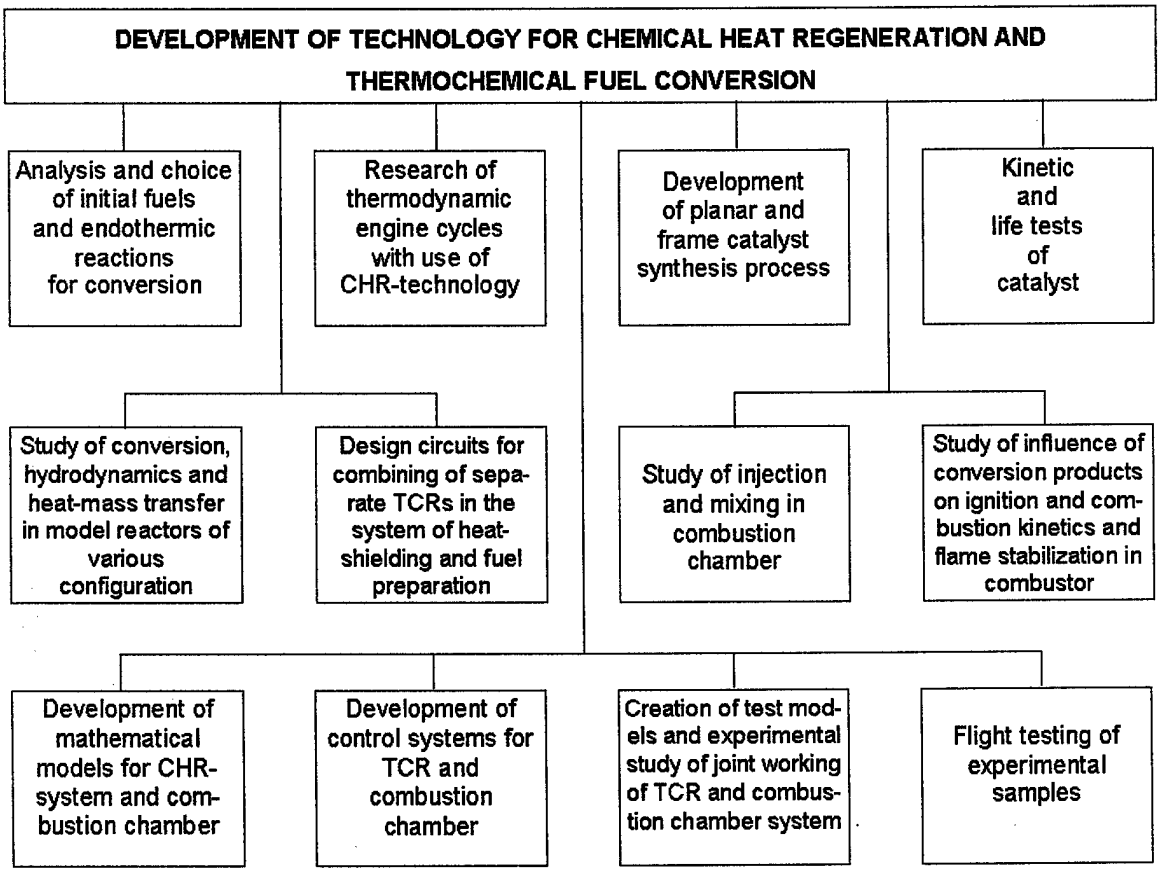

Fig.1. Development stages

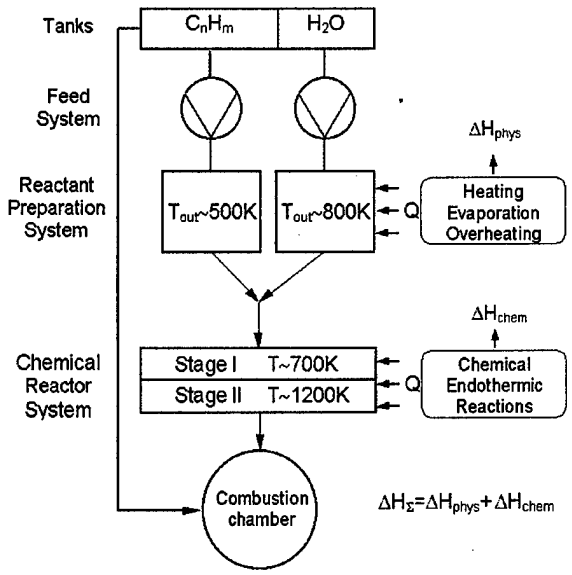

Fig. 1. Two-stage system for the steam reforming of liquid hydrocarbons.

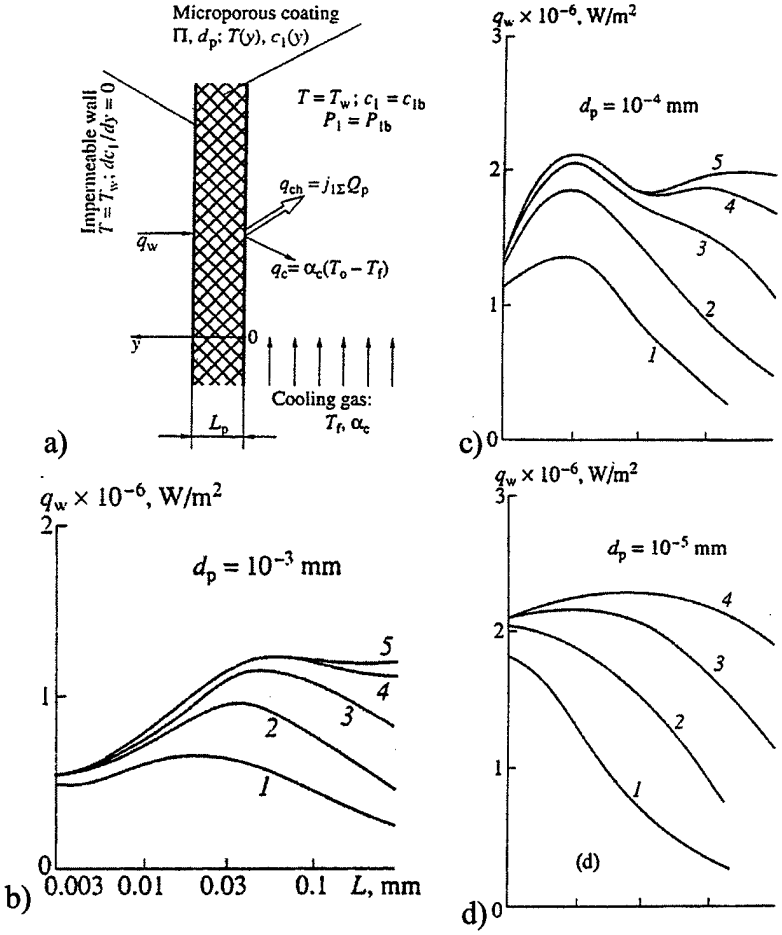

Fig. 3. The model of a heated wall with a microporous catalitic coating; scheme of the heat-and-mass transfer process and local heat flow rates with T_W=1200 K as a function of the thickness and thermal conductivity with a porosity of Π=50% and different diameters of the pores. p_o=0,3 MPa, c_{1o}=0.376, α_c=1150 W/(m²K); T_f=800 K; λ_p, W/(m·K): (1) 0.2; (2) 1.0; (3) 5; (4) 25; (5) 125.

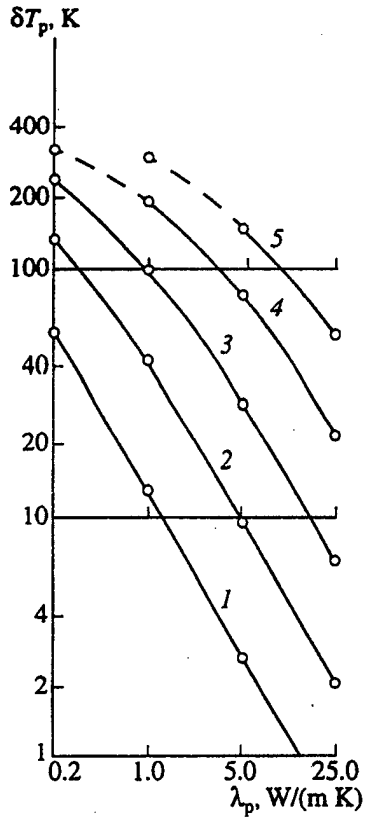

Fig. 4. The thermal resistance of porous catalytic coating (Π=50 %, d_p=10-5 mm) with T_W=1200 K, p_0=0,3 MPa, α_c=2100 W/(m^2·K). L_p=(1) 0.003; (2) 0.01; (3) 0.03; (4) 0.1; (5) 0.3 mm. Insufficiently reliable results of calculations with b_t>3 are shown by the dashed lines.

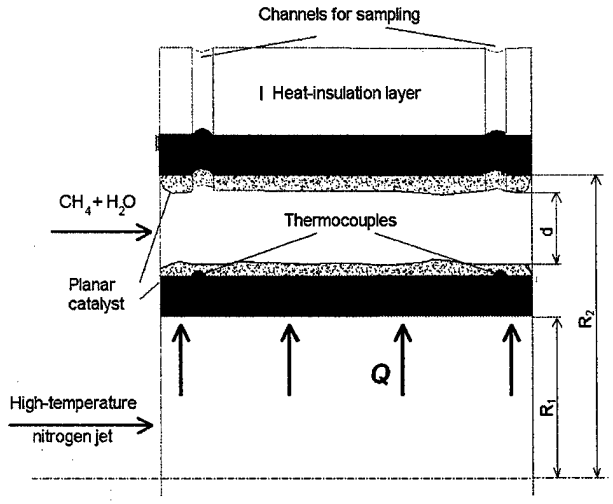

Fig. 5. Fragment of cylindrical thermochemical research reactor.

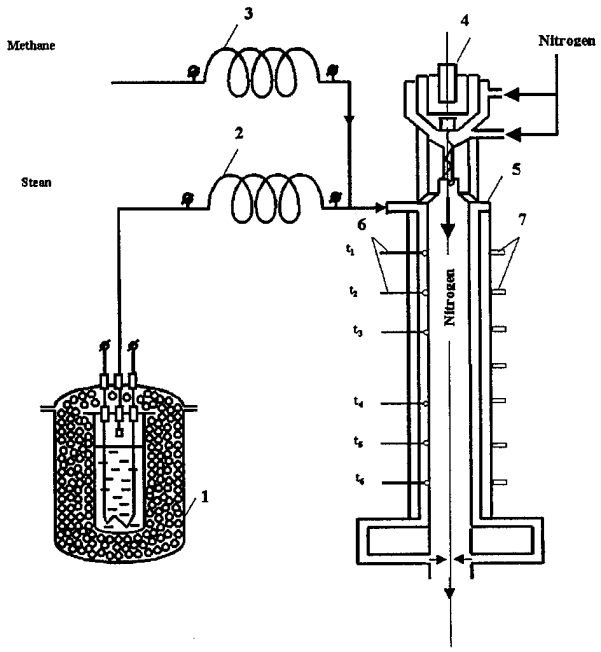

Fig. 6. Experimental set-up.

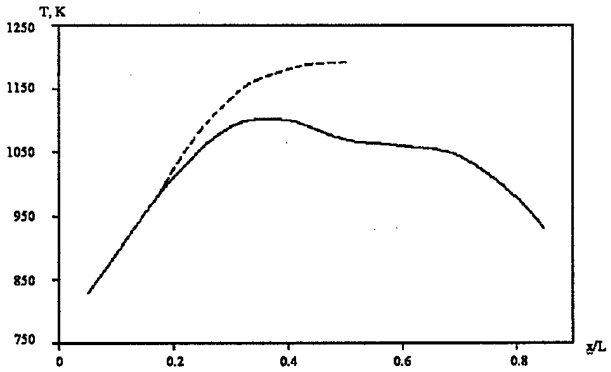

Fig. 7. Temperature distribution along the reactor length

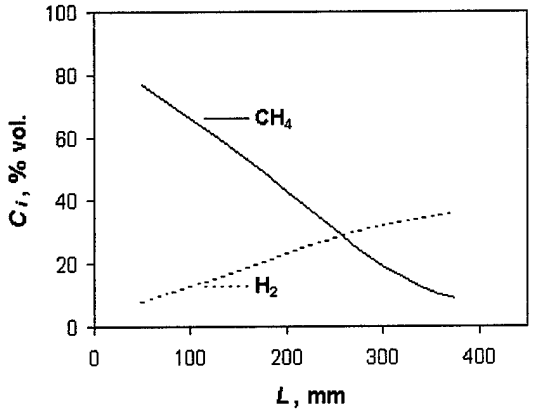

Fig. 8. Concentrations of methane and hydrogen along the length of reactor

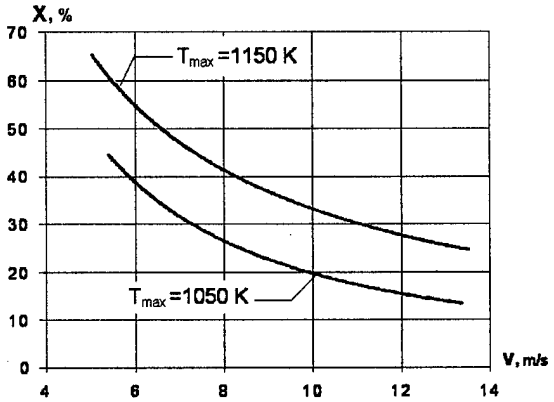

Fig.9. Degree of conversion X vs. mixture speed V at the reactor input

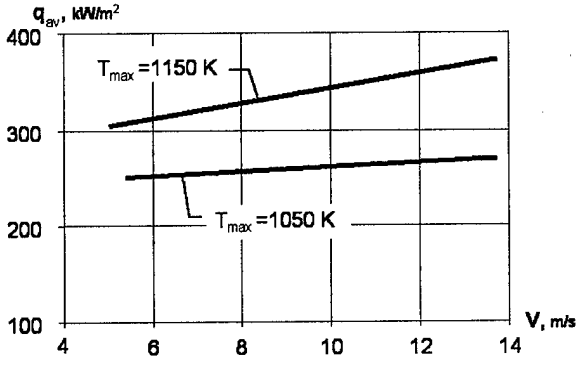

Fig. 10. Average density of heat flux q_{av} vs. mixture speed V at the reactor input

COOLING OF OVERHEATED SURFACES BY THE CATALYTIC METHANE CONVERSION AND AMMONIA DECOMPOSITION

Voskresenskii N.M., Bel'nov V.K., Serdjukov S.I., Safonov M.S., Izmailov L.G.

Department of Chemistry, Moscow State University, 119899 Moscow, Russia

INTRODUCTION

Endothermal processes of methane steam conversion

$$CH_4 + H_2O \Leftrightarrow CO + 3H_2; \qquad (I)$$

$$CO + H_2O \Leftrightarrow CO_2 + H_2 \qquad (II)$$

and ammonia decomposition

$$2NH_3 \Rightarrow N_2 + 3H_2 \qquad (III)$$

may be considered as alternative variants to realize a thermocatalytic way of energy removal from overheated surfaces /1-5/.

In this connection creation of highly effective unified catalytic modules which can be easily included in technological circuits and adjusted to various performance levels under different requirements to reaction completeness is quite actual.

Traditional catalytic modules with a granular catalyst bed do not meet the above requirements and feature low efficiency of catalytic mass use as well as high gasodynamic resistance. Catalysts implemented as coverings applied to regular constructional elements of a module (planar catalysts) are more promising /6/.

The paper considers such a module which is a set of plane-parallel plates made of heat-conducting material with catalyst divided by transport channels wherein gas flows (see fig. 1). Heat is supplied to the plates from the reaction mixture outlet due to high thermal conductivity of the carrier.

Experimental researches of the developed Ni-containing and Fe-containing planar catalysts, prepared by a plasma method, have shown their high catalytic activity in reactions (I), (II) and (III), respectively.

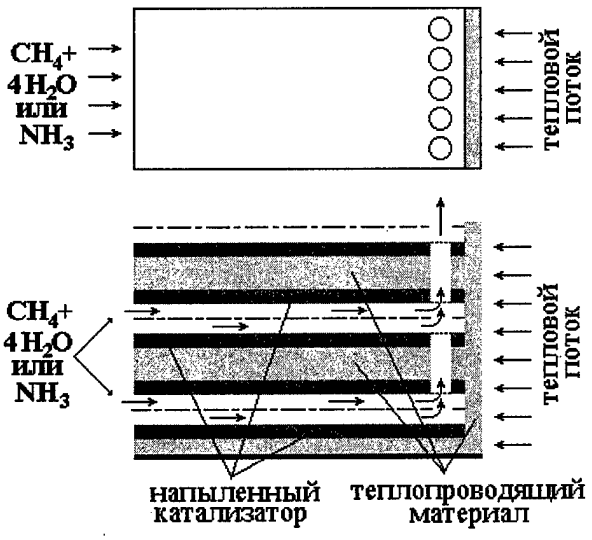

Fig. 1.
A fragment of the catalytic block.

Mathematical model

The processes of methane conversion and ammonia decomposition in a repeating fragment of a catalytic block can be described by the following system of differential equations:

$$\varepsilon\frac{\partial\rho}{\partial t}+\frac{\partial(\dot{m})}{\partial z}=0;$$

$$\varepsilon\rho\frac{\partial x_1}{\partial t}+\dot{m}\frac{\partial x_1}{\partial z}=-AW;$$

$$\varepsilon c_p\rho\frac{\partial T}{\partial t}+c_p\dot{m}\frac{\partial T}{\partial z}=\alpha A(T_k-T); \qquad (1)$$

$$(1-\varepsilon)\rho_k c_{pk}\frac{\partial T_k}{\partial t}=(1-\varepsilon)\lambda_k\frac{\partial^2 T_k}{\partial z^2}-$$

$$-\alpha A(T_k-T)-AW\Delta H,$$

where A - solid material surface area in one unit of package volume, 1/m; b - channel half-width, m; c_p – specific heat capacity of gas, J/(kg·K); c_{pk} - specific heat capacity of the carrier, J/(kg·K); ΔH - increase of gas mixture enthalpy due to chemical reaction per one kilogram of converted methane or ammonia, J/kg; l - half-thickness of the carrier with catalytic covering, m; $\dot{m}$ - gas mass rate per one unit of reactor cross section, kg/(m^2 s); t - time, s; T - gas mixture temperature, K; T_k - temperature of the carrier and catalyst, K; x_1 - fraction by mass of methane or ammonia in the mixture; z - axial distance along the package in gas flow direction, m; W - rate of methane or ammonia transformation per one unit of contact surface area, kg/(m^2·s); α - heat transfer coefficient, J/(m^2·s ·K); $\varepsilon=b/(b+l)$ – fraction of void section in package; λ_k - heat conductivity coefficient of the carrier, J/(m·s·K); ρ - gas mixture density, kg/m^3.

Initial conditions (at $t=0$):

$$x_1=x_0;\ T=T_0;\ T_k=T_0. \qquad (2)$$

Boundary conditions:

$$\text{at } z=0\ (t\geq 0)$$

$$\dot{m}=\dot{m}_0;\ x_1=x_0;\ T=T_0;\ \frac{\partial T_k}{\partial z}=0; \qquad (3)$$

$$\text{at } z=L\ \ (t\geq 0)$$

$$-\lambda_k\left(\partial T_k/\partial z\right)+\left(1-\varepsilon\right)^{-1}\varphi=0, \qquad (4)$$

where L - length of reactor, m; φ - thermal flux per one unit of reactor cross section, J/(m^2·s).

To close the equations system (1), let us use the equations connecting gas mixture density ρ to the current mass fraction x_1 of methane or ammonia.

Let β be water steam-methane mole ratio at the inlet of the catalytic block. Then

$$x_0=\frac{1}{1+\dfrac{M_{H_2O}}{M_{CH_4}}\beta} \qquad (5)$$

and, according to equations (I) and (II), the mass fractions of H_2O, H_2, CO и CO_2 mixture components will be respectively:

$$x_2=\left(1-x_0\right)-\frac{M_{H_2O}}{M_{CH_4}}\left(x_0-x_1\right)-$$

$$-\frac{M_{H_2O}}{M_{CO_2}}x_5;$$

$$x_3=\frac{M_{H_2}}{M_{CH_4}}\left(x_0-x_1\right)+\frac{M_{H_2}}{M_{CO_2}}x_5; \qquad (6)$$

$$x_4=\frac{M_{CO}}{M_{CH_4}}\left(x_0-x_1\right)-\frac{M_{CO}}{M_{CO_2}}x_5,$$

where

$M_{CH_4}, M_{H_2O}, M_{CO}, M_{H_2}, M_{CO_2}$ и M_{NH_3} – – molecular masses of the components, kg/mol. The value of x_5 was calculated based on quasiequilibrium condition of the reaction (II), using the expression for equilibrium constant K_{p2} /7/

$$K_{p2}=\frac{M_{H_2O}M_{CO}}{M_{H_2}M_{CO_2}}\frac{x_3x_5}{x_2x_4}. \qquad (7)$$

Using (6), we can derive the equation for reaction mixture density

$$\rho = \frac{P}{RT}\frac{M_{CH_4}+\beta M_{H_2O}}{3+\beta-2x_1\left(1+\frac{M_{H_2O}}{M_{CH_4}}\beta\right)}, \qquad (8)$$

where P – total pressure, R - gas constant.

In the case of ammonia decomposition to the inlet of reactor comes pure ammonia and

$$x_0 = 1.$$

The ratio of nitrogen and hydrogen (reaction products) is 1:3, hence

$$\rho = \frac{PM_{NH_3}}{RT(2-x_1)}. \qquad (9)$$

In calculation of heat transfer coefficient α the known Reynolds analogy between heat exchange and friction was used, which can be expressed by /8/

$$\mathrm{St} = \frac{\alpha\varepsilon}{c_p\dot{m}} \approx f, \qquad (10)$$

where St – Stanton number, f – friction resistance factor. For completely developed laminar flow in a flat channel the friction resistance coefficient is described by the formula

$$f = \frac{12}{\mathrm{Re}}, \qquad (11)$$

and for turbulent flow

$$f \approx 0.039\,\mathrm{Re}^{-0.25}, \qquad (12)$$

where $\mathrm{Re} \equiv \dot{m}d_э/\varepsilon\eta$, $d_э$ – equivalent diameter (for a flat channel $d_э = 4b$), η – dynamic viscosity, kg/(m s).

Thus, from (10) and (11) we have under laminar modes

$$\alpha = 3\frac{c_p\eta}{b}. \qquad (13)$$

Let us enter the dimensionless variables:

$G = \dot{m}/\dot{m}_0$, $\theta = T/T_0$, $\theta_k = T_k/T_0$, $\sigma = \rho/\rho_0$, where for methane steam conversion

$$\rho_0 = \frac{P}{RT_0}\times\frac{M_{CH_4}+\beta M_{H_2O}}{1+\beta}, \qquad (14)$$

and for ammonia decomposition

$$\rho_0 = \frac{M_{NH_3}P}{RT_0}, \qquad (15)$$

dimensionless coordinate $Z = z/L$ and time $\tau = \frac{\lambda_k t}{\rho_k c_{pk} l^2}$. Using dimensionless variables, let us transform the system and additional conditions (1) - (4) to the form:

$$\frac{\partial\sigma}{\partial\tau}+\frac{\rho_k c_{pk}}{\lambda_k\rho_0}\frac{\dot{m}_o}{\varepsilon}\frac{l^2}{L}\frac{\partial G}{\partial Z}=0;$$

$$\sigma\frac{\partial x_1}{\partial\tau}+\frac{\rho_k c_{pk}}{\lambda_k\rho_0}\frac{\dot{m}_o}{\varepsilon}\frac{l^2}{L}G\frac{\partial x_1}{\partial Z}=$$

$$=-\frac{\rho_k c_{pk}}{\lambda_k\rho_0}\frac{l^2}{b}W;$$

$$\sigma\frac{\partial\theta}{\partial\tau}+\frac{\rho_k c_{pk}}{\lambda_k\rho_0}\frac{\dot{m}_o}{\varepsilon}\frac{l^2}{L}G\frac{\partial\theta}{\partial Z}= \qquad (16)$$

$$=\frac{3\rho_k c_{pk}}{\lambda_k\rho_0}\eta\frac{l^2}{b^2}(\theta_k-\theta);$$

$$\frac{\partial\theta_k}{\partial\tau}+3\eta c_p\frac{l}{b}(\theta_k-\theta)=$$

$$=\left(\frac{l}{L}\right)^2\frac{\partial^2\theta_k}{\partial Z^2}-\frac{\Delta H}{\lambda_k T_0}lW,$$

$$\tau = 0;\quad x_1 = 1, \theta = 1, \theta_k = 1;$$

$$Z = 0;\quad x_1 = 1, \theta = 1, G = 1, \frac{\partial\theta_k}{\partial Z} = 0; \qquad (17)$$

$$Z = 1;\quad \frac{\partial\theta_k}{\partial Z} = \frac{1}{\lambda_k}\frac{\varphi L}{(1-\varepsilon)T_0}.$$

For numerical calculations were used average temperature-independent parameter values of a steel carrier for planar catalysts:

$$\rho_k = 8\times10^3\,\mathrm{kg/m^3};\quad c_{pk} = 0.046\,\mathrm{J/kgK};$$
$$\lambda_k = 46\,\mathrm{J/msK},$$

the known empirical relations for ΔH and c_p /7/.

Gas mixture viscosity was calculated by the approximation formula of the kinetic theory of gases /9/:

$$\eta_m = \sum_{i=1}^{n} \frac{x_i M_i^{-1}\eta_i}{\sum_{j=1}^{n} x_j M_j^{-1}\Phi_{ij}}, \qquad (18)$$

where $\eta_m(T)$ – gas mixture viscosity, $\eta_i(T)$ – viscosity of i-th pure component of the mixture;

$$\Phi_{ij} = \frac{\left[1+\left(\eta_i/\eta_j\right)^{0.5}\left(M_j/M_i\right)^{0.25}\right]^2}{\left[8\left(1+M_i/M_j\right)\right]^{0.5}}, \qquad (19)$$

M_i – molecular mass of i-th component,

$$\eta_i = \eta_{ic}^{*} T^{0.71+0.29/T}, \qquad (20)$$

η_{ic}^{*} – viscosity of the i-th component at the critical temperature T_{ic} and critical pressure P_{ic}:

$$\eta_{ic}^{*} = \frac{3.5 M_i^{0.5} P_{ic}^{2/3}}{T_{ic}^{1/6}}. \qquad (21)$$

For reaction rate of methane with water steam on Ni-containing catalyst the equation derived in /10/ was used:

$$W = M_{CH_4}\frac{kP_{CH_4}P_{H_2O}\left(1-\frac{1}{K_{p1}}\frac{P_{CO}P_{H_2}^3}{P_{CH_4}P_{H_2O}}\right)}{P_{H_2O}+k_1P_{H_2}}, \qquad (22)$$

where $P_{CH_4}, P_{H_2O}, P_{H_2}$ и P_{CO} – partial pressures of components, K_{p1} – reaction (I) equilibrium constant (I) /7/,

$$k = \gamma T_k e^{\left(-\frac{E}{RT_k}\right)},$$
$$\gamma = 0.23\frac{\mathrm{mol\,s}}{\mathrm{kg\,m\,K}},\ \frac{E}{R} = 1.58\times10^4\,\mathrm{K}, \qquad (23)$$
$$k_1 = 1.99\times10^3.$$

Relation between partial pressures and mass fractions of components was defined by the formula

$$P_i = P\frac{x_i M_i^{-1}}{\sum_i x_i M_i^{-1}},\ i = 1,..,5, \qquad (24)$$

where P_i and M_i – partial pressures and molecular masses of components.

For the reaction of ammonia decomposition on Fe-containing catalyst the known relation was used

$$W = M_{NH_3} K \exp\left(-\frac{E}{RT_k}\right), \qquad (25)$$

wherein the constants values for the developed catalyst type were /11,12/:

$$K = 7.10\times10^{11}\,\mathrm{mol/m^2s};$$
$$E = 1.9\times10^5\,\mathrm{J/mol}. \qquad (26)$$

In numerical solution of equation (16) values of parameter $l, b, L, T_0, \dot{m}_0$ and β were varied.

Results and conclusion

The calculation results for steady state processes of methane conversion and ammonia decomposition in a catalytic block for some specific values of design parameters are presented in fig. 2 and fig. 3.

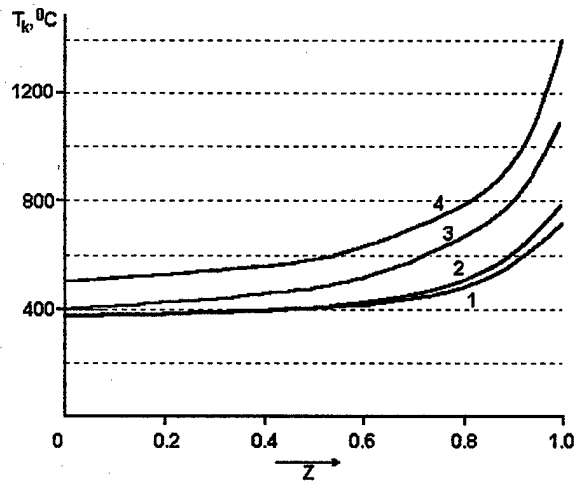

Fig. 2.

Temperature distribution T_k along the block length (L=0.1 m) for ammonia decomposition (φ, MW/m²: (1) 0.5; (2) 1.0) and methane conversion (φ, MW/m²: (3) 0.5; (4) 1.0).

From fig. 2 it can be seen that the length of a catalytic block (determined particularly by the value of thermal flux) for ammonia decomposition process is much less than in case of methane conversion.

Fig. 3 shows that the level of thermal load allowable for heat-resistant steel ($T_k(Z=1) < 1000$ °C), for the process of methane conversion does not exceed 1 MW/m². Further increase of the thermal flux results in significant growth of catalytic block wall temperature.

For ammonia decomposition the allowable thermal flux may achieve 3 MW/m².

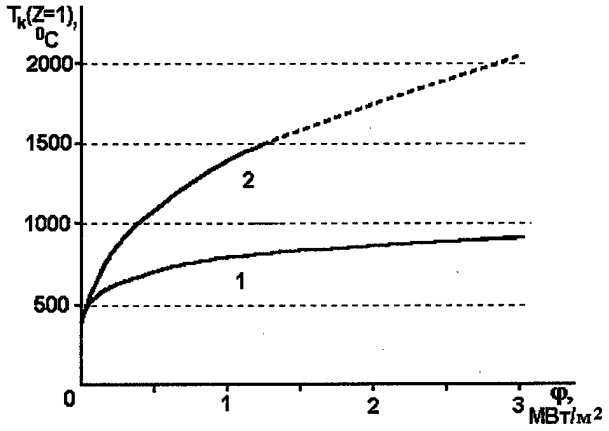

Fig. 3.

Relations between the temperature of a catalytic block wall (L=0.1 m) and the value of heat flux: (1) ammonia decomposition (feed 1 kg/(m² s)), (2) methane conversion (feed 4 kg/(m² s), β = 4).

These results demonstrate a significant advantage of ammonia decomposition over methane conversion in chemothermal cooling of overheated surfaces.

References

1. Nosach V.G. Thermochemical insulation. Doc. AN USSR, Ser. A. 1979. № 11. pp. 941-953.

2. Anikeev V.I., Bobrin A.S., Kirillov V.A. Collected volume of the 1-st All-Russia Conf. Chemical regeneration of heat in air vehicles. 1989. pp 281-294.

3. Anikeev V.I., Hanaev V.M., Bobrin A.S., Kirillov V.A. Analysis of heat removal efficiency from catalyst surface in carrying out perspective thermochemical reactions under diffusion restrictions. Sib. Chem. J. 1991. B. 2. pp. 130-135.

4. Kurganov B.A., Zejgarnik J.A., Korabel'nikov A.V., Maslakova I.V. A thermochemical principle of cooling on the basis of steam methane conversion. Teploenergetika. № 3. 1996.P. 18-29.

5. Korabel'nikov A., Kuranov A. Thermochemical conversion of hydrocarbon fuel under the concept "AJAX". AIAA-99-4921.

6. Safonov M.S., Serdyukov S.I., Voskresenskij N.M. A device for heterogeneous catalytic processes. Patent № 2055635 // 1996. Bul. № 7.

7. Gurvich L.V., Vejts I.V., Medvedev V.A. et al. Thermodynamic properties of individual substances. /Edited by V.P.Glushko. M.: Nauka, 1978. v.1.

8. Heat exchange manual. V. I. M.: Energatomizdat, 558 p.

9. Reid R., Prausnitz J., Sherwood K. The properties of gases and liquids. L.: Chem. 1982. P. 360.

10. Makunin A.V., Bel'nov V.K., Safonov M.S., Serdyukov S.I., Suris A.L. Experimental research and mathematics modeling of a coaxial tubular reactor of steam methane conversion. Teor. Osnovy Chim. Technol., 2000. v.34. №6 (is in the press).

11. Ostoshevskaja O.Yu., Serdyukov S.I., Safonov M.S., Plasma-covered catalyst of ammonia decomposition. I. Influence of preliminary processing conditions on catalytic properties. Kinetika i kataliz, 1996. v. 37. №6. P. 927-930.

12. Ostoshevskaja O.J., Serdyukov S.I., Fabrichnii P.B. Plazma-covered catalyst of ammonia decomposition . II. Research of phase transformations. Kinetika i kataliz, 1996. v. 37. №6. P. 931-934.

THERMAL PROTECTIVE CHARACTERISTICS OF MULTICHANNEL PANELS WITH THERMOCHEMICAL COOLING

Kurganov V.A.*, Zeigarnik Yu.A., Maslakova I.V.

* Institute for High Temperatures of Russian Academy of Sciences (IVT RAN), ul. Izhorskaya, 13/19, Moscow, 127412, Russia

The "AJAX" concept of the hypersonic flight vehicle (HFV) constructing [1], which have been worked up by GNIPGS of the "Leninets" holding company, foresees the usage of the catalytic thermochemical reaction of the steam reforming of the methane in the system of active thermal protection of the various elements of HFV. The great value of the heat effect of this reaction (approximately 5 times greater than the heat of water vaporisation) allows to significantly increase the cooling resource of the fuel, and moreover to partially utilize the mechanical and heat losses of the vehicle and to improve the chemical composition of the fuel by an addition of CO and hydrogen. In the numerical researches, which have been carried out by IVT RAN, there were undertaken an attempts to predict the characteristics of the thermal protection systems with the thermochemical cooling. Considered types of the elements of the thermal protection systems are as following: the tube reactor [2], and the multi-channel and plane-channel reactors of a panel type [3, 4]. The multi-channel thermochemichal reactor (TCR) of a panel type is a matter of interest from the different points of view: as the real module of the HFV covering, and as a reactor which allows to significantly change the macrosurface area of the catalysis in the range of the given (fixed) dimensions. The scheme of such a reactor is shown on fig.1,a. In this work we consider the following characteristic parameters of the TCR: the nominal equivalent diameter $D_0 = 2a$; the density of the inside ribbing a/b; the relative length L/D_0; and the porosity $\Pi = V_0/V$, here V - the total volume of TCR, V_0 - the volume of holes (channels) for a gas pass. Reactors with the identical diameters D_0 and porosity have the same power-to-weight ratio for any value of the a/b ratio.

The numerical research of the hydraulic characteristics of the panel type TCR was based on the integration of one-dimensional system of the equations of conservation of the gas flow bulk parameters. An interaction of the flow and the wall was described with the generalised relations of convective heat and mass transfer, which take into account the effects of the variable properties and laminarisation of the flow at the high heating rates. The processes of the heat conductivity in the metal framework of the TCR and the radiative heat transfer of the channel walls were calculated with the zoning method and with using of the spline-method technique (see [3, 4]).

In case of the non-equilibrium reacting, the kinetic of the reaction of steam reforming of the methane was described with the following equation:

$$j_{1w} = Bp_{1w}\exp[-E/(RT_w)]$$

where j_{1w} is the mass flow rate of the methane on the catalytic wall, p_{1w} is the partial pressure of the methane on the wall, T_w is the wall temperature.

The relation between CO and CO_2 in synthesis-gas was established by the equilibrium condition of the "water gas reaction" on the catalytic wall. In calculations we used the values of B (in kg/(m^{2}sMPa)) and E/R (in K) experimentally obtained in [5] (dense nickel foil: B = 5000, E/R = 15600) and [6] (porous granule: B = 410, E/R = 9760), and theoretically estimated in [2] (microporous thermal conductive catalytic coatings of an optimum configuration: B = 860, E/R = 7850).

The numerical researches of the thermal and hydraulic characteristics of the panel TCR were carried out in the following ranges of parameters: $p = 0.3-2.0$ MPa; $T_{in} = 500-1100$ K; $D_0 = 4\div16$ mm; $L/D_0 = 25-150$; $\Pi = 45-90\%$; $a/b = 0\div5$. In the major of studies the relation H_2O/CH_4 was taken to be 1.5. The law of the heat supply was taken in the form $q_w = \text{const}$. As a result, the permissible values of the heat flux q_w^{perm}, at which the maximum temperature of the wall attains the value of 1225K (~950^{o}C), were determined. Mostly it was considered the case of the one-side heating, as the major in thermal protection systems. Some of the results of the studies fulfilled are presented in fig. 1 and 2. The fig.1,b,c shows the typical values of q_w^{perm} and the level of total methane conversion Z_α, as a functions of the Mach number at the outlet of the reactor. As could be seen from the figure, the Ma_{out} changes monotonous with the flow rate. Meanwhile, because of the changes of the flow and heat-and-mass transfer regimes in the TCR channel, the curves q_w^{perm} and Z_α are not smooth. It has no sense to operate with Ma_{out}>0.4, because in that case the decrease of the reactor power could be happen. So the regime with Ma_{out}=0.4 we call the limit regime, and the corresponding heat flux we denote as q_w^{lim}. At the limit regime for the pressures in range 0.3 - 0.5 MPa, the monolithic steel reactor is able to absorb the heat fluxes levels order of 0.6 – 1.2 MW/m^2, but the considerable values of the conversion level could be achieved only at the high catalytic activity. The significant generation of synthesis-gas is provided at the moderate and small flow rates and Mach numbers for the corresponding levels of q_w^{lim} within 0.2 - 0.4 MW/m^2.

Fig.2,a,b represents the effect of the porosity Π and the inside ribbing density a/b on the characteristics of the TCR in the limit regimes. As could be seen, these parameters has no great influence on the thermal protective ability of the TCR (q_w^{lim}); hence this fact gives some opportunities for the designers.

Increasing of the specific weight power of the TCR (this means power per 1 kg of TCR's weight) with increasing of the porosity can be achieved due to the certain increase of the mass flow rate of the cooling gas. Increasing of the ribbing density allows to significantly reduce the mass flow rate of the cooling gas and to rise up the conversion level. Finally, fig.2,c shows the role of the thermal conductivity of the TCR's metal framework in the process of heat transfer. Using fig.2,c one can compare the values of q_w^{lim} and Z_α for the monolithic steal reactor (solid lines) and for the plane channel with catalytic inserts, which have no good thermal contact with a heated wall (dash-and-dot lines). As could be seen, the monolithic constructions have the evident advantages in comparison with the reactors with free catalytic inserts.

The numerical calculations have been carried out shows that the multi-channel panels with thermochemical cooling by the mixture of methane and water steam:

- is the perspective technology of the thermal protection coverings for the HFV, and

- presents the great opportunities either for heat absorption of the heat fluxes up to the level of 1 - 1.5 MW/m^2, and for generation of the synthesis gas of the great amount. Creating of the microporous catalytic coatings with good heat conductivity and adhesiviness is the main technological problem under designing of such a constructions.

References.

1. The new hypersonic technologies under the "AJAX" concept / A.A. Turchak, V.L. Fraishtadt, A.L. Kuranov // Polet, 1999, No.9, pp. 3-8.

2. The thermochemical principle of cooling based on steam reforming of methane / V.A. Kurganov, Yu.A. Zeigarnik, A.V. Korabelnikov, I.V. Maslakova // Thermal engineering, 1996, v.34, No.3.

3. The cooling of thermal stressed surfaces with chemical reacting gases / V.A. Kurganov, Yu.A. Zeigarnik, F.P. Ivanov, I.V. Maslakova, S.B. Martynov / In "Heat transfer in modern technique". Ed. Zeigarnik Yu.A. et al. Moscow, IVT RAN, 1998, pp. 48-74.

4. High temperature thermal protective panels with thermochemical cooling based on steam reforming of methane / V.A. Kurganov, Yu.A. Zeigarnik, I.V. Maslakova et al // High Themperature, 2000 (in print).

5. Bodrov I.M., Apel'baum l.O., Temkin M.I. Kinetics of the methane reaction with steam, catalizing by nickel on the porous ground / Kinet. Katal., 1967, v.8, No.4, pp. 821-828.

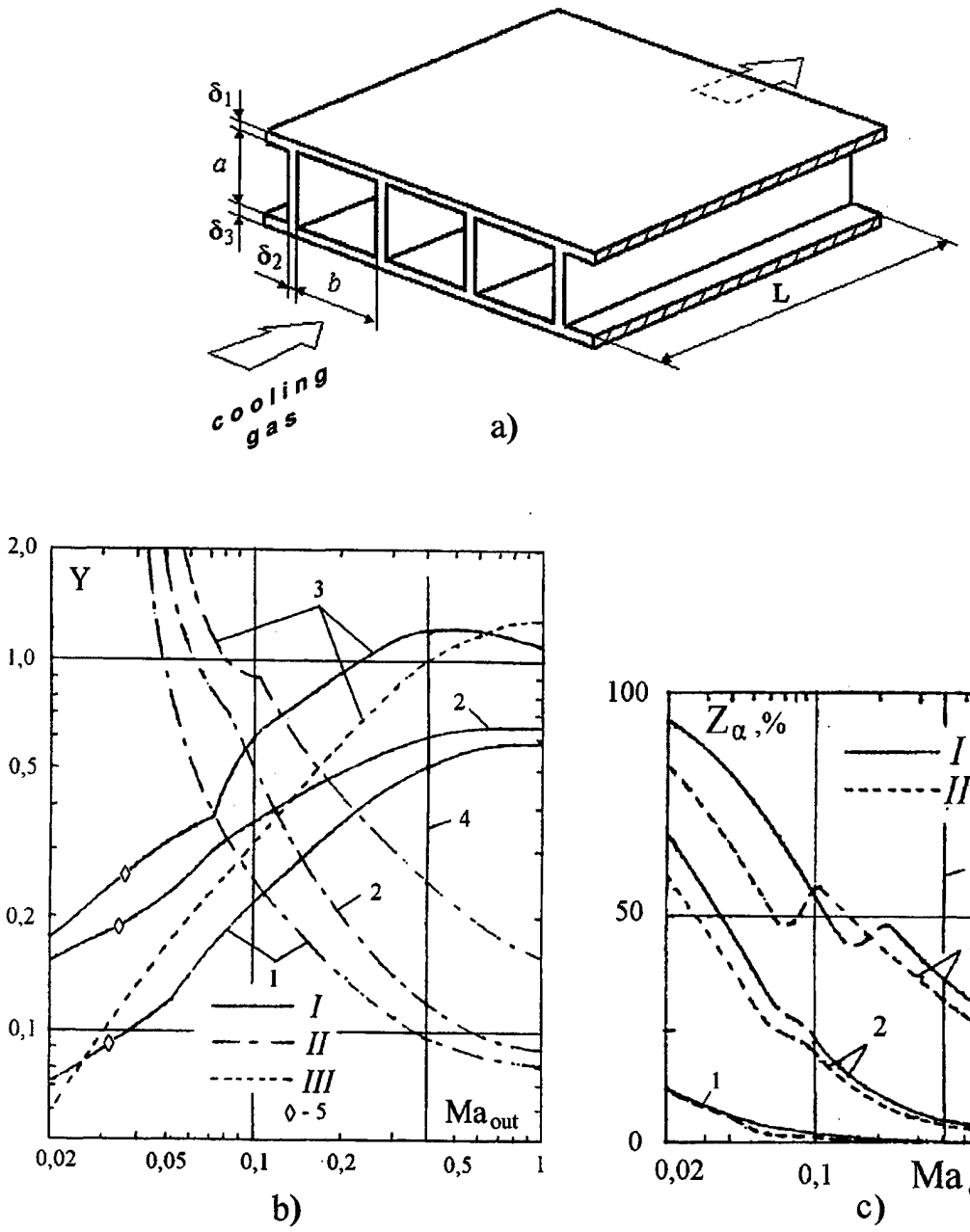

Fig.1. a) the constructive scheme of the panel type TCR; b) characteristics, as a functions of the Mach number in the reactor outlet ($D_0 = 8$ mm): *I* - q_w^{perm} (MW/m^2), *II* - q_w^{perm}/q_{cr}, *III* - the relative flow rate of a gas; c) the total conversion level as a function of Ma_{out}: *I* - $D_0 = 4$ mm, *II* - $D_0 = 8$ mm. Monolithic reactor with one-sided heating ($\Pi = 70\%$; $L/D_0 = 100$; $a/b = 1$; $p_{in} = 0.3$ MPa; $T_{in} = 700$ K; H_2O/CH_4=1.5). Curves 1, 2, 3 corresponds to the low, middle and high levels of the catalytic activity of the walls; 4 - $Ma_{out}^{lim} = 0.4$; 5 - $Re_{in} = Re_{cr} = 2200$.

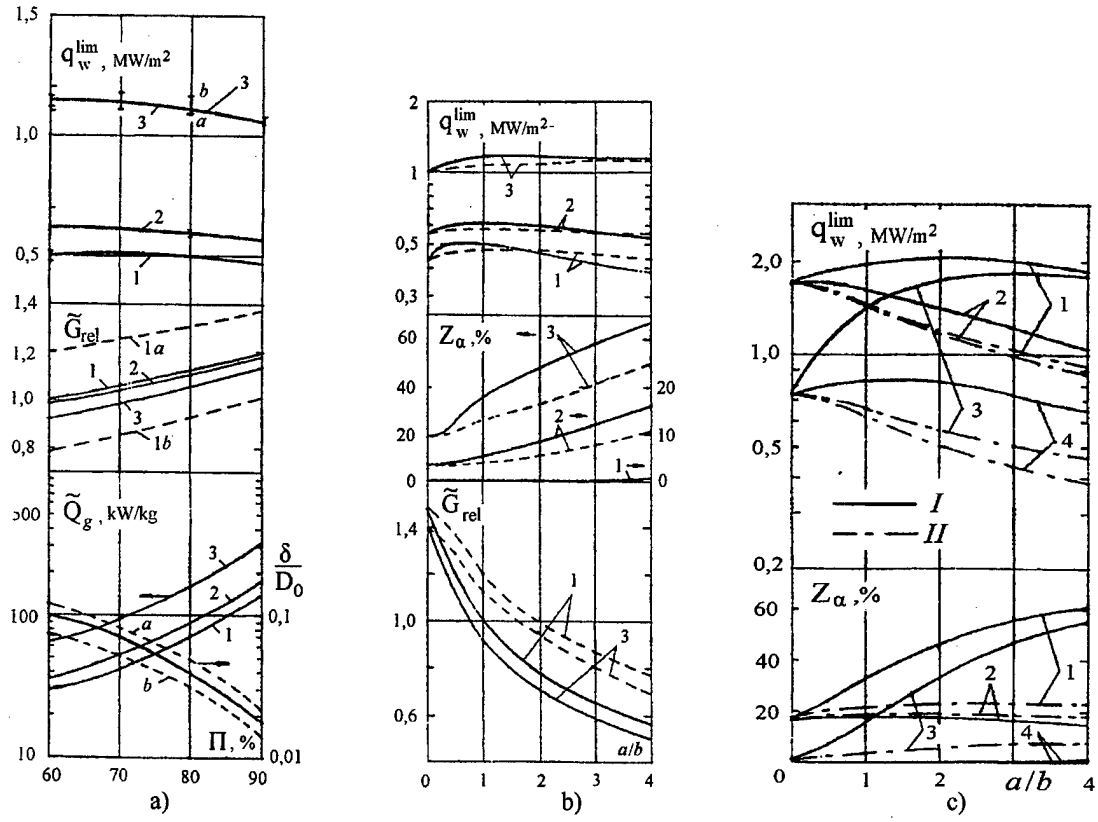

Fig.2. The limit characteristics of the multi-channel panel TCR, as a functions of the porosity (a), of the density of the internal ribbing (b) and of the conditions of the thermal contact of the ribs with the heated wall (c). $L/D_0 = 100$;

a), b): $D_0 = 8$ mm; number of curves and the gas parameters – see fig.1.

c): ($p_{in} = 0.5$ MPa) 1 - all the walls are of the high catalytic activity; 4 - all the walls are of the low activity; 2 - the heated wall is of the high activity, other walls are of the low activity; 3 - the heated wall is of the low activity, other walls are of the high activity.

I - monolithic framework; *II* - bad thermal contact of the heated wall and the catalytic inserts.

THE CHARACTERISTICS OF MICROPOROUS CATALITIC COATINGS

Kurganov V.A.*, Martynov S.B.

* Institute for High Temperatures of Russian Academy of Sciences (IVT RAN), ul. Izhorskaya, 13/19, Moscow, 127412, Russia

In the thermal protective thermochemical reactors (TCR) the cooling effect of the catalytic reaction of the methane reforming is used. To construct such a reactors it is necessary to know the specialties of kinetic of the reaction for the catalizer of the used type. To calculate the heat and mass transfer in the channel reactors with catalytic walls, one needs to know as the activation energy of the reaction, so the specific productivity of the catalytic wall, related to the area of the contact surface of the gas with the wall. Such a data for the dense nickel foil and porous cubic granule of nickel catalizer GIAP-3 were experimentally obtained in [1, 2]. On these data the kinetic of the methane reforming in the temperature range from 700 to 900^{O}C can be described with the equation:

$$j_{1W} = B \exp[-E/(RT_W)]\, p_{1W}, \quad (1)$$

where p_{1W} is the partial pressure of the methane on the wall. For the dense nickel foil B = 5000 kg/(m^{2}sMPa), E/R = 15600K (E = 31000 kcal/mole); for the surface of the porous granule B = 41 kg/(m^{2}sMPa), E/R = 9760K (E = 19400 kcal/mole). At the temperature of 1200K the rate constant of the reaction on the porous surface is 10 times greater then the one on the dense foil. Nevertheless, the numerical studies of the normal turbulent heat and mass transfer in the tube reactors showed that in the range of temperatures up to 1225K (~950^{O}C) which is permissible for the thermal stressed steals, the methane reforming process calculated within eq.(1) with parameters from [1, 2] flows in the regime of the weak damping by the outside diffusion. This speaks to the enhancing of the catalytic activity of the wall. This enhance could be obtained using the microporous coating with active porous surface.

In [3] the heat and mass transfer problem for the micriporous coating was considered. The approximate solution of the problem was analytically obtained using some assumptions. The solutions fulfilled allowed to determine the conditions of the most effective usage of the catalytic coatings. Meanwhile the effect of such a factors as the porosity of the coating, the level of activity of the surface, the gas penetration factor, haven't been studied yet. In this work more accurate technique, based on the method of finite elements, was used. Using this method the possible changes of the activity of microporous coatings under mentioned above factors was studied. The results obtained generally confirmed the conclusions have been made earlier in [3].

Fig.1, 2 presents some of the new numerical results obtained. In fig.1 the effect of the porosity of the coating (with the pore diameter d_p=10^{-5} mm) and the level of activity of the pores surface in relation to

activity of the dense nickel foil [1], on the heat flux removed, at the surface temperature T_c=1225K is shown. The heat flux is given as a function of the thickness and the thermal conductivity of the porous layer. The data presented in fig.1 confirms the advantage of the thin coatings with a good thermal conductivity λ_p=1-5 W/(m K). Meanwhile, such a coatings are under the great effect of the activity level of the porous surface and the porosity of the layer. An increase of the activity g decreases the heat flux removed q_c. As could be seen from fig.1b the porosity of П=50% seems to be most efficient to provide as the sufficient amount of the contact surface area, so the good level of thermal conductivity of the layer. An increase of the porosity up to 70% could give the significant increase of the heat flux q_c, but how to keep the thermal conductivity λ_p of the porous layer on the high level is rather a problem.

Fig.2 shows the relative efficient values of the rate constant of the reaction in formula (1). The values have been used in [3] are compared with the new ones, obtained for the porous coatings with $d_p = 10^{-4}$ and 10^{-5} mm and with thickness L_p = 0.01 mm. In fig.2 the variants of kinetics 1 and 2 corresponds to the above parameters in (1) according to the data [1, 2]; the 3 variant corresponds to the values B = 860 kg/(m^2 s MPa) and E/R = 7850K (15600 kcal/mole) obtained in [3] for the coatings of the high thermal conductivity with П=100%. As could be seen from fig.2, an increase of g substantially reduces the catalytic efficiency of the porous coating; the decrease of the gas penetration factor has the same effect. Enlarging of d_p over 10^{-4} mm at temperatures below 1100K moves the reaction to the kinetic regime and increases the visible activation energy. In the large temperature range, at least from 950 to 1300K, the kinetic parameters are more stable and varies slowly at the pores diameter below $3 \cdot 10^{-5}$ mm.

As could be seen from fig.2 the catalytic activity of the real coatings even of an optimum configurations varies substantially with a manufacturing quality factors of the coatings. Evidently, the 2nd and the 3rd variants of parameters of the equation (1) corresponds to the low and the high levels of the catalytic activity. We should note here that the 2nd variant is realized at the very low quality factors of the coating. Therefore the quite low level of kinetic parameters of the porous cataliser obtained in [2] can be explained by the effect of the thermal and diffusion damping of the reaction, which were not taking into account in [2].

On the results of the studies we can conclude that for the practicable microporous coatings with $d_p < 3 \cdot 10^{-5}$ mm, L_p = 0,01 ± 0,003 mm and $\lambda_p \geq 1$ W/(m K), the following kinetic parameters of eq.(1) are mostly real: B = 380 kg/(m^2 s MPa) and E/R = 7985K (E = 15870 kcal/mole). The thermal resistance of such a coatings can be approximately calculated with a usual formula for the plate wall without inside heat absorption.

Of course to determine the specialties of the kinetic of the methane steam reforming, the experimental investigations should be conducted.

References.

1. Bodrov I.M., Apel'baum L.O., Temkin M.I. Kinetics of the methane reaction with steam on a nickel surface / Kinet. Katal., 1964, v.5, No.5, pp. 696-705.

2. Bodrov I.M., Apel'baum L.O., Temkin M.I. Kinetics of the methane reaction with steam, catalizing by nickel on the porous ground / Kinet. Katal., 1967, v.8, No.4, pp. 821-828.

3. The thermochemical principle of cooling based on steam reforming of methane / V.A. Kurganov, Yu.A. Zeigarnik, A.V. Korabelnikov, I.V. Maslakova // Thermal engineering, 1996, v.34, No.3.

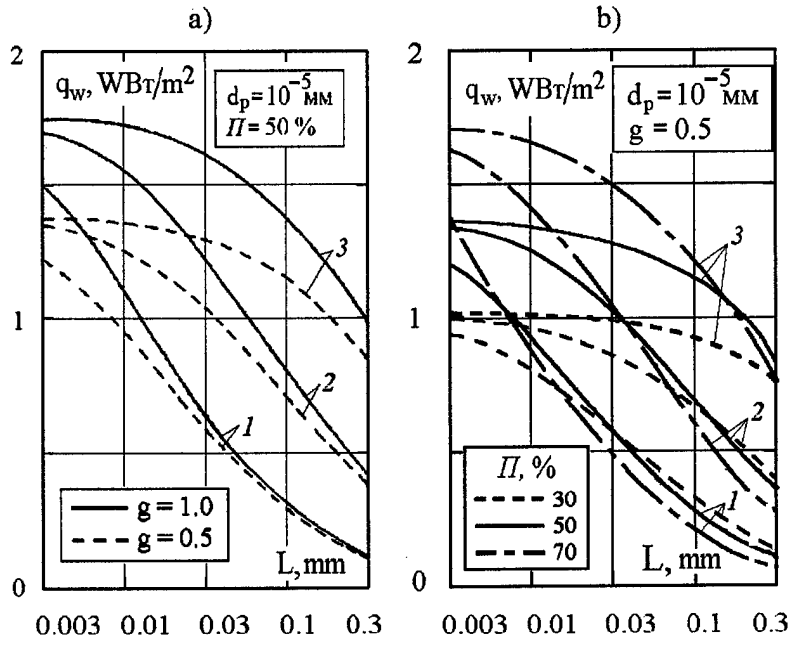
a)
b)
q_w, WBт/m^2
$d_p = 10^{-5}$ мм
П = 50 %
g = 1.0
g = 0.5
L, mm
П, %
30
50
70
0.003 0.01 0.03 0.1 0.3
0 1 2

Fig. 1.

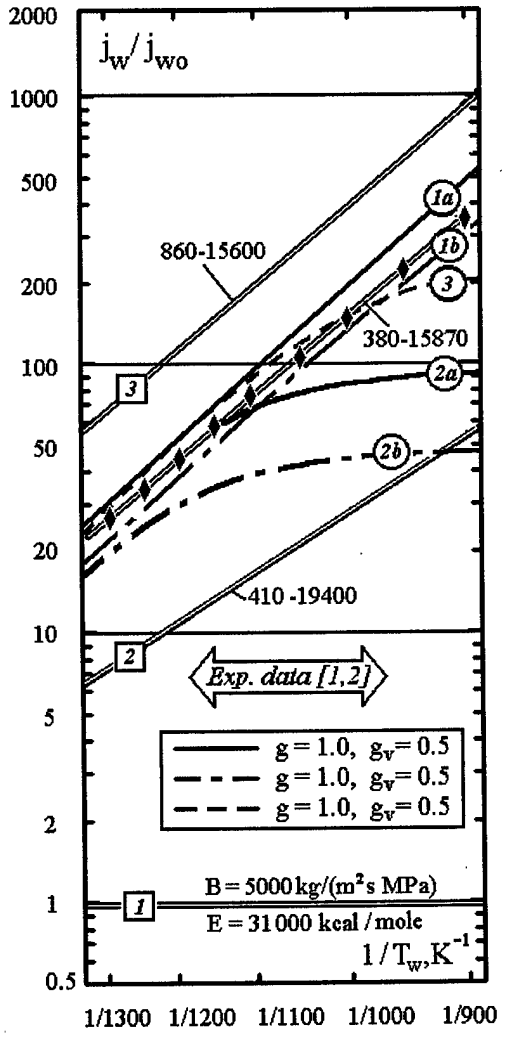
j_w / j_{wo}
860-15600
380-15870
410 -19400
Exp. data [1,2]
g = 1.0, g_v = 0.5
g = 1.0, g_v = 0.5
g = 1.0, g_v = 0.5
B = 5000 kg/(m^{2}s MPa)
E = 31000 kcal / mole
$1/T_w, K^{-1}$
1/1300 1/1200 1/1100 1/1000 1/900
2000 1000 500 200 100 50 20 10 5 2 1 0.5

Fig. 2.

QUASIMONODIMENTION MATHEMATICAL MODEL OF THE HEAT CHEMICAL REACTOR, DEVELOPED UNDER THE "AJAX" CONCEPT

Korabelnikov A.V., Kuranov A.L., Kuchinsky V.V.

212 Moskovsky prospekt, St. Petersburg, 196066, Russia.
Hypersonic System Research Institute
Tel./ Fax:(812) 291-82-94, E-mail:ajax@comset.net

The given operation is devoted to presentation the semiempirical mathematical model of the heat chemical reactor (TCR) and discussion of main legitimacies, determined during experimental research of the first TCR sample. According to the "Ajax" concept, TCR, installed in heat-stressed constructional units of the hypersounic aircraft (HA), play a role the main component of the system of active thermal protection and simultaneously will carry out modification of initial power bearer (air kerosene), supplying to combustion camera a "conventin"- mixture of initial fuel with synthesis-gas. The most important part, where usage of active thermal protection is necessary, is a supersonic camera of combustion of the HA engine. At any function of TCR (cooling and/or modification of fuel) usage of TCR allows to return a part of energy earlier leaving in thermal losses. Given below semiempirical methods will allow, for our opinion, to make the important steps in direction of creation of engineering methods of calculation and optimization of TCR.

The complete task of interpretation obtained in operation [1] of the experimental data on heat-mass transfer in model TCR includes solution of the self-coordinating task under description of the temperature mode in an internal pipe, heat-mass transfer in a wall of a pipe and heat-mass transfer a in the TCR, and solution for everyone of them these areas is a boundary condition for adjacent area and all solutions become correlated. But in a real situation heating of TCR will be made at expense of energy of braking of semi-infinite air stream, and registration of interference of stream and TCR will be carried out in absolutely another way. Therefore it is expedient to develop such mathematical model, in which the effect of thermal stream on TCR is simulated by definition of some function of a thermal source q (X, Y, Z), which generally depends on coordinates X, Y, Z and time t . For the stationary task, which will be considered in the given work, such approach is quite justified. The allocation of thermal sources on length of TCR (by an X axis) is taken as an exponential function $q(X)=q_0\exp(-X/X_0)$, as the exponential dependence is most widespread in a nature, but all obtained formulas easily received also for any other law of allocation of thermal sources (for example, linear).

The approximation of incompressible gas (liquid), density of gas mixture and main parameters describing heat-mass transfer considered constant are used. The independence of thermal conduction coefficients, thermal capacity and diffusion from coordinates is not for us a mandatory limitation, however, as it will be seen of further consideration, the error which is

brought in by such approximation, is much less than an error of experiment.

In the real TCR the process of steam conversion occurring on a reactor wall or on specially organized carrier inside of reactor , is realized with heterogeneous catalyst, i.e. by its nature it is a surface process but not volumetric. Values and allocation of temperature and density of gas mixture in TCR volume are interested for us only in that degree, in which they influence on appropriate surface characteristics. Many volumetric characteristics (for example, the hydraulic resistance) in general are difficult to be accounted and, most likely, will require only experimental definition. Therefore an approximation in which the functions interesting for us depend only on one X coordinate - distance from entrance to TCR will be considered below. Thus the choice of some parameters will be made so as though we make consideration of a complete three-dimensional situation, therefore such approximation is possible to consider quasimonodimension. Further after setting the task the simple formulas for calculating of allocation of temperature and density of components of gas mixture are obtained, the estimation of input parameters of the task is made, comparison to experiment is carried out. After the serviceability of the obtained mathematical methods is shown, it is possible to restore with their help those dependences, which for various reasons were not obtained experimentally in complete size.

Generally system of the stationary equations of heat-mass transfer in three-dimensional TCR looks like:

$$\frac{\lambda}{c_p\rho}\nabla^2 T - \vec{w}\nabla T + \frac{DQ^*}{c_p}\nabla^2\rho_0 - \frac{h_0 - h_\Sigma}{c_p\rho}I_0 + \frac{q}{c_p\rho} = 0, \quad (1)$$

$$D\nabla^2\rho_0 - \vec{w}\nabla\rho_0 + \frac{k_T D}{T}\nabla^2 T - \frac{I_0}{\rho} = 0 \quad (2)$$

The following denotations are entered:

$\vec{w}$ - speed of movement of gas mixture in TCR, [m/s];

λ -coefficient of a thermal conduction, [Wt / (m K)];

ρ -density, [kg / m^3];

c_p - specific thermal capacity at constant pressure [G / (kg K)];

D - coefficient of mutual diffusion, [m\s^2];

Q^*- specific heat of the isothermal process [G/kg];

h_0 and h_Σ - specific methane and second component entalpy of mixture respectfully [G/kg];

I_0 - power of a weight methane source (in the equations it enters with "-", that means decrease of content of methane during reactions of steam conversion), [kg / (м^{3}s)];

q - volumetric power of a heat source [Wt/м3];

k_T- heatdiffusion coefficient.

The relative concentration of methane and second component of mixture by a usual mean are connected to appropriate densities r0 and r_Σ

$$\rho_0 = \frac{r_0}{(r_0 + r_\Sigma)} = \frac{r_0}{\rho}, \quad (3)$$

$$\rho_\Sigma = \frac{r_\Sigma}{(r_0 + r_\Sigma)} = \frac{r_\Sigma}{\rho}, \quad (4)$$

and $\rho_0 + \rho_\Sigma = 1$.

In the equation (1) a coefficient at V2T for an interested range of speeds $w \geq 1$ m/s appears very small, so as at solving of heat-mass transfer problem in the moving medium this addend is usually omited [3]. Thus, passing to an one-dimension case and entering a dimensionless space variable

$$x = \frac{X}{L}, \quad (5)$$

where L – length of TCR, we receive a set of equations

$$\frac{w}{L}\cdot\frac{dT}{dx} + \left(\frac{c_\Sigma}{c_p\rho}T - \frac{Q^*}{c_p\rho}\right)\cdot I_0 - \frac{q}{c_p\rho} - \frac{w}{L}\cdot\frac{Q^*}{c_p}\cdot\frac{d\rho_0}{dx} = 0, \quad (6)$$

$$\frac{1}{L^2}\cdot\frac{d^2\rho_0}{dx^2}-\frac{w}{DL}\cdot\frac{d\rho_0}{dx}+$$

$$+\frac{k_T}{T}\cdot\frac{1}{L^2}\cdot\frac{d^2T}{dx^2}-\frac{I_0}{D\rho}=0$$

If in zero approximation to neglect by the d^2T/dx^2 and in second equations (6), the solution of this equation necessary to us gives linear allocation of methane concentration by the length of TCR:

$$\rho_0(x)=\overline{\rho}_0-\omega x\ , \qquad (7)$$

Input data of our task are expenditure of methane g0 and expenditure of water vapor, which on entrance of TCR is a unique component of mixture $g_0=g_1$ (kg / s). Density of methane in this case is calculated under the formula

$$r_o=\frac{g_o L}{wV}, \qquad (8)$$

where V – volume of TCR, density of water vapor

$$r_1=\frac{g_1 L}{wV}, \qquad (9)$$

that gives for complete density

$$\rho=r_o+r_1=\frac{g_o+g_1}{wV}L. \qquad (10)$$

Density p is saved constant on all length of TCR. Relative weight concentration of mixture components on entrance to TCR (at $x=0$)

$$\overline{\rho}_i=\frac{r_i}{r}=\frac{g_i}{g_o+g_1},\ i=1;2. \qquad (11)$$

(All values, which value are taken at $x=0$, in further will be designated by lining at the top).

The parameter is equal to the ratio of quantity of substance, which can leave as a result of a steam conversion reaction (for 1s of 1 m^3) to appropriate quantity of substance had come to entrance of TCR.

$$\omega=\frac{I_0 V}{g_0+g_1}=\frac{I_0}{\frac{g_0+g_1}{V}}\ . \qquad (12)$$

At derivation of the formulas the obvious equalities are used

$$\chi(1)=1-\frac{\rho_0(1)}{\overline{\rho}_0}, \qquad (13)$$

$$\rho_0(1)=\overline{\rho}_0[1-\chi(1)]$$

where $\chi(x)$ - degree of methane conversion on distance of x.

The calculation of relative weight concentration of other components will be done under the formulas

$$\rho_1(x)=\overline{\rho}_1-\frac{M_1}{M_0}\frac{2k+1}{k+1}[\overline{\rho}_0-\rho_0(x)],$$

$$\rho_2(x)=\frac{M_2}{M_0}\frac{1}{k+1}[\overline{\rho}_0-\rho_0(x)], \qquad (14)$$

$$\rho_3(x)=\frac{M_3}{M_0}\frac{k}{k+1}[\overline{\rho}_0-\rho_0(x)],$$

$$\rho_4(x)=\frac{M_4}{M_0}\frac{4k+3}{k+1}[\overline{\rho}_0-\rho_0(x)]\gamma_H,$$

where index «1» is fixed for H_2O, «2» for CO, «3» for CO_2 and «4» for H_2. These formulas are obtained taking into account a real situation of a relation for hydrogen are broken (that is connected, apparently, to high diffusion coefficient of hydrogen), therefore in the last of formulas (14) correction factor H is entered. The coefficient k shows, what contribution to creation of total concentration of components gives the response with obtaining of carbonic gas in relation to the contribution of reaction with derivation of carbon oxide. The values k, I_0, H are given by the empirical formulas

$$k\approx 1+5.06(z_0-z)(\frac{w}{w_0}-1)(\frac{w}{w_1}-1),$$

$$I_0\approx 0.83+2.4(z_0-z)(\frac{w}{w_0}-1),$$

$$\gamma_H\approx 8z^{3/2}/15, \qquad (15)$$

where $z=g0/g1$, $z0=0.791$, $w0=5.75$ m/s, $w1=6.61$ m/s. Derivative from relative weight concentration

$$\frac{d\rho_0(x)}{dx}=-\omega \qquad (16)$$

allows to calculate the last addend in the first of equations (6), describing allocation of temperature on length of TCR. The solution of this simple equation turns out by a standard method if consider that on input of TCR

($x=0$) temperature was equal to temperature To coming on input of TCR of gas mixture. Obtained at this condition allocation of temperature on the length of TCR is given by expression

$$T(x)=\left(T_0-\frac{Q_0}{H-\varepsilon}\right)e^{-Hx}+\frac{Q_0}{H-\varepsilon}e^{-\varepsilon x},\quad(17)$$

where constants Q_0 and H

$$Q_0=\frac{q_0 L}{wc_P\rho},\ \mathrm{H}=\frac{\mathrm{c}_\Sigma LI_0}{\mathrm{w}\rho\cdot\mathrm{c}_\mathrm{p}}.\quad(18)$$

Thus, at zero approximation the allocations of concentration and temperature on length of TCR are obtained. The further specification is easy to make having substituted the obtained allocation of temperature (17) in the second equation (6) for more exact definition of methane concentration and after this of all other components.

References.

1. Отчет НИПГС за 1998 г. С._Петербург, 1999 г., 58 с.
2. Лыков А.В., Михайлов Ю.А. Теория тепло и массообмена, М., 1963 г.
3. Ландау Л.Д., Лифшиц Е.М. Гидродинамика, М., 1980 г.
4. Лыков А.В. Сопряженные задачи конвективного теплообмена, М., 1971г.

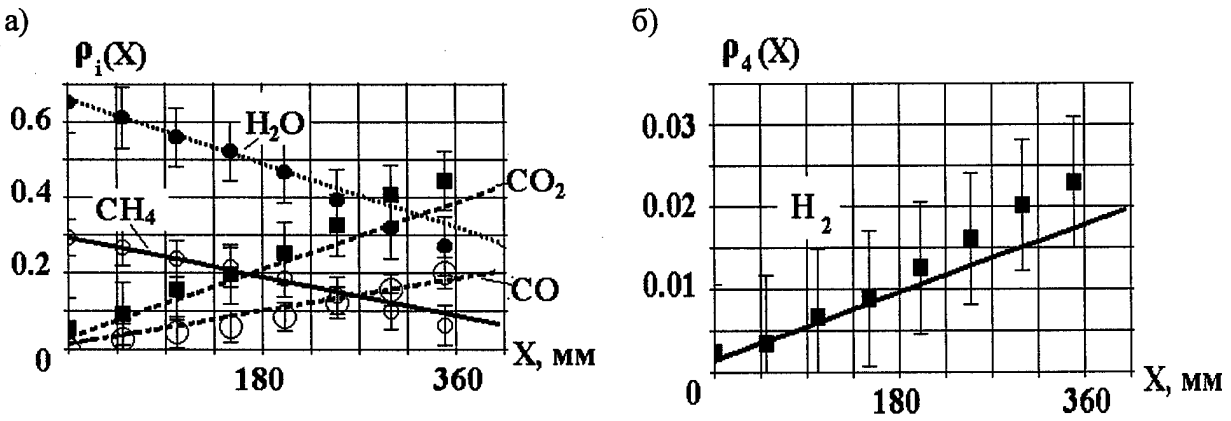

Fig. 1. Allocation of concentration CH_4, H_2O vapor, CO and carbonic gas and allocation of concentration of hydrogen (б) on the length of TXP at speed of gas mixture 5 м/с. Points are the experimentally measured concentration on an exit of TXP, z=0.446.

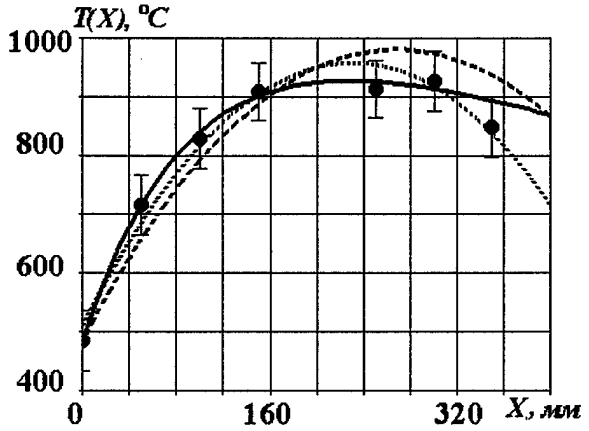

Fig. 2. Allocation of temperature on the length of TXP at speed of gas mixture 5 м/с. Points - experimental data, continuous curve - calculation at the exponential law of allocation of heat sources, dotted line – account at the linear law of allocation of heat sources, dot curve - result of approximating of the experimental data by a square-law polynomial, =0.446.

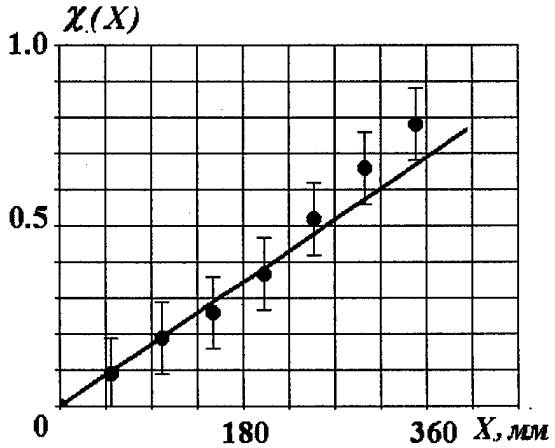

Fig. 3. Allocation of a degree of conversion methane on the length of TXP. A curve - account, points - experimental data.

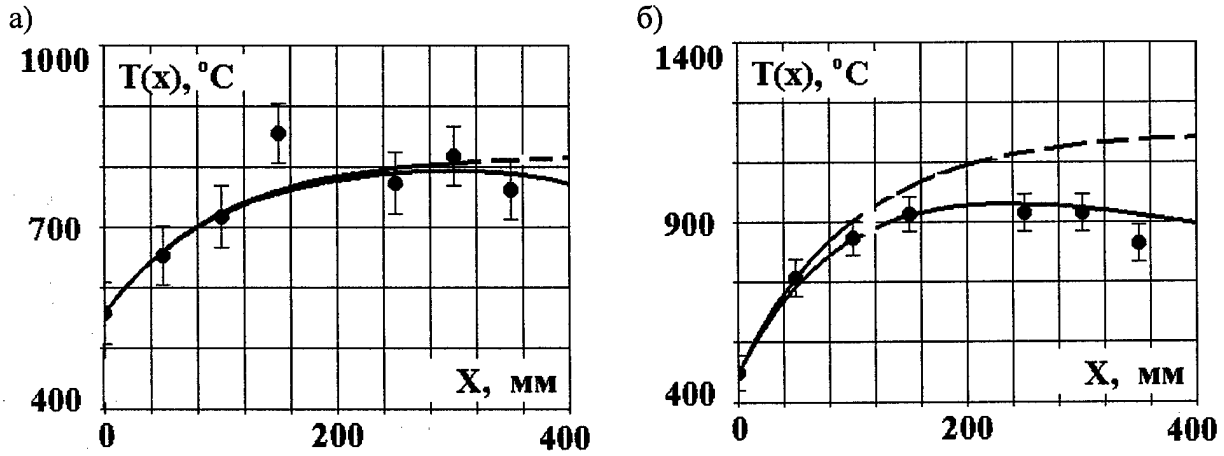

Fig. 4. Allocation of temperature on the length of TXP at speed of gas mixture 20 м/с (а) and 1 м/с (б). Points – experimental data, continuous curve - calculation at the exponential law of allocation of heat sources, dotted line - calculation at absence of reaction of steam conversion.

PROMOTION OF KEROSENE COMBUSTION IN A HIGH ENTHALPY SUPERSONIC FLOW

Tretyakov P.K. and Bruno C.*

Institute of Theoretical and Applied Mechanics, Siberian Division Russian Academy of Sciences, 630090, Novosibirsk, Russia
* University of Rome, Rome, Italy

Doubts in the possibility of using kerosene as a fuel for supersonic ramjet engines stem from difficulties arising in flame stabilization and organization of its effective combustion over the entire range of ramjet parameters and its cooling capacity insufficient for protection of thermally stressed components of the engine and aircraft.

Part of the problems involving the combustion process can be solved by realizing the two-stage combustion scheme [1], where the first combustion (in the inner loop, the gas generator) proceeds with a deficient of the oxidant (equivalence ratio $\alpha=1/\varphi \approx 0.35$). As the flight Mach number increases, the fraction of kerosene being fed into the internal contour may also decrease, and, at high air temperatures when the conditions for ignition improve, the gas generator is used as a pilot device.

The above difficulties with kerosene can be avoided (see the concept "AJAX" [2]) by using part of the kerosene (up to ~20%) for cooling as its decomposes thermally by means of catalysts. This method raises the cooling resources of the aircraft since, the conversion process absorbs heat and the gas-synthesis (converted gas), which contain hydrogen (70% by volume), may improve the ignition characteristics and further stabilize the flame in the scramjet chamber. Hydrogen is also known as an additive by means of which the kerosene combustion efficiency can be improved.

Characteristics of kerosene combustion can be also improved by admixing to it some other additives. Nitrates of organic compounds are examples of promotor additives. At the Institute of Theoretical and Applied Mechanics, Siberian Division of the Russian Academy of Sciences, a cycle of experimental studies has been performed on the ignition delay period of several types of kerosene (T-A, T-15, KO-20) in their pure form, as well as mixed with fatty alcohol nitrates (FAN), cyclohexyl nitrates (CHN) and isopropyl nitrate (IPN). The experiments were carried out in a shock tube and in a constant-volume bomb [4, 5]. It has been established that the promotor effect increases as the temperature is lowered and the percent content of the promotor in the fuel is raised. At high initial temperatures (>1000 K), the ignition delay period for the fuel becomes shorter, and the promotors less effective.

Similar results have been also obtained in studies of self-ignition of methane-air mixtures and $CH_4/O_2/Ar$ mixtures with added hydrogen peroxide (H_2O_2 + 5 ÷ 10% CH_4) [6]. As follows from Fig. 1, the promotor effect is observed in the temperature range 1100 ÷ 2000K and is explained by the catalythic effect due to additives at individual stages of chemical reactions. With increased initial mixture

temperature, the diminishing effect of H_2O on the ignition delay period vanishes.

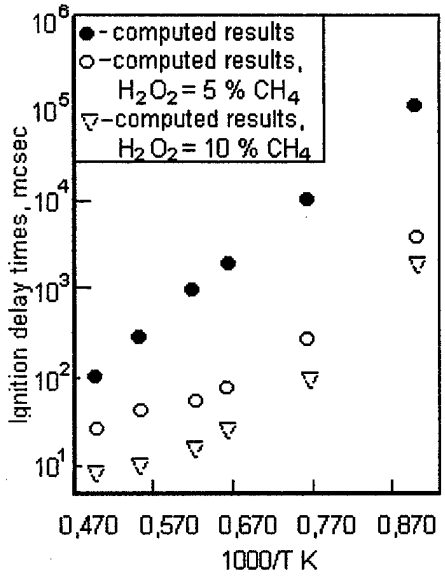

Fig.1. Effect of H_2O_2 on the ignition delay time for methane-air mixtures (P_0=1 atm., φ=0.5)

However, the attempt to experimentally realize the combustion of mixtures promoted with the above-indicated additives (FAT and CHN in concentrations up to 30%) in a planar channel was a failure [5]. The air stream heated up to 1200 ÷ 1800 K (see Fig.2) entered a planar channel with dimensions 40×60×545 mm through a nozzle with an exit flow area 40×40 mm (M_0= 1.7). Kerosene with admixed additives was injected behind a step (20×40 mm) through a fuel screw-centrifugal atomizer. The negative result obtained is presumably caused by short time of fuel residence in the channel, insufficient for pre-flame processes to develop.

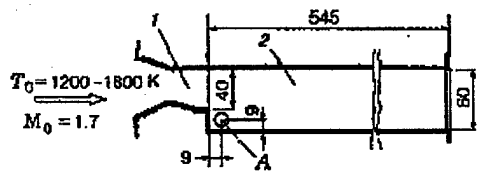

Fig.2. Scheme of the channel: 1 – nozzle; 2 – quartz windows; A – fuel atomizer

The controlling role of pre-flame process, especially, that of evaporation or mixing can be illustrated by the experiments in which the fuel injection place was transferred into the subsonic part of the nozzle.

The residence time of kerosene aerosol droplets in the nozzle turned out to be too short to ensure their complete evaporation and the onset of pre-flame processes (τ= 6 ÷ 7 msec). The ignition of kerosene and its stable burning in the channel was observed at air temperatures as low as T_0 = 1200K.

Cutting the time of mixture-preparation is a most important problem in using liquid fuels. In [7], injection of a gas-liquid mixture was suggested. It has been experimentally shown that for the mass fraction of gas 1 to 3%, the penetration depth of the fuel jet into the supersonic stream substantially increases, the spray cone widens and the drop diameter decreases. All the above factors act to facilitate the mixture formation process and the development of the combustion. In [8], characteristics of the continuous detonation-type combustion were substantially improved by injection of kerosene-air foam.

A certain pre-flame preparation of the kerosene fuel can be achieved by its heating at high pressure prior to the injection into the air stream. The level of heating may be enough for it to start decomposing. For this purpose, we have used a resistive heater. Kerosene was fed into the heater through a stainless steel tube, which served simultaneously as a heating element. The time of kerosene stay in the heater was 0,5 ÷ 2 sec. The kerosene temperature could be varied smoothly by adjusting the heater's consumed power. The scheme of experiments on organizing fuel combustion in a free air jet at M_0 = 2.2, T_0 = 1500 ÷ 2300K and P_0 = 0.5 ÷ 0,9 MPa is shown in Fig. 3. For kerosene temperatures below 1000 K, no self-ignition was observed up to air temperature 2300K. As follows from Fig. 3, the mode with simultaneous injection of steam and kerosene was also possible. Stable ignition of the fuel mixture was observed already at T_0=1500K and P_0=0.56 MPa (the temperature of the heating element was 1120 K and pressure

3 MPa). With gradual displacement of water with kerosene, the flame adjusts and, finally, gets quenched (see Fig. 3). The observed ignition and stable burning can be attributed to conversion of kerosene in the presence of steam. However, no quantitative parameters in this case have been determined.

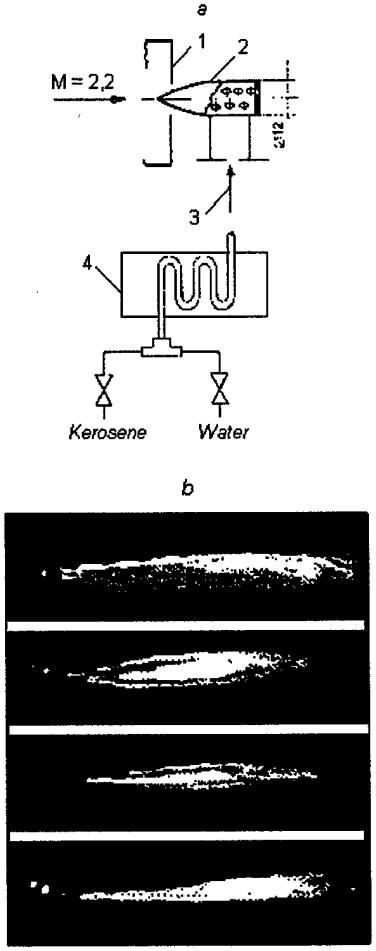

Fig.3. Scheme of the experiments with the combustion of kerosene-overheat products (a) and photographs of flames (b): T_0=2300 K, P_0=0.94 MPa,
kerosene mass-flow rate G_K=17.0 g/sec,
kerosene temperature 920 K;
1 – nozzle; 2 – injector; 3 – fuel feed; 4 – resistive heater

As stated above, one of the ways for intensifying the combustion of kerosene may be combined fuel injection with a chemically more active gas, for instance, hydrogen. The scheme of this experiment is shown in Fig. 4. Hydrogen was injected through three slit pylons. At the inlet into the fuel feed section, a 8,5 mm ledge was provided, whose presence compensated the blockage of the flow area with pylons and aided in stabilizing flame. Kerosene was injected through low-pressure centrifugal atomizers with an aerodynamic shield, The latter was intended to increase the range of the liquid jet and ensure more vigorous mixing. To the constant-area piece, a 264 mm-long conical section was attached. In part of the runs, to the conical section, another constant-area section was adjusted. The hydrogen/kerosene mass ratio, $G_H/G_K \approx 0{,}22$, was sufficient for stable ignition and maintaining combustion of the kerosine. Data on the measured static pressure are shown in Fig.4. The total air-excess coefficient was α=1,0. In the channel with dismounted cylindrical section (diffuser), a pseudo-shock forms in its conic part. During the combustion, the pseudo-shock moves upstream and becomes fixed at the step (see curve 1 in Fig. 4). An analysis of the pressure profiles shows that in the constant-area section, a transonic flow develops in the portion with the constant cross section, with subsequent acceleration of the flow at the beginning of the expanding section and after-burning in the newly formed pseudo-shock flow.

With the cylindrical diffuser installed, the pressure in the forechamber is sufficient to produce a supersonic flow throughout the entire channel when there is no fuel feed (see curve 4 in Fig. 4), and the pressure profile during combustion (curve 2) is typical of such configurations. The estimated extent of burnup is $\eta \approx 0.6 - 0.8$. Another arrangement of hydrogen and kerosene injectors, one after the other, has a significant effect on the combustion process. In this case, the ignition spreads over a longer period and the combustion begins in the diverging section.

When analyzing these results on kerosene combustion in a free jet and in a channel, it should be noted that combustion onsets in the channel at lower initial air flow temperatures. This fact is probably points out to the essential role of wave structures.

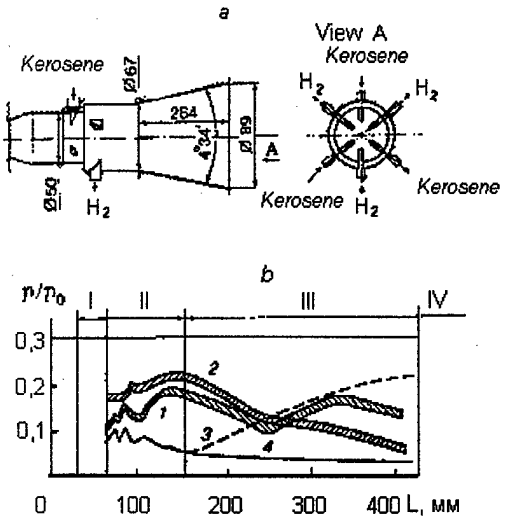

Fig.4. Scheme of the channel (a) and results of runs (b) with kerosene and hydrogen injection (M_0=2.2, P_0=0.7 MPa): I – kerosene feed section, II – hydrogen feed section, III – conical section, IV – cylindrical section (diffuser); test conditions: for experiments with combustion: 1 – without diffuser, T_0=1870÷1900K; 2 – with diffuser, T_0=1970÷2000K; for experiments without combustion: 3 – without diffuser, 4 – with diffuser

Regarding the difficulties faced in organization of effective kerosene combustion, we should note the main shortcoming, its long combustion zone compared to hydrogen for identical initial conditions. The average heat-release rate of kerosene is far less than that of hydrogen, especially in the range of relatively low (for a scramjet) initial temperatures (T_0 = 1700K). Assuming that it is the pseudo-shock mechanism of combustion that is operative [9], we can estimate the required combustion-chamber length for hydrogen, kerosene, and the kerosene/ synthesis-gas mixture. In these calculations, the following initial conditions were adopted: $M_н$ = 2.5; T_0= 1800 K; α = 1.0; we also assumed that the mass fraction of the converted gas in the mixture amounts to 30% of its whole mass, and the volume fraction of hydrogen in the conversion products runs into 70%. The combustion was assumed to proceed by two stages: first, hydrogen burns, and then kerosene does. Effect due to other admixed gases was ignored. An axisymmetrical combustion chamber was considered, which was composed of two sections, a constant-area one (having the length $\Delta l_1 = \Delta l / D$, where D is its diameter) and a diverging section having a length Δl_2. Calculation results are shown in Fig. 5 and listed in the table (here δ°is the full divergence angle of the chamber, and σ is the total-pressure recovery coefficient). As calculations show, the required length of the chamber for kerosene is approximately twice as large as that for hydrogen. The presence of hydrogen in the conversion products causes the chamber length to decrease by ~ 16%. However, the total-pressure losses change only slightly.

Fuel	$\Delta \bar{l}_1 + \Delta \bar{l}_2$	δ°	σ
Hydrogen	6.0	1.30	0.415
Kerosene	11.4	0.75	0.407
Kerosene + synthesis-gas	9.6	0.88	0.410

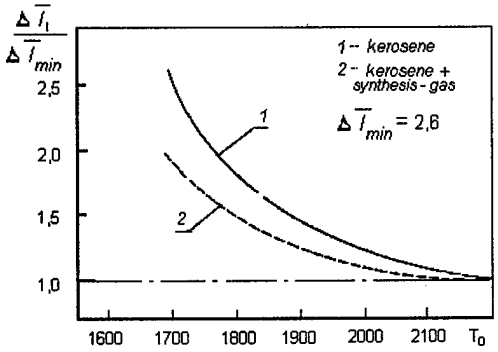

Fig.5. Length of the combustion zone in a channel with F=Const,

In conclusion, we may argue that the preliminary preparation of the fuel-air mixture has a pronounced effect on the efficiency of kerosene combustion. Not all the methods for intensification of combustion have been adequately studied. Initiation of chemical reactions prior to injection of promotor additives results in an improved

kerosene combustion in the temperature range T_0=1200 ÷ 1800K.

References.

1. Voloshchenko O.V., Meshcheryakov E.A., Ostras' V.N., and Sermanov V.N., Analysis of gas generation and conversion of hydrocarbon fuels in a two-mode scramjet, Proceedings of TsIAM, №2572, 1995. P. 3–19.
2. Gurianov E.P., Harsha P.T., AJAX, New Directions in Hypersonic Technology. AIAA Paper 96–4609.
3. Annushkin Yu.M. and Maslov G.F., Combustion efficiency of hydrogen-kerosene fuel in a ramjet channel. Combustion, Explosion and Shock Waves, Vol. 21, № 3, 1985. P. 30–32.
4. Buzukov A.A., Promotor effect of alkyl nitrates on self-ignition of a kerosene/air mixture. Combustion, Explosion and Shock Waves, 1994. Vol.30, № 3, P. 12–20.
5. Tretyakov P.K. and Bruno C., Combustion of kerosene in a supersonic atream, Combustion, Explosion and Shock Waves, 1999, Vol. 35, № 3, P. 245-251.
6. Golovitchev V.I., Pilia M.L., and Bruno C. Auto-ignition of methane mixtures: The effect of hydrogen peroxide // I. Propulsion and Power. 1996. Vol. 12, № 4. P. 699-707.
7. Avrashkov V., Baranovsky S., and Levin V., Gasdynamic features of supersonic kerosene combustion. AIAA, 90-5268, P.8.
8. Bykovsky F.A., Continuous detonation in annular chambers, Theses of Doctoral Dissertation, Institute of Hydrodynamics, SD RAS, Novosibirsk, 2000.
9. Tretyakov P.K. Pseudo-shock combustion, Combustion, Explosion and Shock Waves, 1993. Vol. 29, № 6, P. 33–38.

SUPERSONIC COMBUSTION ORGANIZING IN DUCT WITH PRELIMINARY THERMO - CHEMICAL CONVERSION OF HYDROCARBON FUEL.

Voloshchenko O.V., Meshcheryakov E.A., Ostras V.N.,
Sermanov V.N., Sabelnikov V.A..

Central Aerohydrodynamic Institute (TsAGI) named after Prof. N.E. Zhukovsky
TsAGI, Zhukovsky, Moscow Region, Russia

Many types of propellant being complex hydrocarbon compounds, can be chemically transformed with the heat absorption (endothermic conversion) and forming more simple substances (H_2, CO, etc). Application of such conversion on a aircraft at high flight supersonic spuds opens additional cooling possibility of airframe and engine structural elements. Thus, the cooling capability of a fuel will be enhanced considerably. Fuel serviceability also increases due to heat absorption under conversion [1]. In consequence of fuel transformation into more reactive gaseous substances fuel burning stability and reactivity rise. The principle of chemical heat regeneration based on endothermic conversion of hydrocarbons is used on some types of hypersonic aircraft now [2].

Computational analysis of conversion of enriched kerosene-air mixture with water additions has been performed for an autonomy gasgenerator. In the first example if was assumed that the process ran by the next scheme - partial kerosene burning up to a full consumption of an oxidizer and pyrolysis of residual excess fuel. Analysis shows that as equivalence ratio β_{gg} decreases in the gasgenerator the content of molecular hydrogen H_2 and carbon oxide CO highly reduces. If water is not supplied into the gasgenerator optimal operation regime is realised without soot forming at $1/\rho_{gg} = 0.35$-0.4. This regime corresponds to following process characteristics: decomposition products temperature is $T = 1300$-1600 K, volume content of H_2 - 20-22%, CO - 22-24%, CH_4 - 0.5%.

The most output of free hydrogen occurs under operation of the gasgenerator in regime of direct thermal conversion of kerosene - water mixture. Process goes with the intensive soot generation. It is eliminated with feed of considerable water fraction (55-60% by mass) into the gasgenerator at temperature $T \geq 1200$ K. In these conditions output of H_2 reaches 60-65%, CO - 30-32%, CH_4 - 4% (by volume). Increasing the water feed in excess of pointed value is not advisable because it leads to an abrupt drop of H_2 and CO in conversion products.

To verify some calculation results of kerosene pyrolisis experiments were conducted at a dual - circuit ramjet - type model combustor. Tests were run at following conditions in the facility heater: $P_t \leq 4.2$ MPa, $T_t = 1150$-1350 K, corresponding to flight Mach number $M_\infty = 4.8$-5.3 (for more details, see [3]).

Experiments show that inanition and combustion of the fuel in the main combustor occur only with availability of kerosene thermo-pyrolysis in the inner circuit. In this regard, the best conditions provide regimes with $1/\beta_{gg} = 0.3$-0.4 and $T_t \geq 1250$ K. It is in accordance with the computational analysis.

Reliable stabilization and intensive combustion take place in the combustor. Herewith, there arise a pseudoshock - type flow, located upstream from the place of kerosene decomposition product supply. Combustion efficiency of kerosene decomposition products at the end of the combustor with a length L=370 mm, defined by one - dimensional theory according to pressure, is equal to $\eta = 0.74$. As combustor length increases up to $L = 650$ mm fuel combustion efficiency rises up to 0.992-0.95.

Performed computational analysis and tests showed the possibility and efficiency of endothermic conversion processes use in a two-stage scheme of hydrocarbon fuel burning in ramjets. In this respect, the water conversion of hydrocarbons can provide the most possibilities.

References

1. Favorsky O.N., Kurziner P.U. Teplophyzika vysokikh temperatur, v.28, No 4, 1990, pp. 793-803.
2. Petley D.H., Jones S.C. AIAA Paper 90-3284, 1990.
3. Voloshchenko O.V., Meshcheryakov E.A., Ostras B.N., Sermanov V.N. Trudy TsAGY, vyp. 2572, 1995.

ADVANCED RAMJETS USING THERMOCHEMICAL CONVERSION OF LIQUID HYDROCARBON FUEL

Pavlyukov E.V., Piotrovich E.V., Ostras V.N., Ruch'ev V.M., Sermanov V.N., Starukhin V.P., Chevagin A.F.

Central Aerohydrodynamic Institute named after professor N.E. Zhukovsky
1, Zhukovsky street, Zhukovsky, Moscow region, Russia

Successful solution of a hypersonic advanced vehicle creation problem is defined in many respects by problems of effective power plants developing on the basis of ramjets, integrated with a vehicle airframe, capable to operate using a liquid hydrocarbon fuel over a wide range of Mach numbers M=3…6.

Preliminary computational studies of the advanced multi-mode ramjet showed that a qualitative improvement of power plants, based on ramjets, consuming kerosene, could be provided by radically new working process implementing in a combustor by means of preliminary fuel preparation. It is known that considerable internal losses of a potential serviceability of the hydrocarbon fuel are inevitable at its direct oxidizing due to combustion reaction nonreversibility. The multi-stage process is advantageous from the viewpoint of thermodynamics: fuel conversion (i.e., its preliminary heating and decomposition into high reactive components), and then decomposition products burning in the main combustor. The hydrocarbon fuel conversion can be realized in the special ramjet reactor, located immediately in the main ramjet combustor, consisting of two circuits. Fuel part burning is performed in the first circuit of the reactor. Released heat is used for heating, evaporation and decomposition of the remained fuel part in the second circuit. As a result, combustible gases, supplied into the main combustor, contain high reactive components (H, H_2, CO, C_2H_4, …) with high temperature T=1300…1500K. It favors the combustion process. Combustion efficiency increase in the main combustor results in the necessity to change its configuration and to use diffuser-type chambers in order to prevent thermal choking. Heat balance computations show that to realize such reactor scheme it is sufficiently to supply into the first circuit up to 10…15% of the total fuel, supplied into the combustor. Combustion efficiency in this circuit is comparatively small ~ 0,7 at sufficiently high speed $\lambda \cong 0{,}5$. Herewith, cross dimensions of the first circuit of the reactor must not exceed 15% of cross dimensions of the main combustor. Optimum total air-fuel ratio in the reactor is 0,3. Herewith, a content of high reactive components, going from the second circuit of the reactor, is maximum. The computed value of the induction time of combustible gases at the reactor exit reaches the value of $\tau = 10^{-5}$ sec. It is nearly less by two orders than the induction time of liquid kerosene. The hydrocarbon fuel conversion before fuel burning solves problems of igniting and combustion stabilization at substantially high speeds in the combustor than in existing ramjets with the traditional scheme of combustion implementing. So, in

this case, components, supplied into the chamber, more tend to combustion, and their time of ignition delay is less by two orders.

Preliminary computational studies show that such combustion process implementing provides the possibility to substantially decrease the overall chamber dimensions with maintaining high fuel combustion efficiency and thrust-economic ramjet characteristics. Also, the preliminary preparation (conversion) of the liquid hydrocarbon fuel provides possibility of the multi-mode ramjet combustor. In turn, it permits the vehicle flight over a wide range of Mach numbers M and altitudes.

УДК 536.24: 665.642

THE COMPARATIVE STUDY COMBUSTION PRODUCTS OF THERMOCHEMICAL DECOMPOSED LIQUID HYDROCARBON FUEL IN FLOODED JET

Authors:

Ianovskiy L.S., Sapgir G.B., Sverdlov E.D., Baikov A.V., Ivanov V.F.

CIAM, SNC, Moscow, RF.

One of the most actual development trends of modern aviation is creation of the hypersonic flight vehicles (M ~ 5÷8) with engines working on liquid hydrocarbon fuel. Traditionally, application of endothermic hydrocarbon fuels is considered to be solution of this problem. The endothermic fuels being decomposed under heat flux are capable to be refrigerant. Cooling capacity of the endothermic fuels in count on unit of heating value is comparable with the cooling capacity of liquid hydrogen.

Key tasks are embodying of endothermic effect and organizations of combustion process. Embodying of endothermic effect requires organization of complicated process of thermochemical decomposition of liquid fuel on the flight vehicle. Organization of combustion process specifies a problem how to use the power capabilities of gaseous decomposition products of the endothermic fuel in the engine.

Reaction time of combustion is very important problem for the second task. The small time of combustion reaction is necessary requirement for high completeness of combustion into small combustion chamber. It is clear that maximum reaction velocity results in minimum reaction time.

The theory of chain reactions [1] shows that the reactions which have the greatest difference of kinetic factors of reactions of bifurcation and abruption of chains are valid maximum velocity. According to this theory, velocity of reaction - w can be given by

$$w = a \times n$$

where a - is kinetic factor and n - is concentration of radicals, calling by chain process. Evolution of n in process of the reaction is given by the following differential equation:

$$\frac{dn}{dt} = n_0 + (f - g) \times n$$

This equation has exact solution

$$n = \frac{n_0}{f - g} \times \left(e^{(f-g)\times t} - 1\right)$$

where n_0 - is concentration of radicals arised in process of primary monomolecular reaction when the chain reaction did not start yet;

f,g - kinetic factors of reaction of the bifurcation and abruption of chains.

The burning reaction is appeared when threshold value of the reaction velocity will be reached. When $w > w_t$, the heat generation in a process of reaction results in

thermal, light and acoustic effects. The time for approaching this threshold value can be determined as:

$$t_i \approx \frac{1}{f-g} \times \ln \frac{w_t (f-g)}{a \cdot n_0}$$

Parameter t_i – it is period of an induction or delay of ignition [2].

Thus the period of induction is the important quality index permitting to compare velocities of reaction for different fuels. Different methods for measurement of period of induction in engineering have been proposed and developed. However method of a «hanging» flame receives the application for determination of comparative changes of combustion velocity for various gaseous fuels.

Method for determination of normal flame propagation using flame of the burner has been suggested in XIX century. Mixture of air and some fuel is supplied in the burner. As a rule, the combustion starts near to the end of the burner [3]. Typical flame propagation rates obtained by this method are shown in Table 1.

If clean gaseous fuel flows out from burner nozzle with enough high velocity, then the flame of burning fuel displaces on some distance from end of the burner.

Such kind of flame has titled by diffusive or «hanging» flame ([4,5]). Special researches show that the phenomenon of the «hanging flame» depends on kinetics of chemical reactions. Decreasing of induction period requires increasing of fuel rate in the spray to obtain fixed location of the flame above shear of the burner. Photo of the typical experimental burner and flame is shown on Fig. 1.

Scheme of the burner used in this experiment is shown on Fig. 2. Main part of the burner is the gas receiver for gas outflows in atmosphere. The burner is equipped by a set of replaceable nozzles with diameters 4, 6 and 8 mm for control of the gas flow rate. Oxygen-methane igniter is used for the gas firing. The igniter was actuated during 3÷5 sec in the start mode. After reaching stable gas combustion implied from the receiver, the igniter is turned off. The gas consumption is changed by pressure variation in the gas receiver. Pressure in the receiver is measured by fluid differential pressure gauge.

The height of flame lift-off depends on the outlet velocity of gas jet from the receiver. This value is changed by pressure variation in the receiver. Videoshooting of combustion process is performed during experiments.

The experiments with the torch device shown on Fig. 2 are performed with different gaseous fuels.

Experimental facility shown on Fig. 3 is intended for operating with gaseous fuels. The facility has two lines: the left-hand line is intended for generation of decomposition yields of the endothermic fuel and right-hand line is used for operating with usual kinds of the gaseous fuels (methane and methane-hydrogen mixture).

The left-hand line includes a heat exchanger-reactor (1) for decomposition of liquid fuel. The reactor is a special design. The hot air flow comes into heating line of the reactor. The fuel is decomposed under heat of this flow. Electrical heater (2) is intended for air heating.

High-pressure stand system makes it possible to feed electrical heater by air. In case of need, the heat exchanger-reactor can be used for heating of methane and other gases or to use it for evaporation of liquid fuel. It enabled to perform experiments with combustion of vapors of endothermic fuel without its decomposition, and with methane heated in the heat exchanger up to high temperature. The outlet velocity from the burner nozzle as a function of flame lift-off height is fixed in these experiments. Typical function are relations are shown on Fig. 4. In follows, these relations are redrawn on the general diagram for the comparative analysis. This diagram is represented on Fig. 5.

Fig. 5 shows that from point of view of minimum induction period the most effective fuels are products of thermal decomposition of liquid fuel. It is easily explained by analyzing of their composition. Chemical analysis (Table 2) shows that the decomposition products have not only high

concentration of ethylene and hydrogen (i.e. gases with increased velocity of normal combustion), but also radicals arised at thermal decomposition of liquid fuel. The chain mechanism of reaction generates formation radicals [1,6]. These radicals intensify the process of combustion in the combustion domain and decrease combustion time. It is very attractive feature for application files of this kind for SCRAMJET.

Conclusion:

The performed experiments have shown considerable reduction of induction period at combustion products of thermochemical decomposition of endothermic fuel as contrasted with similar period of usual gaseous fuels or vapors of initial liquid fuel.

LITERATURE

1. N.N. Semenov. Some problems of Chemical Kinetic and Reaction Capacity. Moscow, AS USSR, 1958, 686p.
2. V.C. Zyev, L.S. Skubachevsky. The Combustion Chambers for Air – Breating Engines, Moscow, Oborongiz, 1958, 214p.
3. K.I. Zchelkin, Ya.A. Trochin. Burning Gasodynamic. Moscow, AS USSR, 1963,255p.
4. V.K. Baev, V.A. Yasakov. The Investigation Diffusive Flame Jet Stabulity. Journal "Izvestiya of SD AS USSR", ser. "Technical Sciences", v.1, № 3, 1969
5. I.M. Annushkin, E.D. Sverdlov. The Investigation Diffusive Flame Jet Stability for Subsonic and Supersonis Jets of Gaseous Fuels. Journal " The Physic of Explosion and Burning". Journal "Izvestiya of SD AS USSR", ser. "Technical Sciences", № 5, 1978.
6. L.S. Ianovskiy, V.F. Ivanov, F.M. Galimov, G.B. Sapgir Coke deposits in aviation and rocket engines. Kazan, KSTU, 1999,285p.

Table 1

Maximum normal values of flame velocities for different fuels in mixture with air under atmospheric pressure and temperature 20°C ([3]).

Fuel	Maximum normal rates of flame [m / sec]	Percentage composition of fuel in the mixture with maximum rates of flame	Percentage composition of fuel in stoichiometrical mixture
Hydrogen	2.670	42	29.5
Acetylene	1.310	10	7.7
Ethylene	0.630	7	6.5
Propylene	0.435	4.8	4.5
Methane	0.370	10.5	9.5
H – hexane	0.320	2.5	2.2
Acetone	0.318	6.0	5.0

Table 2

Results of chromatographic analysis of the gas mixture obtained at thermochemical decomposition of the endothermic fuel. (Outflow gas temperature from the heat-exchanger is 670°C. Decomposition degree is approximately 80 %).

Gas	Inclusion volume fraction (in %)
Hydrogen	6.5
Methane	31.5
Ethylene	38.0
Ethane	4.6
Propylene	14.0
Propane	5.4

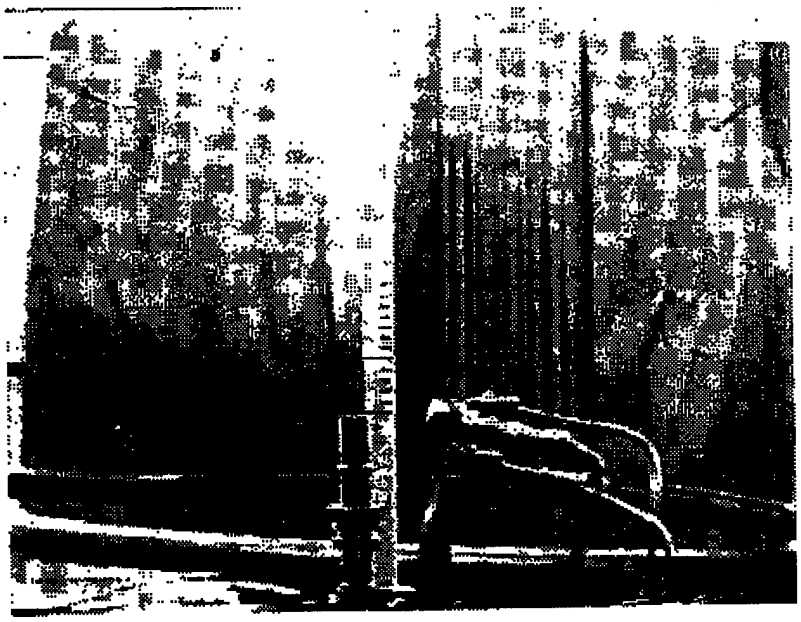

Fig. 1. Combustion of yields of thermal decomposition in the flooded plume

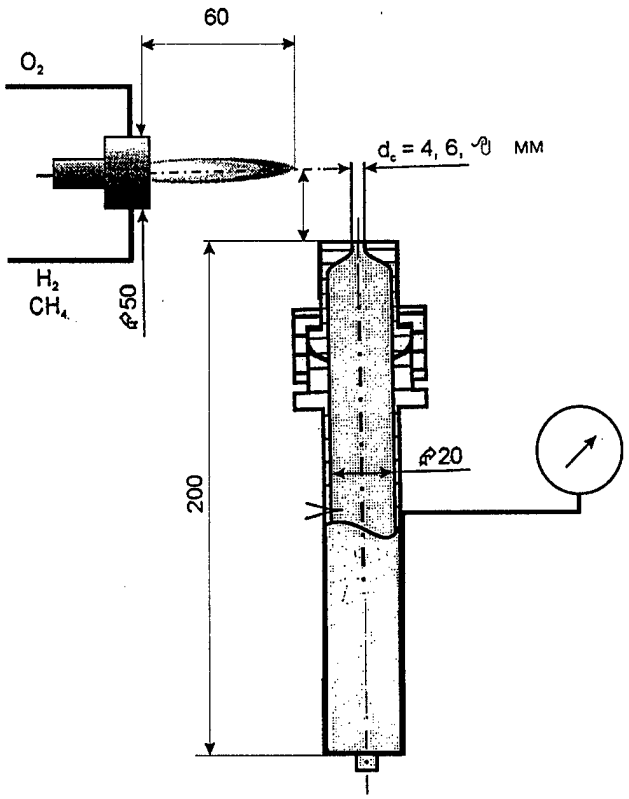

Fig.2. The scheme of the burner for research of the characteristics of combustion of gaseous fuels

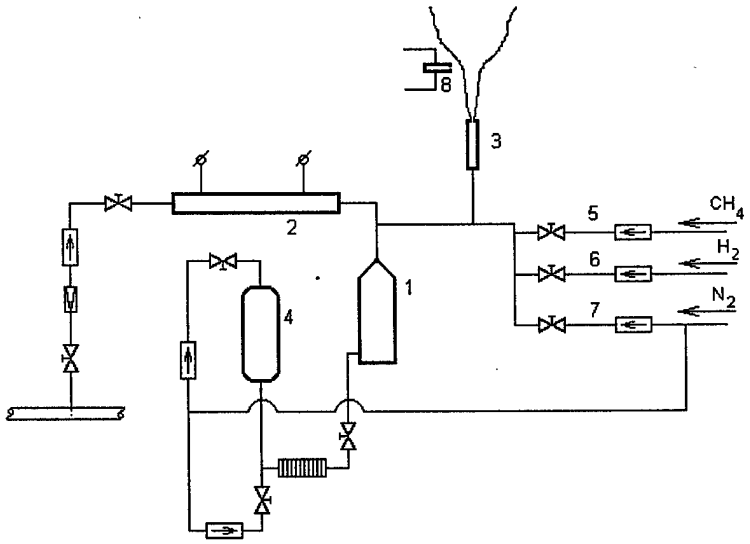

Фиг. 3. Схема факельной установки.

1 - Теплообменник- реактор; 2 - электрический нагреватель воздуха;
3 - горелка; 4 - бак с жидким топливом; 5 - магистраль падачи метана;
6 - магистрал подачи водорода; 7 - магистраль подачи азота;
8 - зажигательное устройство.

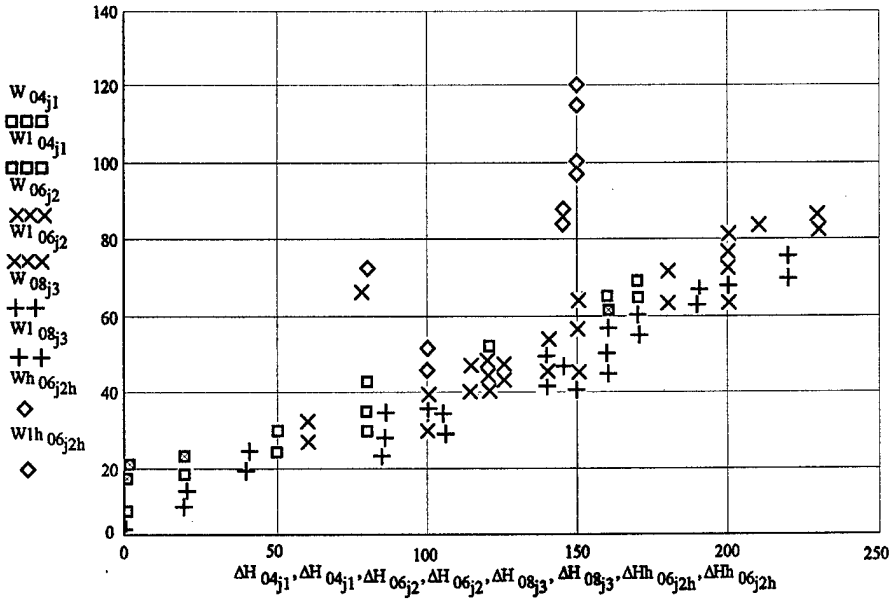

Fig. 4. Exhaust velocity as a function of an altitude of a waste of a flame for methane with various diameters of the nozzle of an injector and for methane with the additives of hydrogen

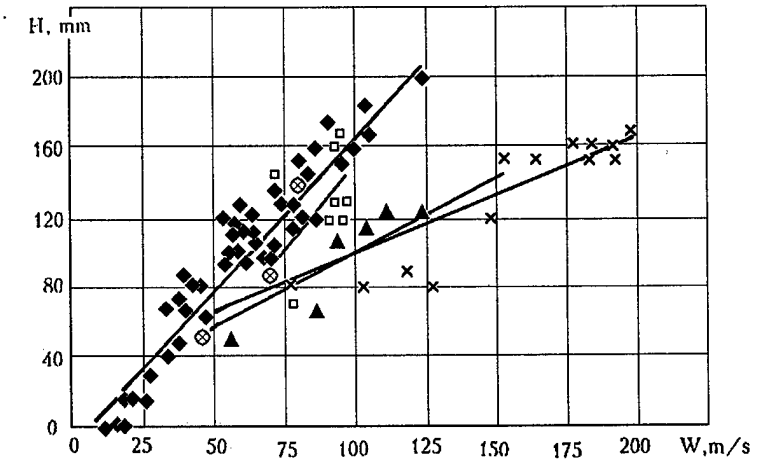

Фиг.5. Результаты сравнительных испытаний горения продуктов ТД ЭУВТ в затопленном факеле.
◆- CH_4
□ - CH_4, t 100 ÷500°C;
▲- CH_4 + H_2;
⊗- пары ЭУВТ.
×- продукты деструкции.

EXPERIMENTAL AND NUMERICAL STUDY OF IGNITION OF METHANE STEAM REFORMING PRODUCTS BEHIND SHOCK WAVES.

Gurentsov E.V., Divakov O.G., Eremin A.V.

Institute for Thermophysics of Extreme States RAS, Moscow , Russia
127412
Moscow, Izhorskaya st. 13/19
Eremin A.V.
E-mail: eremin@aha.ru
Fax: (095) 485-79-90

Introduction

One of the perspective ways of space and aviation technique development is transatmospheric hypersonic vehicle design [1,2]. The scramjet air-breathing engine as propulsion system for transatmospheric flight can be considered. The important problem at scramjet design is the fuel choice. The main criteria are the thermal capacity to serve as regenerative coolant, specific impulse and fuel density in the tanks.

Theoretically, liquid hydrogen is the ideal fuel for scramjet, it have a maximum specific impulse, great cooling resource and a minimum ignition delay times. But the use of liquid H_2 is connected with several difficults. The first, liquid hydrogen has a small density, that causes the tanks volume increase and consequently, the essential enhancement of the plane drug. The second, structure of producing, keeping, transporting and making fill up liquid hydrogen must be build. Besides that, the requirements of safety conditions increase essentially.

The hydrocarbon fuels at high heating loads (the flight Mach number above 8) are less effective as coolant and have less specific impulse relatively to the liquid hydrogen. However methane and other simple hydrocarbons can compete with liquid hydrogen, because of their less cost and wide use in the different areas. The main problem to solve for this goal consists of enhancement of specific impulse, cooling resource and the reduction of ignition delay times of hydrocarbon fuels, which can be used in scramjet engine.

Endothermic hydrocarbons (i.e., liquids which can be gasified, cracked and reformed in the coolant system) are one of the perspective fuels. In [3,4] the using of endothermic reaction of steam reforming of methane ($CH_4+H_2O\rightarrow 3H_2+CO$-226 kJ/mol) for new fuel production is discussed. High endothermic effect of this reaction and essential hydrogen yield [3] gives the hope to get the necessary coolant resource and to increase the specific impulse. In this case, multicomponents mixture consisting of H_2, CO, CO_2, CH_4, H_2O is mixed with the hot air before the entrance of combustor.

The main parameters of supersonic combustion are initial temperature of combustive mixture and the total combustion time. The decrease of initial temperature leads to enhancement of the thrust and the less heating load in the inlet of engine. However, if the initial temperature decreases, the total combustion time rather increases, that causes the growth of the length of combustion chamber and the weight of engine.

The real total combustion time consists of two parts - ignition delay time and namely time of combustion. Combustion time is the function of the kind of the fuel, while

ignition delay time is strongly influenced on the temperature and pressure of the flow. For example, in the work [5] there was shown, that calculated and experimental ignition delay times for $O_2 + H_2$ mixture at the temperature T=1000K and pressure P=1bar differs at about factor of 2, and at temperature T=700-800K this difference increased up to 2-3 orders of magnitude.

For the other hand, modern kinetic schemes also could not give the adequate relationship between ignition delay time andtemperature and pressure. This proceeds because of incomplete knowledge of chain nucleation and branching mechanisms at the early stage of the combustion processes. Another reason could be the influence of excited particles on ignition delay, when even the small change of concentration of active radicals could play the principal role.

The processes of ignition and combustion of hydrocarbon fuels were studied in the number of works (see for example review [6]). But detailed investigations of combustion and ignition kinetic of multicomponent mixtures of endothermic hydrocarbons with promotor additions were not conducted. Thus, one could note, that investigation of multicomponent mixtures and measurement of the actual dependence at ignition delay time on the pressure and temperature, is important problem for scramjet design.

The goal of this work is to study ignition mechanism of different fuels (H_2, CH_4, C_2H_6, C_2H_2) and its mixtures with addition of H_2O, SiH_4, N_2O investigation behind shock waves, in vicinity of low-temperature limit and searching of new ways to control the ignition processes.

Selection of kinetic mechanism

The problem of initiation of ignition in the supersonic flows is very important for internal aerodynamics of supersonic velocity. In this case besides hydrodynamics means the optimization of kinetic mechanisms of ignition plays the important role. It is necessary to underline that to solve this problem the volume of experimental work must be limited as far as possible. For this point of view, the choose of kinetic model plays the principal role. Up to now, the detailed kinetic mechanisms of combustion of H_2, CO and simple hydrocarbons has been elaborated. The most complicated kinetic mechanisms are developed to describe the combustion of hydrocarbons and consist of abundant elemental reactions of formation as light as heavy hydrocarbons. In work [7], the kinetic scheme of combustion of methane-air mixture consists of 433 forward-reverse reactions and accounts for formation of different hydrocarbons C_xH_y up to C_4H_y. This mechanism gives a good agreement with experimental data for combustion times, temperatures and concentrations of products.

However, this scheme for our investigation is too complicative and to analyze our experimental data, we have reduced it up to 321 reactions. The calculations have been carried out by using the most up-to-date CHEMKIN II code.

In Fig. 1 the calculated values of total combustion time (t_i) for some fuels in dependence on initial temperature at the entrance of combustion chamber is shown. Among these fuels CH_4, C_2H_6 and mixture obtained during the steam reforming of methane in different reforming degrees (Z=10; 20; 100%) are considered. Values of t_i in Fig.1 are related to the total combustion time of hydrogen. It is obvious from these curves, that total combustion time for hydrocarbon fuels increases relatively to those of hydrogen with the temperature decrease down to 1000-1200K. One can make a conclusion from the results obtained, that for the use of hydrocarbon fuels it is necessary to found an efficient methods to reduce the total time of combustion.

As has been already noted, the total combustion time can be divided on ignition delay time and combustion time. The combustion time depends on the thermodynamic parameters and kind of fuels, while the ignition delay time (the main part of the total combustion time) depends on the ratio between reaction rate of the chains

nucleation and branching for one side and the reaction rate of chains breakage for another side. This circumstance can be used to affect on ignition delay time by the changing of the kinetic reaction.

For example, the analysis of ignition kinetic of H_2+O_2 mixture behind shock waves in vicinity of low-temperature limits, made in experimental study [8], has shown, that ignition delay time is very sensitive to the concentration of oxygen atoms. An addition of $10^{13} \div 10^{14}$ O atoms to mixture of $10\%H_2+5\%O_2+85\%Ar$ at a pressure of P~1 bar and at a temperature of T~800K , causes the ignition delay time reduction about at 10 times (see Fig.2). To obtain such an initial concentration of O atoms in the flow of the mixture $2H_2+O_2$ with cross-section 10^3 cm^2, and flow velocity 1km/s, there is necessary to apply the source of UV radiation at the corresponding wavelength with the power 1kW. The another way to accelerate the ignition process is adding of promotors in the mixture (less than 1% of the fuel). The species like N_2O, NO_2, SiH_4, O_3 are the good promotors for hydrocarbon fuels and its using can reduce ignition delay times at factor of 10 and more [6].

Experimental part

The experimental part of the study has been carried out in shock tube with inner diameter 50 mm. A driver section was 1.5 m length and driven section was 3.7 m length. The driver gases were pure helium or hydrogen. The initial pressure in the driven section was 50-100 Torr. The pressure gauges were equipped in the wall at 10, 104, 384 mm from the end of the tube. The test mixtures used are presented in the Table 1. The temperature behind reflected shock wave was determined by the incident wave velocity based on the time difference of pressure response between gauges, taking into account the temperature dependence of heat capacity of the gases.

Measurements of emission signals from OH radicals (wavelength 3060 Å) and laser light attenuation (wavelength 6328 Å) were performed through LiF windows equipped on 10 mm from the end of tube, by using PEM . The ignition delay times were detected by peak of OH emission signals. Experimentally measured ignition delay times in the $CH_4+O_2+N_2$ (Ar, He) stoichiometric mixtures have a good agreement with calculations performed (see Fig.3).

The first step to study the multicomponent mixtures was to test the methane-air-steam mixture. Amount of H_2O vapor was up to 6% of the volume. One can see from Fig.3, that ignition delay times decreased a 2-3 times. This effect could not be described by kinetic scheme developed. The similar results were presented in reference [9], were combustion of the mixture of 90%propanol +10%tethradecane in stoichiometry with oxygen, diluted by argon was investigated. Adding in this mixture at 2% of steam caused the essential decrease of ignition delay times.

The resulting experimental data will be base for the following study of multicomponent mixtures which can be used for scramjet fuels.

Authors would like to thank Prof. Y.V. Polezhaev for the valuable remarks during the investigation. The financial support of RFBR is gratefully acknowledged.

Referenses

1. Erdos J.I. Scramjet testing in shock-heated tunnels. // 21-th International Symposium on Shock Waves. Great Keppel, Australia. 1997, paper № 9030.
2. Gurijinov P.T., Harsha. AJAX: new directions in hypersonic technology. //AAIA 96-4609.
3. Korabelnikov A.V., Kuranov A.L. Thermochemical conversion of hydrocarbon fuel under the concept "AJAX". // AAIA 99-4921
4. Kurganov V..A., Zeigarnik Y.V., Korabelnicov A.V. The thermochemical principle of cooling based on steam reforming of methane. // Thermal engineering, 1996, vol. 43, No. 3.

5. Divakov O.G, Eremin A.V., Ziborov V.S. Gas-diluter influence on H_2/O_2 mixtures ignition in a weak shock wave. // 22-th International Symposium on Shock Waves. London. 1999, paper №3974.
6. Zamanskii V.M., Borisov A.A. The mechanism and promotion of the perspective fuels self-ignition. // Itogi nauki i techniki 1989.,v.19, Ser."Kinetika i kataliz" (In Russian).
7. Dautov N.G., Starik A.M. // Kinetika i Kataliz. 1997, vol.38, N2, pp..207-230 (In Russian).
8. Divakov O.G., Eremin A.V., Ziborov V.S., Fortov V.,E. Nonequilibrium ignition of H_2-O_2 mixtures in a weak shock wave front. // Dokladi AN, in print (In Russion).
9. Kunz A., Wang R., Cadman P. Liquid spray combustion of propanol/tetradecane/ water mixtures. // 21-th International Symposium on Shock Waves. Great Keppel, Australia. 1997, paper № 1691

Table 1

	Mixture	P, bar	T, K
a	$10\%O_2+5\%CH_4+85\%Ar$	3÷7.6	1450÷1880
b	$10\%O_2+5\%CH_4+85\%He$	2.1÷4	1400÷1840
c	$10\%O_2+5\%CH_4+85\%N_2$	5.6÷7.2	1440÷1850

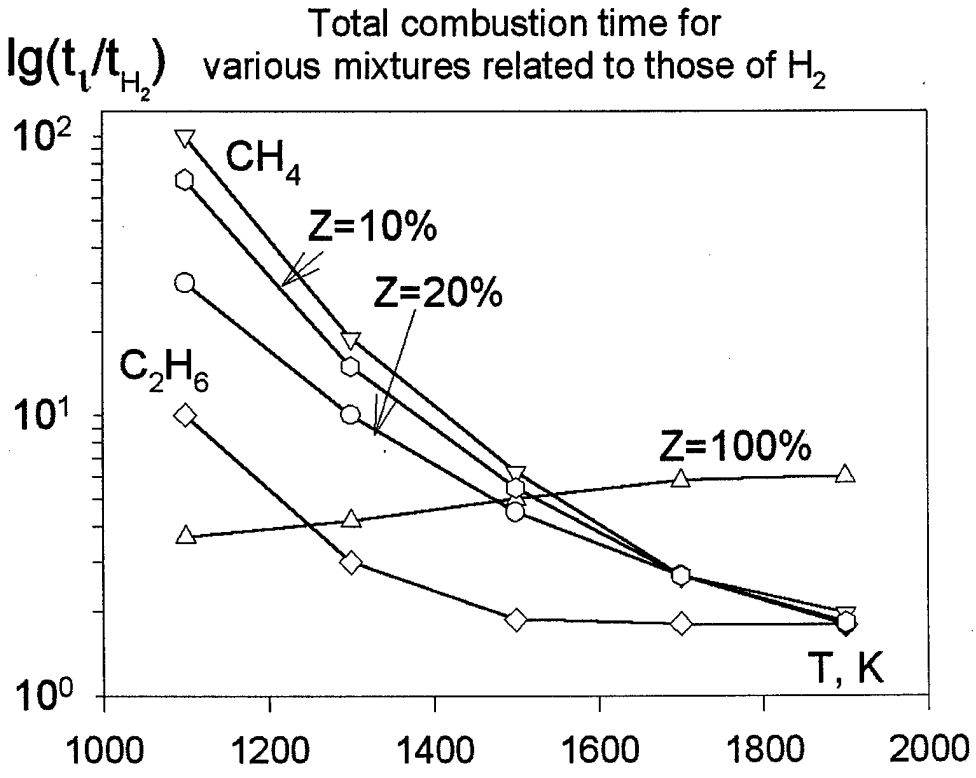

Fig. 1.

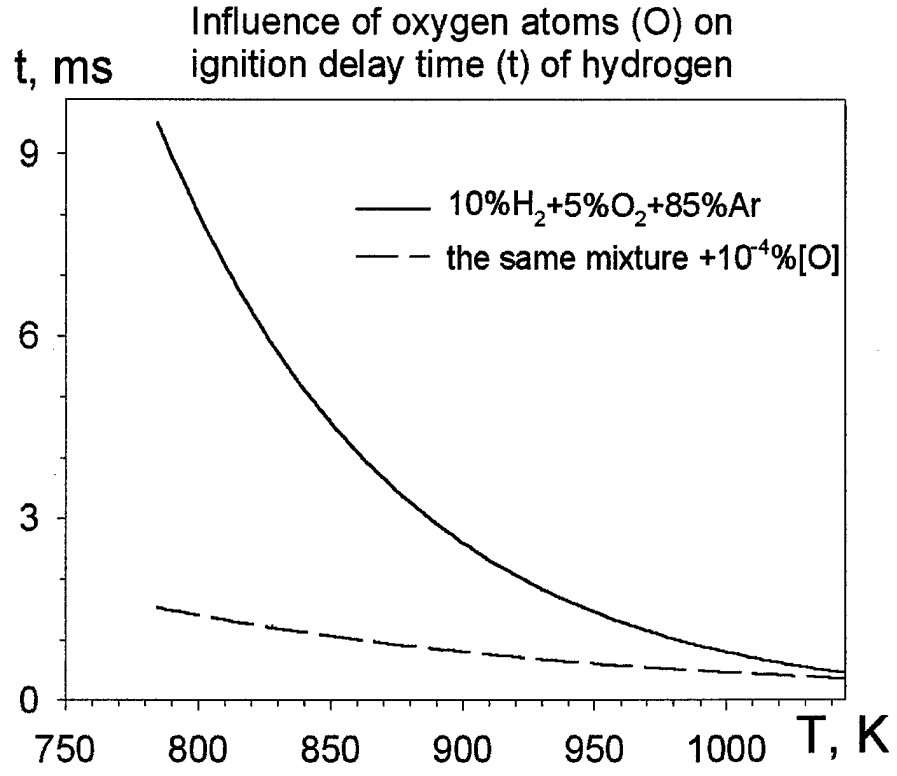
Influence of oxygen atoms (O) on
ignition delay time (t) of hydrogen
t, ms
9
6
3
0
10%H2+5%O2+85%Ar
the same mixture +10-4%[O]
750
800
850
900
950
1000
T, K

Fig. 2.

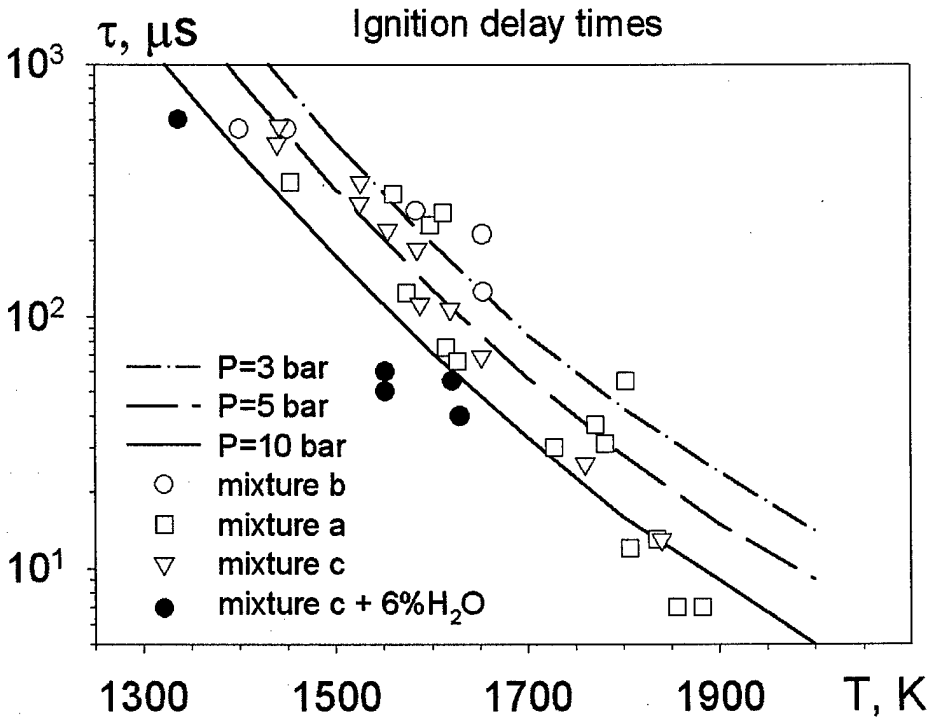
τ, μs
Ignition delay times
10^3
10^2
10^1
P=3 bar
P=5 bar
P=10 bar
mixture b
mixture a
mixture c
mixture c + 6%H2O
1300
1500
1700
1900
T, K

Fig. 3.

PULSE DETONATION ENGINE ON THE BASE OF STEAM REFORMING OF METHANE

Baklanov D.I., Golub V.V., Divakov O.G., Eremin A.V.

Institute for thermophysics of extreme states RAS
127412
Moscow, Izhorskaya 13/19
Dr. Golub V.V.
E-mail: golub@hedric.msk.su
Fax: (095) 485-79-90

The theoretical and numerical studies have shown that pulsed detonation propulsion devices (PDD) offer significant advantages in aviation and rocket propulsion. The burned gas temperature behind the detonation wave is higher then in deflagration. The speed of the detonation wave is about two orders of magnitude higher than the speed of typical deflagration. It allows designing of the propulsion engines with a very high power density. In the detonation propulsion device the effective thermodynamic isochoric cycle is used. The sizes and weight are well compared to those of the current turbojet engines [1,2].

One of the problems in PDD is the great heat flux to the walls. At detonation cycles of the frequency 1 –3 Hz the heat flux to the walls is observed to gain up to 40% of the total heat release in the 16 mm diameter detonation chamber (length 1.5m). In one cycle of hydrogen – oxygen detonation about 1.3 kJ is lost on the wall [3]. The wall temperature rises up to 800K and the self-ignition occurs. In this case it is impossible to control the detonation frequency. If the frequency is increased up to 40-50 Hz the heat flux to the walls during one cycle decreases down to 28% of the total heat of combustion, but it increases in the time unit. Evidently the problem of effective wall-cooling in PDD is very actual.

The problem of thermal protection and thermochemical conversion of a hydrocarbon fuel was considered in [4] under the concept "AJAX". The proposed heat-protection system executes not only usual function, providing temperature conditions of the airframe, but also serves simultaneously as the system of preparation of new modified fuel containing molecular hydrogen.

This combined cooling and fuel preparation system can be used for the PDD-engine's also. One of the variant to accomplish this system on the vehicle is the steam reforming of hydrocarbons, in particular methane via reaction:

$$CH_4 + H_2O + Q \rightarrow 3H_2 + CO \quad (1)$$

The use of methane leads to reduction of carbon deposition on catalythic surfaces comparably with heavy hydrocarbons. The resulting synthesis gas consist of the mixture of H_2, CO, CO_2, CH_4 and H_2O, content of which depends on degree of conversion (Z). The implementation of this fuel allows to reduce the heat flux to the walls due to the less intensity of the working cycle and to remove the additional heat on reforming cycle (1).

In Table 1 the parameters of detonation waves in stoichiometric fuel-air mixtures at initial temperature T_0=750K and pressure P_0=3bar, calculated on the base of up-to-date CHEMKIN-II packet and GRI-Mech 3.0 data, are shown.

In the last row the heat consumption C at methane reforming in reaction (1) are given. It is easy to show, that already at Z=20% this value is more than heat flux to the walls of PDD.

References:

1. S. Eidelman and W. Grossman. Pulsed detonation engine. Experimental and theoretical review. AIAA 92-3168.
2. T. Bazhenova , V. Golub, Pulsed detonation engine. In: The XXIst century scientific base of the technologies, UNPC "Energomash" , Moscow ,2000 , p95-96. (in Russian)
3. D. I. Baklanov et al. Some technical aspects of the detonation combustion employ . Fizika goreniya i vzryva. V12, №1 1976 (in Russian)
4. 4. A. V. Korabelnikov and A .L . Kuranov . Thermochemical conversion of hydrocarbon fuel under the concept "AJAX" . AIAA 99-4921

Table 1.

Fuel	P, bar	T, K	V, km/s	C, MJ/Kg
H_2	19	3120	1.94	—
CH_4	21.2	2960	1.03	—
Z=20%	19.3	2800	1.74	2.7
Z=50%	18	2735	1.70	6.6
Z=75%	16.8	2650	1.65	10
Z=100%	15.5	2536	1.60	13.3

PLASMA COMBUSTION PROBLEM AND ITS FEATURES AT IMPLEMENTATION OF THE "AJAX"CONCEPT

Filimonov Yu.N., Kuranov A.L., Kuchinsky V.V., Pinchuk V.F., Shevchuk V.T., Sheikin Eu.G.

212 Moskovsky prospekt, St. Petersburg, 196066, Russia.
Hypersonic System Research Institute
Tel./ Fax:(812) 291-82-94, E-mail:ajax@comset.net

The combustor is area, where there is the low-temperature plasma in a liquid fuel engine. The magnitoplasmechemistry drive will be used according to the concept "Ajax" as a uniflow air - jet drive, which the principle of operation consists in volumetric inhibiting action of the specially ionized airflow (including before a combustor), the degree of ionization of low-temperature plasma in a combustor can considerably increase and reach values 10^{-8} - 10^{-6}. The presence of charged particles will render noticeable influence on all processes, flowing past in a combustor, and can reduce in evolution both to positive, and to negative processes.

The present work is the first stage in research of course of the most important process - evolution of instability of a spatial charge distribution in the combustor volume. The understanding of specificity of evolution of instability of a spatial charge distribution will enable to avoid failures and nonuniformity of the combustion process and will allow (by electrophysical measurements) to receive the important information on course of the inside-camera processes.

The purpose of the work is the determination of a nature and mechanism of creations of electrophysical mappings of the working process and their link with parameters of the combustion process. The theoretical part of the work consists of a statement and solution of the system of the non-stationary equations circumscribing in one-dimensional approximation the all three main component of low-temperature plasma of combustion products: electrons, ions and neutral atoms at effect on plasma of acoustic perturbations or shock waves. In an experimental part the methods and equipment for measurement electrophysical and gasdynamic parameters of plasma designed and the main data showing of characters of correlation of these two groups of parameters are obtained.

The acoustic effect on combustion products is accompanied by creation of secondary kinetic effects on the process, i.e. the inherent instabilities (for example, instability in a charge distribution by the volume) gain at the expense of energy of acoustic oscillations additional "energy resources " for their evolution.

The evolution of such instabilities carries macroscopic character and is accompanied by carrying-out of an electrical charge from the areas, subject to acoustic effects. The data on character and direction of relaxation processes are obtained, which

depend on many parameters and are defined by a degree of violation of quasi-neutrality of the environment, by the value of an electrostatic potential etc. Three typical modes of evolution of charge instability can be selected: low-temperature, high-temperature and transition mode.

The fulfilled work gives possibility for realization of full-range experiment with usage as an energy carrier the mixture air kerosene with hydrogen.

DETAILED ION KINETIC MECHANISMS FOR HYDROCARBON/AIR COMBUSTION CHEMISTRY

S. Williams, P.M. Bench, A.J. Midey[†], S.T. Arnold‡, A.A. Viggiano, and R.A. Morris
Air Force Research Laboratory, Space Vehicles Directorate
Hanscom AFB, MA 01731-3010

L.Q. Maurice and C.D. Carter¶
Air Force Research Laboratory, Propulsion Directorate
Wright-Patterson AFB, OH 45433-7103

Abstract

The kinetics of reactions between air plasma ions and hydrocarbons typically found in aviation (JP) fuels were studied over 300 – 1400 K using fast ion flow tube techniques. The effects of air plasma ions, namely NO^+ and H_3O^+, on the ignition delay time were studied computationally using the laboratory kinetics data to expand detailed hydrocarbon combustion kinetics mechanisms. The effects of ionization on the ignition delay time for isooctane, ethylbenzene, and a 74 vol% isooctane / 24 vol% ethylbenzene mixture burning in air (P=1 atm, $T_{initial}$=900-1500 K, Φ=1) were examined. Detailed kinetics modeling shows significant decreases in ignition delay in the presence of initial ionization. The most significant decrease in the ignition delay time occurs at lower initial temperatures and higher levels of ionization. In general, H_3O^+ is less effective than NO^+ except for the case of pure ethylbenzene at temperatures below ca. 1000 K.

Introduction

The effects of ionization on hydrocarbon-air combustion chemistry are being investigated at the Air Force Research Laboratory for the purpose of developing techniques to reduce the ignition delay time and increase the rate of combustion of hydrocarbon fuels. The models being developed focus primarily on the development of plasma-based ignition and combustion enhancement techniques for scramjet combustors. However, the methods pursued are based on detailed fundamental kinetics treatments and are therefore broadly applicable to a range of problems such as combustors for gas turbine engines, spark inhibition, improved engine performance, service life, explosion limits in blended fuels, hydrocarbon molecular growth, and high altitude relight.

In the present contribution, the latest progress on the development of the ion-hydrocarbon kinetics database and on the investigation of the effects of ionization on hydrocarbon/air combustion is reported. The effects of ionization on ignition delay for isooctane, ethylbenzene, and a 76/24

[†] Air Force Research Laboratory Scholar.
‡ Wentworth Institute of Technology, Research Scientist.
¶ Innovative Scientific Solutions, Inc., Senior Member AIAA

isooctane/ethylbenzene mixture were examined. The investigation continues to yield promising results supporting the concept of using ionization to promote and enhance hydrocarbon/air ignition and combustion.

Kinetics Experiments

The plasma chemistry of ionized air reacting with hydrocarbons was investigated using fast ion flow tube kinetics instrumentation. The Variable Temperature - Selected Ion Flow Tube (VT-SIFT)[1] instrument at the Space Vehicles Directorate was used to quantify the reactivity and products of a large number of ion-molecule reactions. Measurements included both reaction rate constants and branching percentages as a function of temperature. The VT-SIFT is temperature variable from 80 to 550 K. Additional measurements of selected ion-molecule reactions using a second fast flow tube instrument, the High Temperature Flowing Afterglow (HTFA)[2,3] apparatus, capable of much higher temperatures have also been completed. The HTFA provides data from 300 to 1800 K enabling the study of ion-molecule reactions at relevant ignition temperatures. Both instruments operate at ca. 1 Torr helium buffer pressure, and the kinetics are observed over ca. 1 ms reaction time.

Kinetics Results

Previous experimental investigations in our laboratory revealed very fast chemistry between the major air plasma ions and a series of alkanes found in aviation fuel. Specifically, reactions of C_1 to C_{12} straight-chain alkanes (methane to dodecane) and C_4 to C_8 branched-chain alkanes (isobutane to isooctane) with the most relevant atmospheric positive (NO^+, O_2^+, N_2^+, O^+, N^+, H_3O^+) and negative (O^-, O_2^-, CO_3^-, NO_3^-) ions have been studied.

In brief, the positive ions O^+, O_2^+, N^+, and N_2^+ are highly reactive with all alkanes larger than methane and yield products resulting from C-H and C-C bond cleavage. The cations NO^+ and H_3O^+ become highly reactive with the larger alkanes, and chain branching greatly enhances their reactivity. For example, while NO^+ reacts at 0.2% of the Langevin collision rate (0.2% efficiency) with n-pentane, its efficiency increases to 50% for isopentane. Likewise, the efficiency of NO^+ reaction increases from 28% for n-octane to 95% for isooctane.[4,5] The negative ions O_2^-, NO_3^-, and CO_3^- are unreactive with the smaller alkanes and display little reactivity even with the largest alkanes studied. By contrast, the reactivity of O^- is significant and increases with alkane size. Two product channels are observed: a hydrogen abstraction channel yielding OH^- and a reactive detachment channel yielding neutral products and a free electron. The reaction becomes 100% efficient for butane and larger alkanes, and the dominant (96%) pathway becomes electron detachment for decane and larger.[6]

At present, the positive ion chemistry with aromatic hydrocarbons (C_6-C_{10}) has been studied.[7-9] Temperature dependent rate constants and product branching percentages have been measured for the reactions of benzene, toluene, ethylbenzene, n-propylbenzene, and naphthalene with the air plasma ions. Overall the reactions of NO^+, O_2^+, O^+, and N_2^+ show a progression toward greater extent of dissociative charge transfer (vs. nondissociative) as both the reactant ion recombination energy increases and the flow tube temperature increases. However, the total reaction rate constants remain at the Langevin collision rate which is approximately 2×10^{-9} cm^3-$molecule^{-1}$-s^{-1} for all reactions studied. With regard to benzene and naphthalene, the major product channels are charge transfer, H elimination, and C_2H_2 elimination. Alkyl substituted benzene reactions produce $C_7H_7^+$ ions predominately, and eliminate H, CH_3, or C_2H_5 depending on the size of the alkyl substituent. The reactions of H_3O^+ with the aromatics proceed exclusively through proton transfer (dissociative and nondissociative) at the collision rate.

Computational Modeling

The chemical kinetics of ion-hydrocarbon reactions in macroscopic systems were studied using detailed hydrocarbon combustion kinetic models formulated by Maurice and coworkers.[10-12] The kinetic mechanism features alkane molecules up to C_{12} (dodecane), an aromatic sub-mechanism including mono-substituted and polycyclic aromatic hydrocarbon oxidation chemistry, and a NO_x sub-mechanism. The complete mechanism has been extensively evaluated in a broad range of combustion devices.

The CONP program of the CHEMKIN II software series[13] was used for the computations. The CONP model assumes perfect mixing and is essentially a streamtube computation at a specified constant pressure and initial temperature. This approach enables the detailed chemistry and the mechanisms for flame initiation to be evaluated without the computation time required for calculations coupling fluid mechanics with detailed chemistry.

Table 1: Comparison of authentic JP-8 fuel and a 76 vol% isooctane /24 vol% ethylbenzene mixture.

Property	Mixture	JP-8*
Aromatics, Vol %	24.1	22.0
Olefins, Vol %	0.0	2.7
Hydrogen Content, Wt %	14.0	13.7
Density, kg/l	0.734	0.800
Net Heat of Combustion†, MJ/kg	43.7	43.1

*WPAFB, TANK S-15
†Refers to gas phase reactants and products.

Computations have been performed for the combustion of pure isooctane, pure ethylbenzene, and a 76 vol% isooctane / 24 vol% ethylbenzene mixture with a $H_3O^+/NO^+/e^-$ ionization kinetics scheme. This early model considers a neutral plasma composed of NO^+ and/or H_3O^+ as the positive charge carriers and thermal electrons as the negative charge carriers. The key ion chemistry of the JP-8 fuel constituents studied to date is well represented by the reactions with NO^+ and H_3O^+, however, the addition of other air plasma ions is forthcoming. Isooctane and ethylbenzene are chosen because a mixture is a reasonable fuel ignition surrogate for JP-8 fuel based on the close similarities shown in Table 1. Other characteristics such as distillation boiling point, viscosity, and freezing point are not as well represented because species like dodecane have not yet been included. Since the modeling is purely kinetic at this point, differences in the fluid properties are not very significant.

The key ionic reactions included in the model are listed below where i- and t- connote the iso- and tert- prefixes, respectively, and no prefix refers to normal.

Initiation

$NO^+ + i\text{-}C_8H_{18} \rightarrow HNO + i\text{-}C_8H_{17}^+$ (1a)
$NO^+ + C_8H_{10} \rightarrow NO + C_8H_{10}^+$ (1b)
$H_3O^+ + i\text{-}C_8H_{18} \rightarrow H_2O + i\text{-}C_4H_{10} + t\text{-}C_4H_9^+$ (1c)
$H_3O^+ + C_8H_{10} \rightarrow H_2O + C_8H_{11}^+$ (1d)

Dissociation/Decomposition

$i\text{-}C_8H_{17}^+ \rightarrow i\text{-}C_4H_8 + t\text{-}C_4H_9^+$ (2a)
$C_8H_{11}^+ \rightarrow C_2H_4 + C_6H_7^+$ (2b)
$C_8H_{10}^+ \rightarrow CH_3 + C_7H_7^+$ (2c)

Secondary Reactions

$t\text{-}C_4H_9^+ + i\text{-}C_8H_{18} \rightarrow i\text{-}C_4H_{10} + i\text{-}C_8H_{17}^+$ (3a)
$t\text{-}C_4H_9^+ + C_8H_{10} \rightarrow i\text{-}C_4H_{10} + C_8H_9^+$ (3b)
$C_8H_{11}^+ + i\text{-}C_8H_{18} \rightarrow C_8H_{10} + H_2 + i\text{-}C_8H_{17}^+$ (3c)
$C_7H_7^+ + i\text{-}C_8H_{18} \rightarrow C_7H_8 + i\text{-}C_8H_{17}^+$ (3d)
$C_7H_7^+ + C_8H_{10} \rightarrow C_7H_8 + C_8H_9^+$ (3e)
$\rightarrow C_6H_6 + C_9H_{11}^+$ (3f)
$C_6H_7^+ + i\text{-}C_8H_{18} \rightarrow C_6H_6 + i\text{-}C_4H_{10} + i\text{-}C_4H_9^+$ (3g)
$\rightarrow C_6H_6 + i\text{-}C_3H_8 + i\text{-}C_5H_{11}^+$ (3h)
$C_6H_7^+ + C_8H_{10} \rightarrow C_6H_6 + C_8H_{11}^+$ (3i)

Dissociative Recombination

$C_nH_m^+ + e^- \rightarrow$ products (4)

Reactions (1)-(3) involve only ion-fuel reactions. Obviously reactions with O_2 and N_2 must also be considered, especially

since several possible reaction channels are exothermic. The reactivity of some of the secondary alkyl and aromatic ions has been investigated, and to date none exhibit any significant reactivity with either N_2 or O_2. Specifically for $C_8H_{17}^+$, $C_4H_9^+$, and $C_7H_7^+$ the upper limits for the rate coefficients with N_2 and O_2 are 10^{-13} molecule-cm^3-s^{-1} at 300 K which is the current detection limit of the instruments.

The ion cycles shown in Reactions (1)-(3) are completed though neutralization reactions with thermal electrons. These molecular ions undergo dissociative recombination as opposed to three body recombination which is the only channel available for atomic ions. Hence, the dissociative recombination processes implied in Reaction (4) are very fast, typically ca. 10^{-6} cm^3-molecule^{-1}-s^{-1}. Total dissociative recombination rate coefficients of the majority of these ions are known,[14-16] but the products have not been measured directly. The lowest energy channels are the most commonly assumed and are typically two body processes involving hydrogen atom and methyl radical elimination. However, higher energy three body processes producing one or more radical species have been observed.[17-19]

The reaction sequences shown in Reactions (1)-(4) describing the ionization kinetics as well as the main air ionization steps including the dissociative recombination of NO^+ and H_3O^+ have been added to the mechanism. The reactions between NO^+ and H_3O^+ and C_2H_4, C_3H_7, i-C_4H_8, t-C_4H_9, i-C_4H_{10}, C_6H_6, and C_7H_8 fuel fragments and the major secondary chemistry between the product ions and the fuel constituents are also included. The ionic submechanism consists of 42 reactions and 17 species. The detailed hydrocarbon combustion mechanism and individual submechanisms are available upon request.

Computational Results

Results of the preliminary constant pressure streamtube kinetics computations over the 900-1500 K temperature range are shown in Figure 1 for isooctane, ethylbenzene, and the mixture. Additional initial conditions for the streamtube computations included equivalence ratio, Φ = 1.0, and initial pressure, P = 1 atm. The ignition delay time, τ_{ig}, is defined as the time at which the gas reaches a temperature 500 K above the initial temperature, $T_{initial}$. In all cases, τ_{ig} increases monotonically as the temperature is decreased.

Apparent in Figure 1 is the contrast between the ignition of ethylbenzene and isooctane. Fortunately, the mixture exhibits ignition characteristics nearly identical to those of pure isooctane. The mixture contains 24.1% by volume aromatics which is close to the maximum specification of 25% by volume aromatics for JP-8 fuel. Therefore these computations suggest that, although the aromatics act as ignition inhibitors, they do not have a severe detrimental impact on the overall ignition kinetics of the fuel.

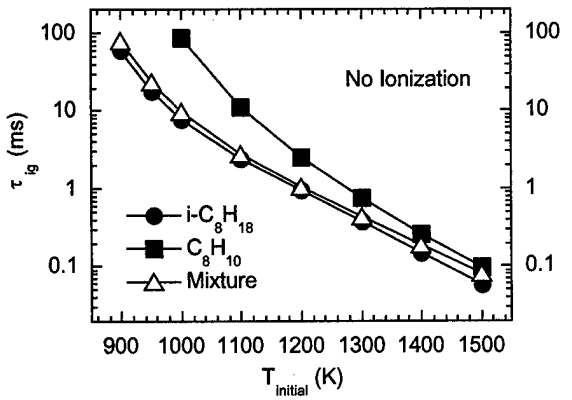

Figure 1. Variation of the ignition delay time (τ_{ig}) as a function of initial temperature ($T_{initial}$) over 900-1500 K for isooctane, ethylbenzene, and a 76 vol% isooctane / 24 vol% ethylbenzene mixture.

The computational results shown in Figure 1 vary over three orders of magnitude as the temperature varies from 900 to 1500 K. It is useful to plot the ignition delay effect as

a function of temperature as shown in Figures 2 and 3 for NO^+ and H_3O^+, respectively. The ignition delay effect at a given temperature is defined as the ignition delay for a specific ionization condition divided by the ignition delay with no initial ionization ($X_{\pm}=0$). The ignition delay time decreases as the ionization level increases. The effect is most pronounced at low temperatures. This result follows from the fact that the ion-molecule and dissociative recombination rate coefficients included in the model either remain constant or decrease with temperature, whereas the majority of the neutral reaction rate coefficients increase with temperature. Therefore, the fast ion chemistry dominates and has a larger effect at low temperatures.

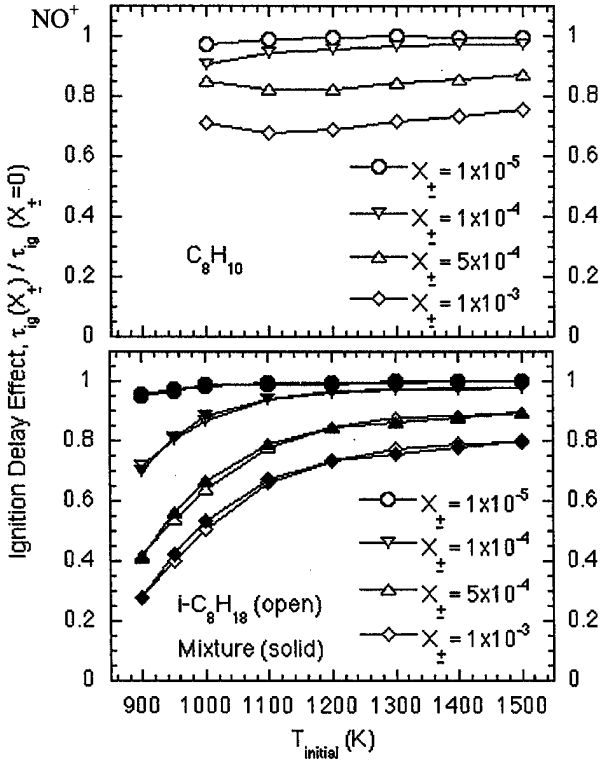

Figure 2. Ignition delay effect versus initial temperature as a function of NO^+/e^- ionization mole fraction.

The computational results plotted in Figures 2 and 3 show that ionization mole fractions greater than 10^{-6} are effective in reducing the ignition delay time and the effects are most dramatic for high levels of ionization. Both pure isooctane and the mixture exhibit a large reduction in τ_{ig} in the presence of either NO^+ and H_3O^+ with NO^+ being more effective. However, NO^+ is not as effective as H_3O^+ in reducing the ignition delay for pure ethylbenzene at low temperature.

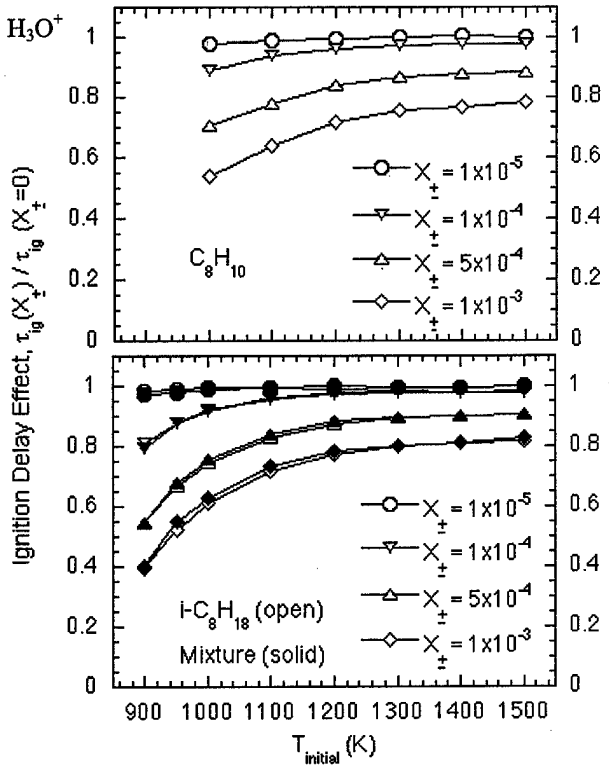

Figure 3. Ignition delay effect versus initial temperature as a function of H_3O^+/e^- ionization mole fraction.

Discussion

Reactions (1)-(4) exhibit considerable exothermicities, however, these exothermicities are small compared to the heats of combustion of the fuel constituents. Furthermore, considering the fact that the ion concentrations are at least an order of magnitude lower than the fuel constituents, little heat is added by the ion chemistry cycles. This conclusion is supported by the modeling results which show that at the completion of the ion chemistry, which occurs within 0.1 microsecond at 1 atm pressure, the temperature has only increased by 10 K for the maximum ionization mole fraction of 10^{-3}. Given the temperature

dependence of the computations shown in Figure 1, a rapid increase in temperature of 10 K leads to an approximately 17% decrease in the ignition delay time at an initial temperature of 900 K. This effect is not significant for initial ionization levels less than 10^{-4} which are associated with ≤1 K temperature increases.

Second, reactions of the air plasma ions with the fuel molecules result in the rapid decomposition of the fuel to smaller fragments with lower ignition temperatures. Thus, fuel breakdown may also play a role, but in general only a few percent of the fuel is reduced to smaller fragments under most conditions.

Important chain initiating and propagating atomic and radical species are produced in reactions (1)-(4). Reduction of the ignition delay time due to radical production is consistent with other experimental and modeling results supporting plasma torch development for hydrogen fuel scramjet combustors where enhanced ignition and flameholding in the presence of plasma torches has also been attributed to radical production.[20-22]

To compare the effect of radicals versus ionization in reducing the ignition delay, computations involving selected atomic and radical species important in chain branching and propagation reactions were performed. Figure 4 shows the ignition delay time as a function of initial mole fraction of these species. The ignition delay time is reduced as the mole fraction of all species is increased, and hence, these species promote ignition as expected. In general, O, H, OH, and CH_3 are equally effective, and C and H_3O^+ are more effective and essentially equivalent. For isooctane and the mixture, NO^+ is the most effective whereas H_3O^+ is the most effective for ethylbenzene. The results plotted in Figure 4 suggest that atomic, radical, and ionic species are effective in reducing the ignition delay time and are nearly equivalent on a mole fraction basis. Ionization the most effective because the ion/fuel chemistry involves heat release and fuel breakdown in addition to the production of atomic and radical species.

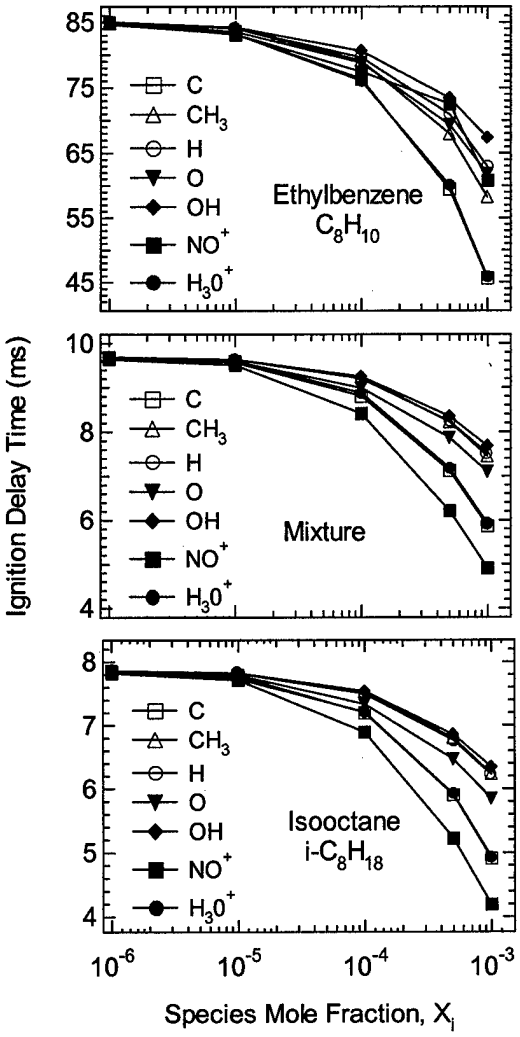

Figure 4: Ignition delay time, τ_{ig} (ms) for the combustion of isooctane, ethylbenzene, and a 76 vol% isooctane / 24 vol% ethylbenzene mixture vs. species mole fractions, $X_{\pm}$, at T=1000K, P = 1 atm, Φ = 1.0.

Summary and Conclusions

Flow tube kinetics measurements show that ions found in air plasmas do indeed react rapidly (ca. 10^{-9} cm^3-$molecule^{-1}$-s^{-1}) with aliphatic and aromatic fuel constituents. These reactions are typically much faster than the reactions between neutral species involved in hydrocarbon combustion initiation.

Detailed kinetics modeling shows significant decreases in ignition delay in the presence of initial ionization in the form of an $H_3O^+/NO^+/e^-$ plasma at levels greater than 10^{-6} ionization mole fraction. The effects are largest for both isooctane and for a isooctane/ethylbenzene mixture. In general, H_3O^+ is less effective than NO^+ except for the case of pure ethylbenzene at temperatures below ca. 1000 K. The ignition delay time is decreased most significantly (by approximately a factor of four) at the lowest ignition temperatures studied, 900 K, which is at the upper range of temperatures encountered in scramjet combustor cavities. The computational results suggest that even larger effects will be observed at lower temperatures.

For this early model, the ignition delay effect is primarily attributed to additional amounts of atomic and radical species produced by the air plasma ion/fuel chemistry followed by dissociative recombination of molecular ions. However, heat release and fuel breakdown also play a role.

Acknowledgements

The financial support of the Air Force Office of Scientific Research (AFOSR) under task 2303EP4 and the Air Force Research Laboratory Hypersonic Technology (HyTech) program are gratefully acknowledged.

References

1 A. A. Viggiano, R. A. Morris, F. Dale, J. F. Paulson, K. Giles, D. Smith, and T. Su, J. Chem. Phys. 93, 1149 (1990).
2 T. M. Miller, J. F. Friedman, M. Menendez-Barreto, A. A. Viggiano, R. A. Morris, A. E. S. Miller, and J. F. Paulson, Phys. Scripta T53, 84 (1994).
3 P. M. Hierl, I. Dotan, J. V. Seeley, J. M. Van Doren, R. A. Morris, and A. A. Viggiano, J. Chem. Phys. 106, 3540 (1997).
4 S. T. Arnold, A. A. Viggiano, and R. A. Morris, J. Phys. Chem. A 101, 9351 (1997).
5 S. T. Arnold, A. A. Viggiano, and R. A. Morris, J. Phys. Chem. A 102, 8881 (1998).
6 S. T. Arnold, R. A. Morris, and A. A. Viggiano, J. Phys. Chem. A 102, 1345 (1998).
7 S. T. Arnold, S. Williams, I. Dotan, A. J. Midey, R. A. Morris, and A. A. Viggiano, J. Phys. Chem. A 103, 8421 (1999).
8 A. J. Midey, S. Williams, S. T. Arnold, I. Dotan, R. A. Morris, and A. A. Viggiano, Int. J. Mass Spectrom. 195, 327 (2000).
9 S. T. Arnold, I. Dotan, S. Williams, A. A. Viggiano, and R. A. Morris, J. Phys. Chem. A 104, 928 (2000).
10 R. P. Lindstedt and L. Q. Maurice, Combust. Sci. and Technol. 107, 317 (1995).
11 R. P. Lindstedt and L. Q. Maurice, Combust. Sci. and Technol. 120, 119 (1996).
12 L. Q. Maurice, Ph.D. Thesis, Unversity of London, 1996.
13 R. J. Kee, F. M. Rupley, and J. A. Miller, CHEMKIN II: A Fortran Chemical Kinetics Package for the Analysis of Gas Phase Chemical Kinetics, Sandia National Laboratories, Report SAND89-8009B - UC-706, Livermore, CA, April 1992.
14 H. Abouelaziz, J. C. Gomet, D. Pasquerault, B. R. Rowe, and J. B. A. Mitchell, J. Chem. Phys. 99, 237 (1993).
15 L. Lehfaoui, C. Rebrion—Rowe, S. Laube, J. B. A. Mitchell, and B. R. Rowe, J. Chem. Phys. 106, 5406 (1997).
16 C. Rebrion-Rowe, L. Lehfaoui, B. R. Rowe, and J. B. A. Mitchell, J. Chem. Phys. 108, 7185 (1998).
17 N. G. Adams and D. Smith, in Rate Coefficients in Astrochemistry, edited by T. J. Millar and D. A. Williams (Kluwer Academic Publishers, The Netherlands, 1988), pp. 173.
18 J. B. A. Mitchell and C. Rebrion-Rowe, Int. Rev. Phys. Chem. 16, 201 (1997).
19 J. Semaniak, A. Larson, A. Le Padellec, C. Stromholm, M. Larsson, S. Rosen, R. Peverall, H. Danared, N. Djuric, G. H. Dunn, and S. Datz, Astrophys. J. 498, 886 (1998).
20 K. Takita, T. Sato, Y. Ju, and G. Masuya, "Effects of Addition of Radicals Supplied by Plasma Torch on Burning Velocity," AIAA 99-2247, 1999.

21 T. Nagashima and H. Kitamura, "Supersonic Combustion of Hydrogen in Tandem Transverse Injection with Oxygen Radicals," ISABE 97-7055, 1997.
22 Y. Sato, M. Sayama, K. Ohwaki, G. Masuya, T. Komuro, K. Kudou, A. Murakami, K. Tani, Y. Wakamatsu, T. Kanda, N. Chinzei, and I. Kimura, "Effectiveness of Plasma Torches for Ignition and Flameholding in Scramjet," AIAA 89-2564, 1989.

PLASMADYNAMIC DISCHARGES AND PROSPECTS OF THEIR APPLICATION IN PULSED PERIODICAL COMBUSTION AND DETONATION INITIATION AND CONDUCTING LAYERS FORMATION IN SUPERSONIC FLOWS

Chuvashev Sergey N., Timofeev Boris I.

Computer Science Faculty, Moscow State University, 119899 Moscow, Russia, tel. (007) 095-939-37-95, e-mail schuv@cs.msu.su, snchuv@orc.ru

Abstract

On base of an extensive experimental and theoretical material [1-12], it is shown that such problems of creation of the hypersonic vehicle as:

1. supersonic flow volume ignition,
2. pulsed-periodical initiation of detonation,
3. formation of transversal periodical high conductance layers in a supersonic airflow (for MHD interactions) –

can be solved with use of the plasmadynamic discharges

1. Plasmadynamic Discharge Physics and Properties

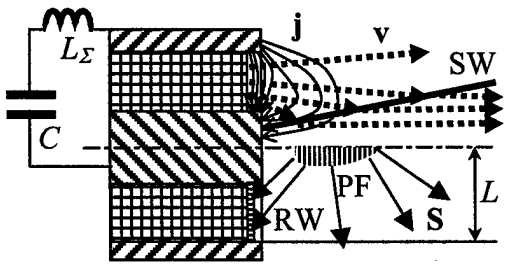

Fig.1. A schematic draft of the plasmadynamic discharge with the previously evacuated gap – the magnetoplasma compressor

The plasmadynamic discharges with the erosive mechanism of plasma formation differ radically from the other types of discharge (arc, corona, glow discharges a. o.) [1].

Such discharges are observed at high current (I = 10-10000 kA) pulses formed, say, at discharges of low inductance (L_Σ = 50-1000 nH) high voltage (U = 2-50 kV) capacitors. The most widely used design of the electrode unit (see Fig.1) is characterized by a couple of coaxial cylindrical electrodes and a dielectric insulating insert between them. The discharge is formed in the inter-electrode gap near the crosscut end of the pencil-like electrode unit (see Fig.1). Due to a considerable compression of the erosive plasma on the axis it is often called "the magnetoplasma compressor".

If the discharge gap is previously evacuated, the processes are as follows. Nearly a half of the discharge electric current flows near the surface of the dielectric insert. Plasma is formed of products of decomposition of the dielectric. The decomposition and further ionization and heating of the products is a result of absorption of a powerful radiation flux S_0 from the plasma focus PF in the

radiation wave RW (see Fig.1) to be formed near the surface. The balance of energy for the radiation wave yields:

$$\rho_0 v_0 = S_0 m_i / h_{i0},$$

here ρ_0, h_{i0} (T_{i0}), m_i, v_0 are plasma density, enthalpy, mean ion mass, and speed below the RW, correspondingly. The plasma temperature T_{i0} is shown to be the temperature of equilibrium single ionization (at which the number of neutral atoms becomes negligible); say, for the Teflon insert, T_{i0} = 1.65 eV. This fact results from an analysis of radiation heat transfer in the plasma and the gaseous products of decomposition [2].

The plasma formed is accelerated by the Ampere force of the discharge current. Due to a considerable radial dependence of the length of the acceleration zone, the plasma flow is focused to the symmetry axis. As the flow is hypersonic, it results in a formation of a strong shock wave SW (see Fig.1).

Note that the dielectric erosion rate is rather low. Actually, the major part of the electric energy release in the discharge E_Σ is transferred into the kinetic energy of the plasma flow:

$$E_\Sigma = M_\Sigma v_0^2/2,$$

here M_Σ is the total plasma mass. This mass corresponds to an evaporation of the dielectric layer with a thickness

$$\delta = M_\Sigma /(\rho_d \pi L^2),$$

here ρ_d is the density of the dielectric. E.g., at E_Σ = 1 kJ, ρ_d = 2 kg/m^3, L = 0.5 cm, v_0 = 50 km/s, the total mass is M_Σ= 0.8 mg, and only δ = 5 μm of the dielectric surface is gone. One should also take into account, that even a considerable erosion with $\delta < L$ does not alter significantly the discharge gap geometry (see fig. 1) and thus does not affect the main parameters of the discharge. This corresponds to $N = L/\delta$ = 1000 discharges. Moreover, it looks possible to synchronize the processes of erosion of the electrodes and the dielectric so that the geometry of the inter-electrode gap would be the same at even more pulses (the electrode unit would be diminishing slowly, like a candle). In such a case, N could be much higher than L/δ. Thus, the plasmadynamic discharge units are very durable. It can be still improved, say, with use of a supply of a liquid or gaseous matter through pores in the dielectric insert and/or the electrodes (for the formation of the discharge plasma of this matter instead of the erosive mechanism of formation of the plasma of the dielectric material). The durability of the plasmadynamic discharges corresponds with the experimental practice.

These discharges can be optimized to be effective sources of either plasma jets with a high pressure head, or strong shock waves in a dense gas, or powerful flows of ultraviolet radiation. All of these three modes can be effectively applied for the plasma aerodynamic applications. Consider at first the possibility to generate plasma jets which can penetrate deeply into a gas and ignite it far from the walls, then the possibility to generate shock waves sufficient for the combustible mixture detonation, the positive effect of the powerful radiation, and the new concept of a pulsed periodical detonating hypersonic jet engine based on this discharge.

2. Long Penetration Modes of the Plasmadynamic Discharge Jets. Volume Ignition. Creation of Transversal High Conductance Layers in an Airflow for the MHD Applications

If the inter-electrode gap before the discharge is filled with a dense gas, the discharge passes through several stages: the surface discharge (like an arc), the discharge with a current sheath, the plasmadynamic discharge with a double cumulating, and the quasi-vacuum plasmadynamic discharge. The last stage is of the most interest for the purposes of formation of long plasma jets and strong shock waves. It can be roughly considered as

a combination of two independent complex processes: 1 – the formation of the plasma jet at the plasmadynamic discharge (see above), 2 – the interaction of the hypersonic plasma jet with the dense gas.

To the first approximation, one can consider a one-dimensional interaction of the gas with a cylindrical hypersonic plasma jet, with a formation of two strong shock waves. This simplified approach results in a good correspondence with experimental data [9-11] on the jet's length, speed, etc.

If one considers the shock waves to be very strong, one can apply the following approximate expressions for the parameters of the shock structure [11]:

$$v_j = v_{pl}/[1+(\rho_g/\rho_{pl})^{1/2}],$$

$$p' = (\gamma_{pl}+1)\rho_{pl}\,(v_{pl}-v_j)^2/2,$$

$$\rho_{pl}' = G_g\,\rho_{pl},\ G_g = (\gamma_g+1)/(\gamma_g-1),$$

$$T_{pl}' = (\gamma_{pl}-1)\,m_{pl}\,(v_{pl}-v_j)^2/(2k_B),$$

$$\rho'_g = \rho_g[G_g\,p'/p_g + 1]/[G_g + p'/p_g],$$

$$v_j = [(p'-p_g)/(V_g - V')]^{1/2},\ V' = 1/\rho',$$

$$D' = [(p'-p_g)/(1/\rho_g - 1/\rho')]^{1/2}/\rho_g,$$

$$T'_g = m_g\,p'/(\rho'_g\,k_B),$$

here v_j is the speed of jet propagation, p' is the pressure between the shock waves, γ_g, γ_g are the adiabatic exponents of plasma and gas, ρ_{pl}', ρ'_g and T_{pl}', T'_g are the densities and temperatures of the compressed plasma and gas, D' is the speed of the shock wave in the gas, k_B is the Boltzmann constant, m_g is the mean molecular mass of the compressed gas. The speed v_{pl} and density ρ_{pl} of the plasma flow can be taken from the model of the vacuum plasmadynamic discharge [1].

The axial size of the plasma jet is

$$x_j = {}_0\int^t v_j\,dt.$$

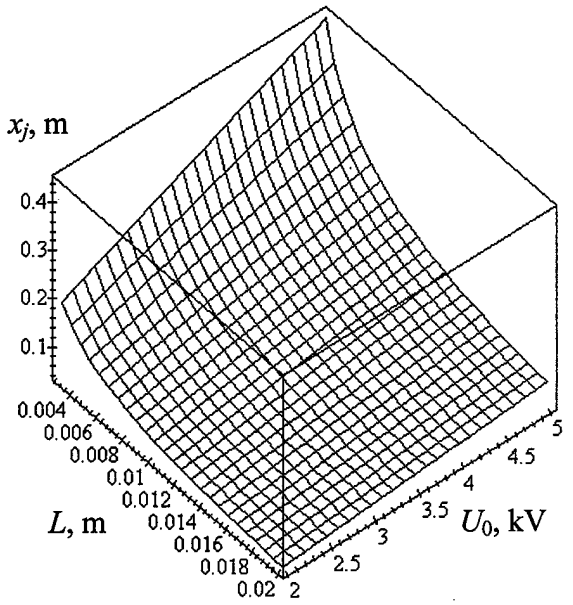

Fig.2. Characteristic length of the plasma jet over the initial voltage and the electrode unit characteristic size at the gas density $\rho_g = 0.26$ kg/m^3

The formulated model has been tested with use of the experimental data [11], a good correspondence has been achieved. The calculations have been produced for a broad range of all the parameters. Computations in terms of parameters of the capacitor based power supply source show that a very deep (up to 0.5 m) penetration is available with use of a capacitor battery with moderate parameters (see Fig. 2). The plasma temperature T_{pl}' = 3...30 eV is far much higher than that needed for the ignition (1500...3500 K). The main mechanism of energy transfer between the plasma jet and the gas is the turbulent heat conductance. It means that a continuous temperature profile ranging from T_{pl}' to $T_g \approx$ 200...300 K is formed, and there surely exists a region in the gas with the parameters optimal for the ignition.

Thus, an effective ignition of supersonic air-fuel mixtures can be provided far from the walls with use of a reliable, durable, low

energy, small size device on base of the plasmadynamic discharge.

The deep penetration of the plasmadynamic discharge jets into a dense supersonic airflow, as well as an ignition of the kerosene vapors in the atmosphere have recently been demonstrated in experiments [13].

Note that the long jets can be applied for a formation of periodical transversal conducting plasma layers in the airflow near a hypersonic vehicle, which can make it possible to implement the concepts of magnetic hydrodynamics now being considered for hypersonic vehicles [14]. For a longer lifetime, the jet plasma may contain elements with low ionization potentials.

3. Detonation Initiation by the Plasmadynamic Discharge. On the Concept of Pulsed Periodical Detonating Engine

It is well known that, say, if the temperature of the combustible mixture is enhanced suddenly, a considerable latent period τ_{lat} precedes the energy release stage. The temperature rise after the latent period is very fast, and one can consider the front of heating as a discontinuity. The total reaction period of time $\tau_{ch} \approx \tau_{lat}$ determines the condition of formation of the detonation wave: the shock wave in the combustible mixture must provide such parameters (pressure p' and temperature T') that the reaction period of time $\tau_{ch} = \tau_{ch}(p', T')$ would be much less than the characteristic time τ' of existence of these parameters. The necessary strong shock wave in the combustible mixture can be formed by the plasmadynamic discharge (see above). It means that it is possible to form the detonation wave just near the ignition system. As these shock waves are not planar, τ' here depends on the shock wave initial radius of curvature r_c and on its speed D'. The detonation condition is

$$\tau_{ch}(p', T')\, D' << r_c.$$

Assume that the parameters of the shock waves are not far from that of the cylindrical strong shock waves formed by a sudden energy release on the axis [15]. The shock wave parameters – radial coordinate r_c and speed D_c, pressure p_c , density ρ_c, and temperature T_c just behind the shock – change with time as

$$r_c = r_{c0}(t/t_{c0})^{1/2},\ D_c = 0.5\, r_c/t,$$
$$p_c(t) = 2/(\gamma_g+1)\ \rho_g D_c^2[1-(\gamma_g-1)/(2\gamma_g)\ v_{sg}^2/D_c^2],$$
$$\rho_c(t) = (\gamma_g+1)/(\gamma_g-1)\ \rho_g/[1+2/(\gamma_g+1)\ v_{sg}^2/D_c^2],$$
$$T_c(t) = p_c m_g/(\rho_c k_B).$$

The characteristic time t_{c0} can be expressed through the initial pressure between the shock waves p' with use of a condition $p_c(t_{c0}) = p'$. The initial radius of the shock wave curvature $r_{c0} \approx 0.45\ L$ (it results from a gas dynamical similarity and the experimental data [9]). Thus, the condition of detonation at the plasmadynamic discharge can be formulated as

$$P_D = \tau_{lat}(p', T')\, D'\, C_8 / r_c > 1.$$

Say, in case of the RLC circuit, P_D depends on the capacity and the initial voltage of the storage condenser, and the values of inductance and resistance of the electrical pathway to the discharge gap.

Formulae of "gross" reactions can be applied for estimates of the function $\tau_{lat} = \tau_{lat}(p', T')$. Say, for the stoichiometric air-methane mixture the rate of the gross reaction of activation is [16], [17]

$$K_M = n_{O2}\, n_{C2H4} C_M/T \exp(-E_M i(k_B T)),$$
$$C_M,\ E_M = \text{const}.$$

With a respect to the practical inefficiency of the reactions of association at high temperatures [18],

$$\tau_{lat} = k_B T^2/[(T_{max}-T)\, E_M K_M],$$

here T_{max} is the maximal possible temperature after combustion at V=idem.

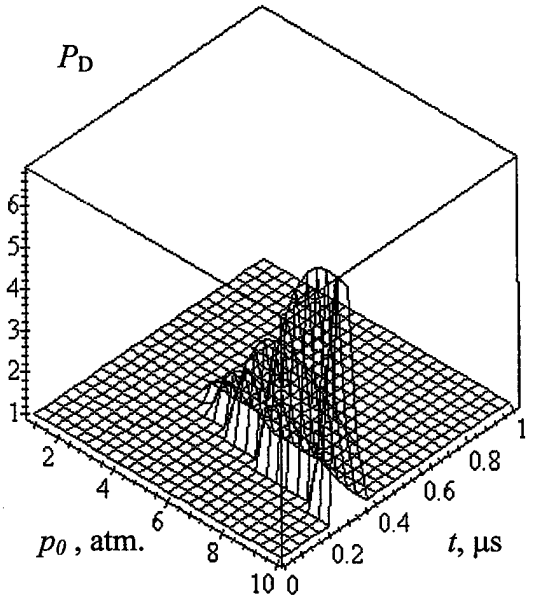

Fig. 3. On the detonation conditions under the effect of the shock wave over the expansion time and the initial pressure (at the normal temperature) before the nozzle for a formation of a supersonic (M=2) flow of the stoichiometric methane-air mixture. The plasmadynamic discharge parameters: initial voltage 5 kV, inductance 5 μH, capacity 30μF, electrode characteristic size L = 1 cm

The relations listed above form an approximate model of detonation at the plasmadynamic discharges in an air-fuel mixture. Results of calculations (Fig. 3) show that the conditions of detonation initiation are achieved at a certain separation from the initial position of the shock wave (or at a certain delay time t). For a less separation, the gas temperature behind the shock wave is too high. Later, the temperature would be insufficient for the ignition to take place during the pass time. Anyway, if with time growth the value of P_D achieves 1, the detonation will be initiated. For some modes corresponding to lower gas density, the value P_D never exceeds 1. Then the probability of the immediate detonation is poor.

Our computations also show that the detonation probability is less for the electrode systems with less characteristic size L. It means that the principles of optimization are different for the volume ignition and for the detonation initiation. The detonation probability is not very sensitive to the initial energy store, i.e. the pulse energy can be rather low.

Note that it can be possible to improve the conditions of detonation ignition by a change of the shock wave geometry (say, with an insertion of the plasma jet into a tube).

The plasmadynamic discharges are known to be effective sources of powerful short wave electromagnetic radiation. Their radiation efficiency (i.e. the ratio of the radiated energy over the total electric energy input) can achieve η = 30...50% [1,5,6,10,11]. The radiation of the plasmadynamic discharges in vacuum lies mainly in the far vacuum ultraviolet with quantum energy $h\nu$ = 20...50 eV. The plasmadynamic discharges radiation in rare gases occupies primarily the vacuum ultraviolet spectral region between 5...7 eV and the gas ionization potential. At the discharges in the air, the radiation at the plasma-gas boundary is characterized by quantum energy between 4..5 and 10...15 eV, but its short-wave component is absorbed near the boundary primarily by the oxygen and water molecules. The total efficiency η can be still high enough even in the air, due to a secondary irradiation of the absorbed energy [12].

The radiation absorption in the vicinity of the plasma-gas boundary is bound primarily with a dissociation of molecules. The interaction takes place either in the form of radiation wave (see Fig.4,*a*), or in the continuous absorption mode (see Fig.4,*b*). The actual mode depends on the optical properties of the molecules, their concentration, and the primary spectrum of the radiation. In a combustible mixture, it can result in a creation of a number of active particles (primarily atoms and radicals) sufficient to

promote the processes of burning dramatically, and to improve the conditions for detonation initiation radically (see Fig.4).

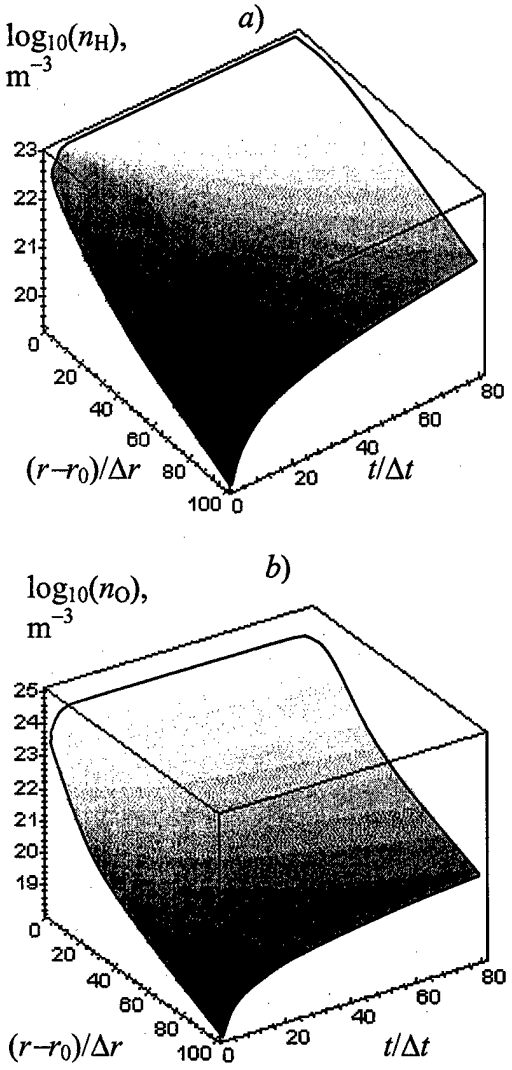

Fig. 4. Spatial and temporary distributions of the atoms of hydrogen (*a*) and oxygen (*b*) due to the photo-dissociation in the radiation field of a 200 J, 50 μs plasmadynamic discharge in the 10^{25} m^{-3} mixture of air with 1% of H_2S and 6% of CH_4 (no other reactions are accounted for, $r = 5$ mm, $\Delta r = 0.5$ mm, $\Delta t = 0.2$ μs)

It means that the energy needed for the pulse can be reduced to ≈100 J or less. The necessary frequency of detonation initiation (corresponding to the gas transit time) is available for these discharges, the durability of the discharge gap unit is high enough.

This makes it possible to consider a development of a pulsed-periodical detonating ramjet engine on base of the low weight, durable, low power, small-size igniting system with no moving mechanical parts.

References

1. Chuvashev S.N., Protasov Yu.S. On the Scaling of the Plasmadynamic Radiating Discharges of the Magnetoplasma Compressor// Sov. Applied Mechanics and Technical Physics. 1990. N 4. Pp. 19-26.

2. Chuvashev S.N., Kamrukov A.S., Kozlov N.P. On an Effect of Ionization Energy on the Processes of Formation of the Plasma Focus in the Erosive Type Plasmadynamic Discharge // High Temperature. 1984. V.22. No. 4. Pp.789-792.

3. Ardelyan N.V., Chuvashev S.N., Kosmachevskii C.V. a.o. Numerical Modeling of Radiating Plasmodynamic Discharges of Erosive Type Magnetoplasma Compressors. // Sov.Physics: Doklady. 1987. V.292. N 3.

4. Thermodynamic and Optical Properties of Plasma of Metals and Dielectrics //Boyko Yu.V., Chuvashev S.N., Grishin Yu.P., a.o. Moscow: Metallurgiya. 1988. 450 pp. (There is an English translation by "Hemisphere", 1989).

5. Kamrukov A.S., Kozlov N.P., Protasov Yu.S. Dynamics and Radiation of the Open (Vacuum) Plasmadynamic Discharges of the "Plasma Focus" Type.// High Temperature. 1982. V. 20. N 2. Pp. 359-375.

6. Vladimirov V.V., Divnov I.I., Zotov I.N. a.o. The Magnetoplasma Compressor with the Explosive Magnetic Energy Generator. //Sov.J. Technical Physics. 1980. V.50. N 7. Pp. 1521-1524.

7. Ardelyan N.V., Chuvashev S.N., Kosmachevskii C.V. a.o. Phenomena of Magnetic Gas Dynamics at an Interaction of Erosive Plasma Flows of the Magnetoplasma Compressor with a Gas. // Sov.Physics: Doklady. 1987. V.292. N 1. Pp.78-81.

8. Chuvashev S.N., Kamrukov A.S., Kozlov N.P., Protasov Yu.S., Schepanyuk T.S. On an

effect of Hydrodynamic Instabilities on Spectral and Brightness Characteristics of Radiating Discharges. The Turbulent Modification.// Sov.J. Technical Physics. 1987. V. 57. N 7. Pp. 1412-1416.
9. Chuvashev S.N., Protasov Yu.S., Schepanyuk T.S. Experimental Study of the Internal Structure of the Radiating Plasmadynamic Discharges of the Magnetoplasma Compressor in Gases. // High Temperature. 1990. V.28. No. 3. Pp.444-454
10. Kamrukov A.S., Kozlov N.P., Protasov Yu.S. On a Possibility of Creation of High Brightness Radiation Sources on Base of Shock Wave Generation in Hypersonic Plasma Flows in Dense Gases // Sov. Physics: Technical Physics (J. Tech. Phys.). 1982. V.52. No.11.
11. Kamrukov A.S., Kozlov N.P., Protasov Yu.S. Plasmadynamic Sources of High Brightness Radiation, and Generators of Strong Shock Waves// In: Radiating Plasma Dynamics. Moscow: Energoatomizdat. 1991. Pp. 10-156.
12. Chuvashev S.N., Kamrukov A.S., Kozlov N.P., Protasov Yu.S. Radiation Gas Dynamical Processes in the Cumulating Plasmadynamic MPC discharges // J.Technical Physics. 1985. V. 55. N 3. Pp. 533-543.
13. Chernikov A.P., Chuvashev S.N., Ershov A.P., Shibkov V.M., Timofeev I.B. Crossed Supersonic Jets of Plasma and Dense Gas// The 2-nd Workshop on Magneto-Plasma-Aerodynamics in Aerospace Applications (Abstracts). Moscow: Inst. High Temperatures.2000. P.68-69.
14. The 2-nd Workshop on Magneto-Plasma-Aerodynamics in Aerospace Applications (Abstracts). Moscow: Inst. High Temperatures.2000. 107 pp.
15. Sedov L.I. Methods of Similarity and Dimensions in Mechanics. Moscow: Nauka. 1987. 432 pp.
16. Williams G.C., Hottel H.C., Morgan A.C. The Combustion of Methane in a Jet Mixed Reactor. Proc. 12th Symp. Combustion. Pittsburgh:1969. P.913-920.
17. Todes O.M. Theory of Thermal Explosion. 1. Thermal Explosion of Zero Order Reactions. // Sov.J.Physical Chemistry.1939.V.13.N 7. P.868-879.
18. Zel'dovich Ja.B., Barenblatt G.I., Librovich V.B., Mahviladze G.M. Matematical Theory of Burning and Explosion. Moscow. Nauka.1980. 480 pp.

PLASMA GENERATORS FOR COMBUSTION.

Bityurin V, Brovkin V., Klimov A., Leonov S.

Institute of High Temperature RAS/ MTC

In the our previous works [1-8] it was underlined, that for generation of non equilibrium plasmoids (NP), with optimal parameters for plasma aerodynamic experiment and combustion experiment, it is necessary to fulfil a number of contradictory requirements, namely:

- to insure maximum high level of non equilibrium ($T_e >> T_g$, $N^* \sim 10^{15} \div 10^{17}$ cm^{-3}, N^* - is concentration of electronically excited molecules, atoms etc.);
- to insure anomalous long periods of plasma decay (long "lifetime" of plasma);
- to create cold, not overheated plasma, with $T_g < 600$ K, etc.

It can be seen that such conditions can be realised only in pulse discharge (PD), at specific conditions (for example, discharge inside the capillary or sliding discharge etc.). Indeed, high values of reduced electric field strength E/N can be achieved only in PD, with sharp fronts. Remember, that parameter E/N determines types of main plasma chemical processes and level of non equilibrium in plasma.

Application of PD with definite parameters gives possibility to achieve:

- cold, non overheated plasma;
- high values of Ne and N* without generation of different types of instabilities, including thermal one, in plasma;
- high current and high power in discharge during short pulse, etc.

Interactions of NP, created by PD, with different gas dynamic disturbances and using of these NP for ignition and plasma assisted combustion are described in [1-8]. It was shown that plasma obtained by means of PD is characterised by three important parameters:

- -time period of activation, tact;
- -time period of plasma "memory", tpm.
- -optimal value gas discharge parameter E/N

The authors of this work designed and constructed the perspective plasma generators for aerodynamic and combustion applications on the base of experimental results, obtained in studies of PPD. HF Tesla's coil PG (PG HF) is one of them.

HF Tesla's PG has the following characteristics:

- Working frequency 13.6 MHz.
- Mean HF power < 2 kW.
- Output voltage <5 kV.
- Operation mode continuous and pulse repetitive modes.
- Pulse repetitive frequency Fm= 10 Hz ÷ 50 kHz .

Physics properties of HF discharge.

1. In the supersonic flow before the head shock wave near the aerodynamic model there was created one- electrode HF discharge by means of Tesla's PG, Fig.1,2.
2. It was revealed that the HF discharge burns very stable in a supersonic flow at M~2 and P_s= 40÷ 300 Torr. Various types of the plasma formations (PF) and plasma

structures were generated in gas flow in respect to the PG's power, static pressure, outputting voltage etc.:

- Diffusive spherical PF at $P_s \leq 100$ Torr. Sizes of such a PF does not exceed 1÷ 5 cm, Fig. 1 ;
- Streamer filamentary corona, Fig. 2. Diameter of the separate streamer does not exceed 1 mm, its length can reach 10 cm.

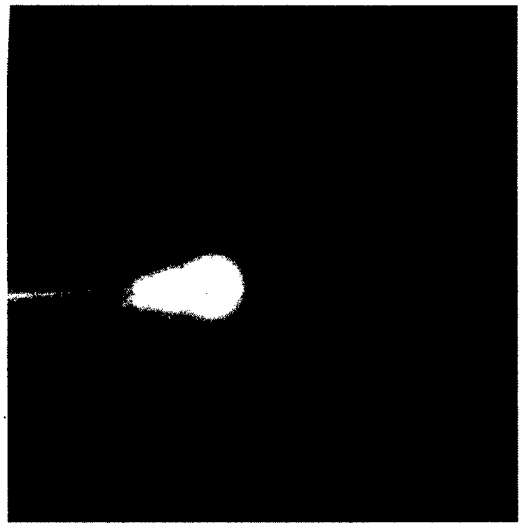

Fig.1. HF discharge near hot electrode in supersonic flow (M~ 2, P_{st}~100 torr).

Fig. 4. Streamer corona HF discharge in supersonic flow (M~ 2, P_{st}~ 200 torr). Small injection of Propane/ Argon mixture (1: 9) throw small nozzle in ball electrode. (Nozzle is located in bottom part of this figure).

3. In the course of optical spectroscopy measurements it was revealed that
   - gas temperature inside streamer
     $T_g \sim 400 \div 1000K$,
   - vibration temperature inside streamer
     $T_V \sim 2000 \div 4000K$.
4. Estimations of other plasma parameters, based on measured value of discharge conductivity:
   - Electron concentration inside streamer
     $N_e \sim 10^{-15}$ cm^{-3}
   - Electron temperature
     $T_e \sim$ 1-2 eV.
5. The change of Tesla's PG resonant frequency (up to 10%) tooks place during the creation of a discharge in a gas flow. Therefore it is required PG tuning with the help of variable capacity.
6. It was revealed that the density of streamers in the HF plasma corona increases at resonant conditions. Streamers concentrate near the model's axis at resonant conditions also.
7. It was revealed that HF-discharge was easily ignited and stable burned inside of the separation zones with decreased density and decreased pressure.
8. Additional heating of gas destroys streamers. Torch HF discharge is created in hot gas.
9. In experiments there was studied the possibility of the additional stabilizing and concentration of the streamer HF discharge near the model' s axis by means of:
   - dielectric and metallic needles,
   - ejection of the Argon- jet,
   - additional external DC electric field

   In the second case there was used the Argon- jet injection with small consumption. It was revealed that the use of Argon jet considerably decreases the thresholds (up to 5 times) of the electric breakdown and burning of HF discharge near a model in the supersonic gas flow. In experiment we succeeded in obtaining of the streamer corona in a flow at high static pressure $P_s \sim 1$ Bar.
10. It was revealed that the application of the additional modulation HF radiation

considerably stabilizes the streamer corona in supersonic gas flow.

11. Calorimetric measurements of HF discharge have shown that power input in streamer corona is about ~60÷70 % total PG power at the resonance. It means that Tesla 's PG is high effective one.

Study of control of ignition and combustion of fuel/ air mixture (propane/ argon / air mixture) by means of HF discharge in supersonic flow.

This mutual experiments were fulfilled together with our colleagues from Moscow Aviation Institute and NIIRP [8].

Main Goal of these experiments:

- Study of ignition, combustion and mixture of propane (kerosene) in supersonic airflow by means of plasma formation at the conditions, closed to scram jet ones.

We use HF PG for creation structural plasmoid (streamer HF discharge) in a supersonic flow. Activated fuel molecules and radicals are generated by this HF PG. Plasma-gas burner consists of the following units (Fig.2):

- Dielectric cylindrical body with HF transformer (Tesla's coil),
- Top conical (or spherical) metal electrode,
- Tubes and small nozzle for ejection Argon (air) and Propane inside of this burner.

Diameter of this gas- burner is 40 mm.

This gas- burner is located inside wind tunnel (WT) near the supersonic nozzle. We can change position of this gas- burner along supersonic jet axis in range of 2 ÷ 20 cm, measured from nozzle end.

Supersonic flow in WT has following parameters:

- Mach number M~ 2.
- Static pressure P_{st}~ 100 torr.

Fraction of Propane in Propane/ Argon mixture was changed from 0.1 up to 1. Note that Propane/ Argon mixture (1: 9) is non-burning one in normal conditions.

Experimental results.

1. Streamer (filament) HF discharge was created near the top of metal electrode of gas- burner. Strong non- equilibrium cold HF plasmoid was generated in supersonic flow.
2. Study of stable ignition, combustion of Propane/ Argon/ air mixture controlled by HF plasma was fulfilled in WT. It was revealed that HF discharge considerably activates chemical reactions of burning of fuel/air mixture in a supersonic flow. It is need to note that we succeeded in ignition and stable burning of very poor Propane: Argon mixture (1: 9).
3. We have realized very stable operation mode of burning of Propane in supersonic flow (M~ 2) at atmosphere pressure (1 Bar). The form of burn reaction zone was closed to ball shape. The ball had bright green-blue color.
4. Small HF power is needed for propane/air ignition and generation of radicals in supersonic flow. The value of HF power was closed to minimal threshold of generation of HF discharge, about ~100W, in WT experiment.
5. It was revealed that fuel could deeply penetrate throw supersonic flow inside HF streamer channel. This result helps us to create principal new type of plasma fuel/ air mixing in scram jet.
6. Parameters of reaction zone are depended on HF power, total pressure of Propane, total pressure of Argon and static pressure of supersonic flow.

References.

1. Review of Experimental and Theoretical Studies of Methods of Reduction of Drag Body Force and Sonic Boom by Use of Special Plasma, Moscow, 1995.
2. Klimov A.I., Mishin G.I., Fedotov A.B., et. al. Propagation of SW in non stationary glow discharge, Pisma v Zhurnal Technicheskoi Fiziki (Sov. Tech. Phys. Lett.), 1989, V.15., N. 20, p. 31-36

3. Klimov A.I., Koblov A.N., Mishin G.I., et.al. SW propagation in a decaying plasma, Sov. Tech. Phys. Lett.,1982, V.8, N.5, p.240-241.
4. Mishin G.I., Serov Yu.L., Yavor I.P. Flow around a sphere moving supersonically in a gas -discharge plasma, Sov. Tech. Phys. Lett., 1991, V.17, N.6, p.413-415.
5. Klimov A.I., Gorshkov V.A., Mishin G.I., et.al. Behaviour of electron density in a weakly ionized non equilibrium plasma with a propagating SW, Sov. Tech. Phys. Lett., 1987, V.32, N. 10, p. 57.
6. Gritsynin S.I., Kossyi I.A., Silakov V.P. et al. Long lived plasma in gases of high pressure, created by sources UV radiation. Teplofizika Vysokhikh Temperatur. 1986. V.24. N. 4.P.662.
7. Ball Lightning in Laboratory .Editors: Avramenko R.F., Bychkov V.L., Sinkevich O.A., Klimov A.I. Moscow. Chimia publishers. (in Russian) 1994. p.291.
8. Bityurin V.A., Klimov A.I., Lebedev P.D. and others. Study of ignition and burning of fuel-air mixture in supersonic flow stimulated by HF streamer discharge. TVT, 2000, (in publishing).

EFFECT OF HYDROGEN FUEL BURNING NEAR TO AIRCRAFT SURFACE ON ITS AERODYNAMIC PROPERTIES

Kirillov I.A., Krasilnikov A.V., Panasenko A.V.

A numerical modeling of the flow near cone in result of the supersonic hydrogen jet injecting at the tip of the aircraft nose into the oncoming supersonic flow is conducted. The unsteady Euler equations in integral conservative form for mass, impulse and energy of the multicomponent gas mixture jointly with the chemistry kinetic equations were considered. The well-known McCormac difference scheme was used.

The calculations were fulfilled at the different hydrogen jet stagnation temperature, concluding the value up to the ignite temperature. In last case the much attention was to study the oncoming flow interaction with the exothermal reaction zone, which at the detonation absent is a factor for the aerodynamic drag reduction.

ROLE OF THE DISSOCIATION PROCESSES IN CHEMISTRY OF FLOWS OF HOT GASES , EXCITED BY ELECTRON BEAMS

Bytchkov V.

Institute for High Temperature RAS, 127412 Izhorskaya 13/19 Moscow Russia

1. Attention to studies of chemically active gas ionization by electron-beams is caused by low sensitivity of the electron - beam method of ionization to the conditions of plasma creation, namely to gas properties and gas-mixture properties as well, including different additives, such as aerosols and powders [1]. It caused appearance of a number works on the molecular oxygen ionization [2,3]. In the reference [2] was considered the penetration of strong electron beams (E_b ~0.5 MeV and current density j_b =10-10^3 A/cm^2) in this gas at the atmospheric pressure at the supposition that the excited gas temperature equals to the room temperature the calculations of excited and ionized particle appearance were carried out during the pulse time ~10-60 ns. At this high level of the excitation the generation of vibrationally excited molecules of oxygen was obtained (up to 10^{16} cm^{-3}), oxygen atoms (up to $5 \cdot 10^{15}$ cm^{-3}) and ozone (up to 10^{15} cm^{-3}). In this case the mane type of ions was O_3^+. In the reference [3] calculations of the oxygen's electron - beam excitation was carried out for a gas density N=10^{+17} cm^{-3} and the current density j_b =2.6 10^{-7}A/$см^2$, and also at N=10^{+19} $см^{-3}$ and j_b =10^{-5}A /$см^2$. During the time about 100 s in the first case up to 10^{+14} cm^{-3} of ozone molecules were generated and up to 10^{+12} $см^{-3}$ of excited O_2 ($^1\Delta$) molecules, the main negative ion type was O_3^- with the concentration about 10^{+9} cm^{-3}. In the second case the concentration of ozone was about 10^{+16} cm^{-3}, and O_2 ($^1\Delta$) up to 10^{+14} cm^{-3}. These facts demonstrated the high level of chemical non equilibrium caused by fast generation of atoms and their reactions. In so doing [3] with the gas heated up to 1500 K demonstrated the ozone destruction, and the atomic oxygen, which is the active radical, becomes the main chemically active particle, its concentration reaches the value 5 10^{+15} cm^{-3}. In this case the gas was chemically active as well but with another main chemically active component.

2.From references follows that the heating of the oxygen dramatically changes the composition of main generated components. Since the medium of the heated oxygen is a very rare experimental object then the investigation of heated electron - beam plasma of air is of interest from the point of view of treatment of surfaces of materials and of creation of non equilibrium MHD generators. Properties of this ionized media can differ significantly from properties of the cold air. It is connected with the difference of the initial composition of a gas mixture where molecules O_2 and NO represent greater parts in comparison with cold air [5].

For investigation of hot electron - beam excited air the physical model was developed [4]. Schemes of positive and negative ion transformation (at the absence of CO_2 molecules in the mixture) are represented in Fig.1-2. (it is possible to vary the water vapor concentration starting from

natural ~ 0.1 %, for which the results are obtained). In the model is accounted the neutralization of charged particles through electron-ion (pair and triple) and ion-ion (pair and triple) recombination [6]. In the model the heating of electrons in the processes of attachment and recombination is accounted. For calculations the numerical scheme of solution of a system of the stiff differential equations was used. It can be seen from the Fig.1-2 that the atoms play important role in kinetics of charged particles in electron - beam plasma. They appear in the result of straight dissociation by fast electrons and during dissociative recombination of slow electrons with molecular ions. From ~40 to 95% (in respect to excitation conditions) of inputted energy goes to this channel [1]. In Fig.3. the results of computations for electron concentration temporal dependence (pressure as the parameter) are represented. Excitation was modeled by the electron - beam pulse with the amplitude's value given in the figure, with the duration τ_b=1.2 μs, characteristic times for the current's rise and fall was 0,2 μs, energy of the electron - beam electrons was E_b=200 кэВ. In the Fig. 4. the electron temperature and plasma composition at P=0.1 atm, and current density j_b=1 A/cm^2 are represented. In the Fig.5. plasma composition at P=0.5 atm, and current density j_b=0.01 A/cm^2 are represented. From the pictures it can be seen that main types of positive ions at the computation times and humidity are NO^+, NO_3^+ and N_2H^+, at the same time the main negative particles are NO_3^-, NO_2^- and electrons (at higher humidity results in respect to ions would be different [4])

The time of electron-ion recombination is determined by the dissociative recombination of electrons with ions NO^+ (with the rate constant $\alpha_{disrec} \sim 10^{-8}$ см^3/с at given gas temperature)

$\tau \sim (N_{NO^+} N_e)^{-1} \sim 10^{-5}$ s it proves to be very long in comparison with the duration of the current's pulse. So the electron - beam plasma of the hot air can be used in devices where the high level of electric conductivity is required, namely, in non equilibrium MHD in particular in systems [7] in frames of the project of the supersonic aircraft Ajaks, where the electron - beam ionization of air is supposed.

References

1. Bychkov V.L., Vasiliev M.N., Koroteev A.S. Electron - beam plasma. Moscow. Moscow state open university publishers. 1993. 168 P. (in Russian).
2. Zaitseva N.S., Skvortsov V.A. in collection of papers "diffraction and radio wave propagation. MPTI. Moscow. 1985. P. 119-125. (in Russian).
3. Mnatsakanyan A.Kh., Naidis G.V., Solozobov Yu.M. Khimicheskaya Fizika. 1987. V 6. № 6. P. 820-824.
4. Bytchkov V.L., Kuranov A.L., Yurovsky V.A. Materials of 8-th All-Union conference Physics of low temperature plasma. Minsk. 1991. Part.3. P.47-48.
5. Kuznetsov N.M. Thermodynamic functions and Hugoniot air adiabats at high temperatures. M. Mashinostroenie. 1965. 463 P.
6. Flannery M.P. In a book: Gas lasers. Editors I.Mc.Daniel and W.Nighan Moscow. Mir. 1986. P.177-215.
7. Brichkin D.I., Kuranov A.L., Sheikin E.G. AIAA 99-4969. 9-th Int. Space Planes Hyper. Syst. &. Tech. Conf. 1-4, November, 1999, Norfolk, VA.

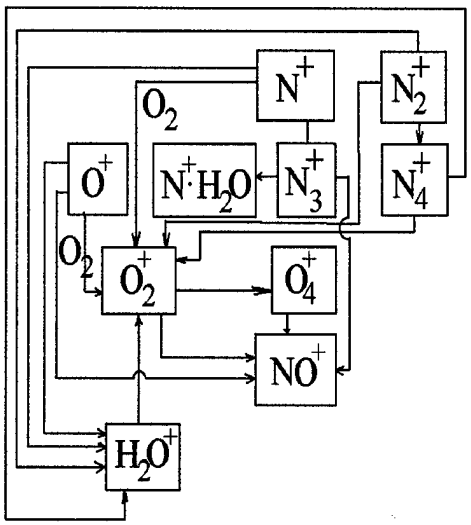

Fig.1. Scheme of positive ion transormation in electron-beam ionized hot air.

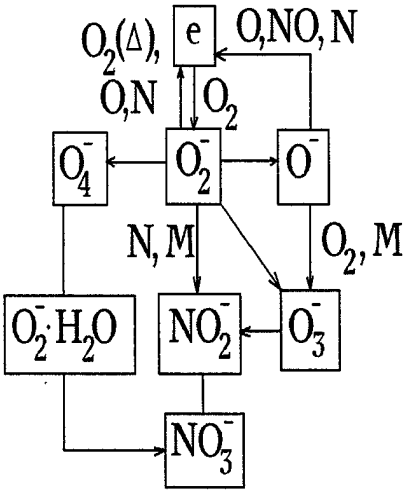

Fig.2. Scheme of negative ion transormation in electron-beam ionized hot air.

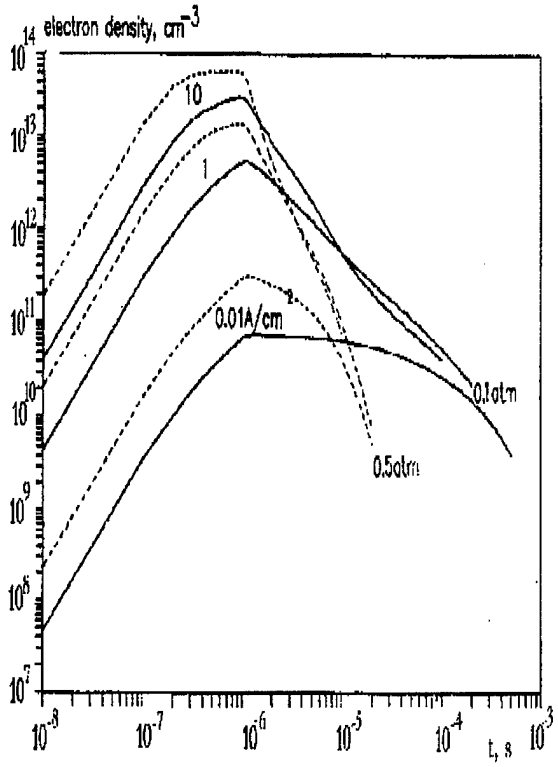

Fig.3. Temporal evolution of electrons in elec-tron - beam ionized hot air at a gas pressure 0.1 and 0.5 atm and current density 0.01, 1 и 10 A/cm^2.

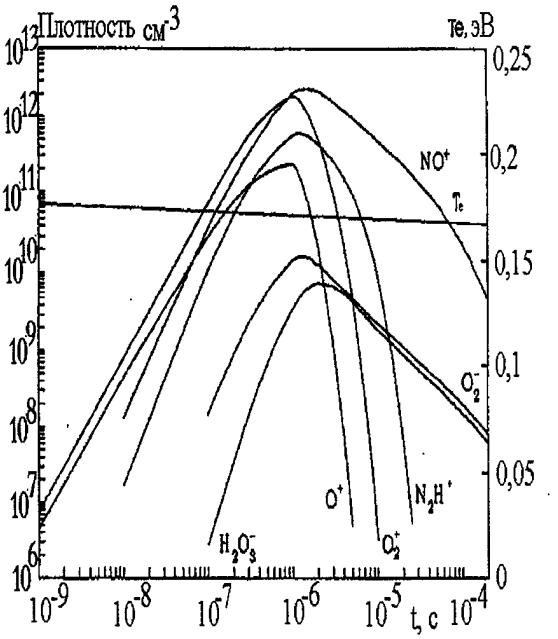

Fig. 4. Composition's evolution in electron-beam hot air plasma at a gas pressure 0.1 atm and current density 1 A/см^2.

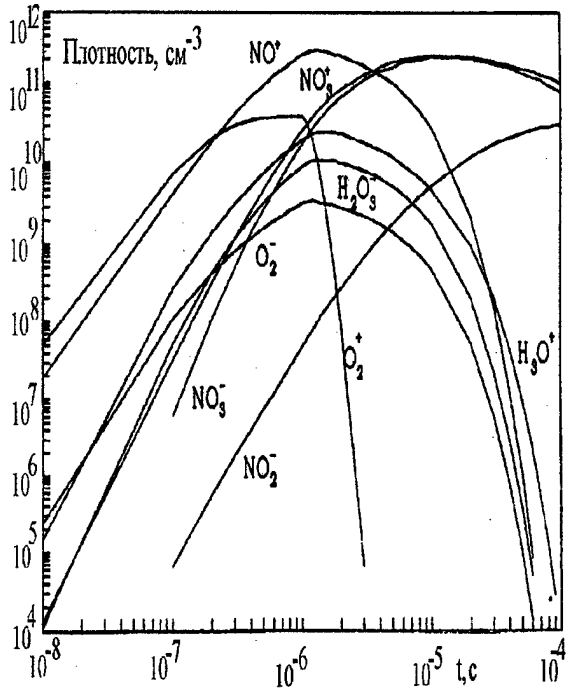

Fig. 5. Composition's evolution in electron-beam hot air plasma at a gas pressure 0.5 atm and current density 0.01 A/см^2.

PROCESSES OF FORMATION OF LARGE POLYMER STRUCTURES IN PLASMA MIXTURES WITH POLYMER COMPONENTS

Bytchkov V.

Institute for High Temperature RAS, 127412 Izhorskaya 13/19 Moscow Russia

1. Creation of macro structures in ionized medium is of interest from the point of view of technology development of powder and thin film polymeric (organic and inorganic) creation and of solution of a number of principle problems connected with appearance of heterogeneous particles in gases in low pressure gas discharges, so called dusty clusters. In particular they appear at the etching of material surfaces during production of chips, appear as aerosol clusters in ionized gases and at laboratory modeling of artificial long lived macro structures with solid framework - so called "laboratory fire balls" with the life time reaching several seconds.

It is worth to note that experiments with water clusters that appear during the humid air ionization by the radioactive source [1-3] show that such clusters disappear at the switching of the source off. With the aim of analysis of the possibility of appearance of large cluster structures with sizes up to several cm at high pressure (about the atmospheric one) the inves-tigations were carried out their results are represented below.

2. Analysis of experimental results with different gas discharges showed that the addition of organic components or molecules that can play part in polymerizing processes in the ionized medium often leads to the appearance of long lived structures of different types that resemble in the appearance interknitted thread tangles. To the first group of experiments can be attributed those with the application of high frequency discharges at low pressure (less than 1 Torr) in mixture of organic and inert gases [4-6]. In these experiments was often observed the appearance of so called "pow-ders" - particles with sizes 10^{-4}- 0.3 cm. Analysis of such powders under the micro-scope [5] showed that these structures represent interknitted links of macromo-lecules.

To the second group can be attributed the experiments with brush and pulse discharges at high pressure (~760 Torr) [7-10]. In these experiments forma-tions resembling glowing spheres appeared in discharge volume when flammable (orga-nic) gases or organic aerosols were added to the gas mixture. Photos from [9], and descriptions given in [10] show that these formations resemble glowing tangles that consist of polymer threads. The nature of these spheres was often connected with the combustion of organic components in a discharge [11], however, experiments [12] showed the following. In the spark dis-charge in air the formation of fireballs with the lifetime ~2 s (in mixture of air with ethane and cotton wool fibers or ethane or methane) took place. In this process concen-trations of organic components were consi-derably smaller than those at which the igni-tion of the mixture takes place. Hence refe-rence [12] showed that these fire balls do not represent some form of the combustion, but can be the autonomous objects created in ionized gas mixture.

To the third group of works we can attribute experiments with erosive or capillary discharges with evaporated walls of organic materials [13-15]. Sometimes du-ring the jet

injection from such plasma gene-rator into water vapor the autonomous for-mations of spherical or the spindle type appeared, their lifetime reached ~3 ms (at the discharge pulse time ~1.2 ms). In case of the capillary in organic glass the amount of carried away material was ~ 1.25 10^{-3} g. It is evident that in this case organic particles can play important role in the formation of the glowing structure.

The only known to us reference devoted to appearance the theory of structures in ionized medium with the additives of organic components is [4]. There was considered the growth of polymer structures as compact spheres that increased their size in plasma chemical processes. This approach [4] allowed to estimate the tem-poral dependence of the particle number in a growing sphere at low gas pressure, but the spatial characteristics were not considered. So one of the targets of this work is the development of the approximate theory of polymer structure growth in the ionized gas at high pressure.

3. In this part we will develop the simple model of the tangle molecular structure in the ionized gas at high gas pressure (100-760 Torr). In so doing we will use data about fractal [16] and physical properties of macromolecules [17-18]. In order to determine the main features of the process we will use the minimal necessary information about plasma chemical processes.

Let us separate into stages the processes of formation of the polymer structure. To the first (kinetic) stage we will attribute the processes with particles with size r less than the mean free path λ of molecules in a gas, $r \ll \lambda$ ($\lambda = (N\sigma)^{-1}$, N-concentration of neutral gas molecules, σ-elastic cross section). These processes take place until macromolecules with sizes $r \sim \lambda$ are not formed.

To the second (hydrodynamic) stage we can attribute processes with the participation of large particles that satisfy $r \tau \lambda$, when, strictly speaking, we can con-sider macromolecular formations as struc-tures.

Estimates show that in experiments [12] with additives of organic gases and aerosol components these two stages realize simultaneously, but in experiment with polymer films [5] at low pressure only kinetic stage took place.

Further we will consider gases at typical discharge temperature in the range T=300-400 K, when polymer macromolecules are characterized by high mobility of links.

4. Within kinetic stage the formation of oligomers from monomers takes place. Then in collisions with a gas molecules the oligomer form is changed. At these col-lisions the accidental changes of directions of monomers in the macro molecule take place. General theory of polymer chains [17-18], from which for the sake of simplicity we use the model of freely joint chains, shows that the average square size of a chain $\bar{r}^2$ is connected with the number of links in it N_1 and the length of the link l by the relation

$$\bar{r}^2 = N_1 \cdot l^2. \qquad (1)$$

In case of rigid chain molecules it becomes more complex

$$\bar{r}^2 = N_1 \cdot l^2 \cdot F(\gamma, \vartheta), \qquad (1')$$

where $F(\gamma, \vartheta)$ is the factor that accounts rotation of atomic groups around the valence bonds, usually $F(\gamma, \vartheta) > 1$, in particular for the cellulose molecules $F(\gamma, \vartheta) \cong 20$. Formulas (1), describe well at the links number in the macro molecule $n \geq 10$.

During collisions with gas particles the macromolecule transforms into the tangle, i.e. the relaxation of directions of its links to the Gauss distribution takes place, the time of this process can be estimated as [17-18]

$$t_{tr} = 6N_1 (N K_r)^{-1}, \qquad (2)$$

where N is the concentration of a gas particles, K_r-rate constant of the translational relaxation of atoms in case of a discharge in inert gas and rotational relaxation in the molecular gas $K_r = K_{tr} Z_{rot}$. K_{tr} is the constant of the translational relaxation, Z_{rot}-number of gas kinetic collisions necessary for rotational relaxation. So for nitrogen molecules Z_{rot} ?3-6, K_{tr} ?2·10^{-10} cm^3/s and for the macro molecule with N_l=10-100 links at P=1 Torr we have $t_{tr} \cong 3 \cdot 10^{-6} - 3 \cdot 10^{-5}$ s,

and at the atmos-pheric pressure $t_{tr} \cong 3 \cdot 10^{-9} - 3 \cdot 10^{-8}$ s, that is less than characteristic times of elemen-tary processes in ionized by a discharge medium. So we can consider the transformation of the macromolecule into a tangle as the independent on other pro-cesses. The process of a tangle trans-formation into a globule is considered in [17], where the following equation for the mean globule's radius is obtained

$$\bar{r} = N_1^{1/3}(-2C/B)^{1/3}, \quad (3)$$

where B and C are the second and the third virial coefficients. In particular for molecules CH_4 at temperatures T=298 and T=400 K we have [18, 19] at N_l=10 $\bar{r} \cong 1.3 \cdot 10^{-7}$ and $\bar{r} \cong 1.6 \cdot 10^{-7}$ cm, respec-tively. It can be shown that the dependence $\bar{r}^2$ on temperature is weak for considered discharge conditions and we can consider macromolecules with N_l>10 as compact globules with effective cross section $\sigma_{eff} = \pi \bar{r}^2$, with corresponding value of average square radius.

For the sake of the simplicity of the following analysis let us divide the process of the macro molecule growth into two stages. In the first one the processes with oligomers with number of links $N_l \leq 10$, take place, in this case we can not use statistic macromolecular properties, and the second one when the number of links in the growing macro molecule N_l>10, for it we use the scaling approach.

Simple system of balance equations for molecule concentrations N_k, that consist of k ($k = N_l$) monomers, has a form:

$$\frac{dN_k}{dt} = K_{k-1,k}N_{k-1}N_{pe} + K_{d1}N_{k+1}N_{pd} - K_{k,k+1}N_k N_{pe} - K_{d1}N_k N_{pd} - K_{d2}N_k N^* + D_k \nabla^2 N_k, \quad (4)$$

where N_{pe} is the monomer concentration with two or more free bonds, at collisions with them the number of links in the molecule increases. N_{pd} - concentration of monomers with free bonds less then two, in collisions with them the decrease of link's number in a polymer molecule takes place. N^* is a concentration of excited molecules, during collisions whit them the decrease of links in macromolecule takes place also. D_k is a diffusion coefficient of a polymer molecule. $K_{i,j}$- rate constants of processes leading to the increase of number of links in a polymer molecule; $K_{d,i}$ -rate constants of processes of destruction of this molecule. At derivation of this equation we used results of works [4-6], where the main processes in the ionized air with hydrocarbon additives were considered.

Analysis of the system of equations (4) shows that optimal conditions for growth of the macromolecule can be realized at the fulfillment of the following equations:

$$K_{k,k+1}.N_{pe} > c \cdot D_k/R_0^2, \quad (5$$

$$K_{k,k+1}.N_{pe} > K_{d2}.N^*, \quad (6)$$

$$K_{k,k+1}.N_{pe} > K_{d1}.N_{pd}, \quad (7)$$

where c is a factor, connected with the form of the experimental device with the characteristic size R_0. Following the standard methods of elementary processes physics we can determine the effective rate constant for the formation of the macromolecule $K_{k,k+1}$:

$$K_{k,k+1} = (\sigma v) \cong \frac{\gamma \pi \bar{r}_k^2 \bar{v}}{4}, \quad (8)$$

where γ-coefficient of the attachment of the monomer to the oligomer with the effective size r_k, $\bar{v} = (8T/\pi m)^{1/2}$ - average velocity of a monomer in a gas, m -its mass. Using formulas (1'), (3) and (8), we get the rate constant for the oligomer growtrh for molecules with freely joint chains

$$K_{k,k+1} \cong \gamma k^{2/3} K_0, \quad (8a)$$

and for rigid joint chains

$$K_{k,k+1} \cong \gamma k \, K_0, \quad (8б)$$

For hydrocarbon monomers like CH, C_2H_2, C_2H_4 the value K_0 proves to be in the range $5 \cdot 10^{-11}$ - $3 \cdot 10^{-10}$ $cm^3 \cdot s^{-1}$, it is comparable with experimental data for formation of dimers and trimers at $\gamma \cong 1$, i.e. the rate constant increases with the growth of the molecule.

Estimates made on the basis of formulas (8) show that in air, or in inert gases with additives of hydrocarbon components, where $K_{d1}, K_{d2} \sim 10^{-9}$ cm^3/s [4-5] conditions (6) and (7) are fulfilled at

$N^*/N \cong 10^{-4} - 10^{-3}$, $N_{pe}/N \cong 10^{-4} - 10^{-2}$, $N_{pe}/N_{pd} > 10$, at $k \le 2 \div 10$ and these conditions can be easily realized in expe-riments.

The condition (5) for processes in discharges in cylindrical tubes transforms to

$$K_{k,k+1} N_{pe} N > 3 \cdot 10^{19} / R_0^2, \text{ cm}^{-3}\text{s}^{-1}, \quad (9)$$

where for the diffusion coefficient of mo-lecules the typical for hydrocarbon dimers and trimers value $D_k \cong 0.1 - 0.2$ cm^2/s [19] is used. The condition (5) is realized in gas discharge tubes of R_0 =1-3 cm at molecule concentrations $N > 10^{16}$ cm^{-3}, it is typical for the conditions of powder particle appe-arance in high frequency discharges [4-6].

From the equation (4) at the fulfillment of conditions (5)-(7) one can estimate the characteristic time t_{tr} of appearance of mole-cules with number of links k>10: $t_{tr} \cong (K_0 \bullet N_{pe})^{-1}$. This estimate for typical conditions in plasma with total concen-tration of polymer monomers $N_p >$ 10^{16} см$^{-3}$ and $N_{pe}/N_p = 10^{-4}$ -10^{-2} gives the following value of time $t_{tr} \cong 10^{-4}$ -10^{-2} с, which is small in comparison with the characteristic hydrodynamic times.

On the later stage (second), when the growth of globules up to hydrodynamic sizes takes place, it is necessary to take into the account that at the sticking of molecules the change of the form and the conformation of the structure and of inter molecule bonds caused by collisions with particles of media takes place. Hence for the description of processes at this stage it is usually necessary to start from the experimental data or theory about interaction of complex macromolecule particles that require, in its turn, the information about interaction potentials for such particles or some models about these processes, based on experiments leading to scaling characteristics. In the considered case when the collisions of the globule with monomers take place the whole process of the growth up to hydrodynamic size can be the described as follows. Monomers that randomly move in a gas stick to the molecule on the surface of the globule. When sticking to the surface they change its form and the probability for the moving monomer to interact with the monomer attached to the surface becomes greater than the probability to get to the surface. So there appear chains on the surface of the globule and with time they also transform into globules. Starting from some size there appear new chains on each of the globule, they are also transformed into globules and so on. In the result the fractal structure is formed. As show investigations of pro-perties of polymer fractals [20], the number of links N_f in them are connected with the size R of the fractal structure by the equation

$$N_f = (R/R_0)^D, \quad (10.a)$$

and the mass m_f of such fractal particle depends on the size by the following law

$$m_f = m_0 (R/R_0)^D, \quad (10.б)$$

where m_0 and R_0 are the mass and size of elementary link in the fractal structure and D - its fractal. In case of polymers D = 2.6±0.3 [20] as show experiments with dif-ferent macromolecules. This dimension lies between the dimension of brownian tra-jectory D = 2, by which the ideal polymer chain with equal links is modeled, and dimension of the solid particle D=3. This scaling relation allows simplify the solution of the problem and to go around the ques-tion about the interaction potential intro-ducing effective interaction cross section.

By applying this approach let us write down the equation for determination of rate constant of interaction of the mono-mer with the polymer fractal aggregate (structure)

$$K_f \cong \frac{\pi R^2 v}{4}, \quad (11)$$

here $v = (8T/\pi M)^{1/2}$ is average velocity of the interacting with the aggregate monomer in a gas M -its mass, T -gas temperature. With the help of this equation at the fulfillment of conditions (5)-(7) we get the following equation for the increase of the monomer number in the polymer fractal structure:

$$\frac{dN_f}{dt} = \frac{N_f^{2/D} v \pi R_0^2 N_{pe}}{4} \equiv K_2 N_f^{2/D} N_{pe}. \quad (12)$$

This equation allows connect the effective radius of the structure R_x with its time of formation $t(R_x)$, namely

$$t(R_x) = \frac{(R_x / R_0)^{1-2D}}{(1-2D) K_2 N_{pe}}. \qquad (13)$$

As shows estimates made with a help of this formulae results for the structure with initial monomer size $R_0 \sim 10^{-7}$ cm, are weakly de-pendent on D in the range 2.5±0.3 at the aggregate size $R_x = 10^{-5} \div 0.1$ cm. This shows that the scaling approach can be applied for the estimates of the time of growth of the fractal particles when the detailed information about elementary processes of growth in unavailable.

Let us apply obtained results for estimation of structure growth charac-teristics in conditions of the experiment [5]. In microwave discharge at pressure 0.5 Topp the maximal size of observed particles reached $R_x \sim 0.3$ cm. These particles did not diffuse to walls and did not fell down. So we can suppose that the condition (5) was fulfilled (it can be shown that long des-cending of particles is connected with the action of free molecular forces). Conditions of the experiment correspond to the kinetic stage of growth since the mean free path $\lambda \sim 0.1$ cm. Estimated by equation (13) time of growth at $N_{pe}/N \sim 10^{-4}$ -10^{-2} proved to be in a range 70-1 s, at the same time the evaluated experimental observed time of growth was $50 < t_{exp} < 100$ s. It allows to conclude that there was not high level of excitation of the polymer monomers in experimental conditions.

The same approach allows to estimate the range of time of growth of the hydrocarbon particles up to hydrodynamic sizes in air at the atmospheric pressure at $N_{pe}/N \sim 10^{-4}$ -10^{-2}, which probes to lie in the range $10^{-5} < t_{exp} < 10^{-2}$ s. These results show that the growth of particles up to hydrodynamic sizes can be in the optimal conditions rather fast in comparison with the growth of aerosol particles in the hydrodynamic stage to analysis of which we come in the next paragraph.

5. Globules that appear in the process of growth or deposited into gas discharge volume in the form of aerosol take part in collisions with other globules. For description of this process we can use the approach developed in references [21,22] where the growth of large fractal clusters at collisions of spherical aerosol particles was considered. In our case it realizes as the growth of aggregates at globule collisions. Taking into the account brownian diffusion, gravitational capture and association of globules in external electric field E it is pos-sible to obtain the following equation for the time of the structure's growth at the initial concentration of globules N_0

$$t(D) = \int_0^\infty \frac{F1(D)\, dt}{N_0\, K1}, \qquad (14)$$

where

$$F1(D) = 1 + t^{(1+1/D)} + K2\, t^{(4/3-1/D)};$$

$$K1(D, R_0) = K_{Br} \cdot \left(K_{Gr} / K_{Br}\right)^{D/(D+1)};$$

$$K2(D, R_0) = \frac{K_{el} N_0^{2/3} E^2}{K_{Br} \cdot \left(K_{Gr} / K_{Br}\right)^{(4D-3)/(3D+3)}},$$

$$\equiv K2_0(D, R_0) \cdot N_0^{2/3} E^2$$

here the coefficient K_{Br} is connected with the brownian aggregation and is equal

$$K_{Br} = \frac{4}{3}\frac{T}{\eta}\left(1 + \frac{\pi/D}{\sin(\pi/D)}\right), \qquad (15)$$

here T is a gas temperature, η-coefficient of gas viscosity. Coefficient K_{Gr} is connected with the gravitational capture of globules by the falling globule

$$K_{Gr} = \frac{g\, m_0 R_0\, f(D)}{12\eta}, \qquad (16)$$

where g -gravitation constant, m_0, R_0 - mass and size of a monomer, $f(2.5) \approx 27.6$, $f(2.2) \approx 66.6$. K_{el} is connected with electrically induced attraction of globules in the external electric field E

$$K_{ei} = C R_0^5 \cdot 2 \cdot \Gamma(2-1/D) \cdot \left[(\varepsilon_p - \varepsilon_g) \cdot \varepsilon_g / (\varepsilon_p + 2\varepsilon_g)\right]^2 / \eta$$

here C=0.354, ε_p, ε_g-dielectric permittivity of the polymer and of a gas. During derivation of (14) we used formulae for dielectric permittivity of mixture of particles from [23] for determination of dielectric

constant ε_1 of polymer fractal structure with voids filled by air.

Presented formulas show that in the absence of external electric field the aggregation time is, $t(2.5) \approx 4.0 \cdot 10^{18} / N_0$ and $t(2.5) \approx 4.0 \cdot 10^{19} / N_0$ s at the size of elementary links of growing structures $R_0 \cong 2 \cdot 10^{-8}$ and $R_0 \cong 10^{-7}$ cm, respectively. But in the external electric field the aggregation time significantly decreases, for example at E=3·10^4 V/cm, $R_0 = 10^{-7}$ cm and $N_0 = 10^{19}$ cm^{-3} the aggregation time becomes $t(2.5) \approx 3.0 \cdot 10^{-4}$ s.

Hence according to these results we can suppose that in case of experiment [12] the appearance of glowing spheres at presence of polymer components was connected with polymerization and aggregation. In this experiment 2.7 % (volume) of ethane and 100 см^3 of cotton wool fibers were deposited to the chamber with air at atmospheric pressure. According to the observations fireballs up to 3 cm diameter appeared during the time less than 1 s. Estimates based on these formulas give the time range for the structure growth $t \cong 140 - 3$ c. We see that obtained formulas for the growth of fractal structures allow qualita-tively explain experimental observations.

References

1. Huertas M.L., Marty A.M., Fontan J. J. Geophys.Res. 1974. V.79. P.1737.
2. Smirnov V.V. Works of IEM N. 24(89). M. Moscow division of Gidrometeoizdat. 1980. P.3-28.
3. Fuks N.A. Mechanics of aerosols. AS USSR Publishers. Moscow. 1955.
4. Ivanov Yu. A., Epshtein I.L. Khimia Vysokikh Energii. 1984. V.18. №5. P.461-467.
5. Vinogradov G.K., Imanbaev G. Zh., Polak L.S., Slovetsky D.I. Ibidem. 1983. V.17. №4. P.372-377.
6. Yasuda H. Plasma polymerization. M.: Mir. 1988.
7. Corum K.L., Corum J.F. Uspekhi Fizicheskikh Nauk V. 160. № 4. P.47-58.
8. Clusarev N.M. in collectrion Fireball Editor prof. B.M. Smirnov M.: IVTAN. 1990. Part.1. P. 18-29.
9. Barry J. Ball lightning and bead lightning. M.: Mir. 1983.
10. Cawood W., Patterson H.S. Nature. 1931. V.128. P.150.
11. Singer S. Nature of ball lightning. M. Mir. 1973.
12. Ofuruton H., Ohtsuki Y.H. Il Nuovo Cimento. V. 13 C. N. 4. P.761-768.
13. Avramenko R.F., Bakhtin B.I., Nikolaeva V.I. et al. Zhurnal tekhnicheskoi fiziki. V.60. № 12. P.57-64.
14. Avramenko R.F., Nikolaeva V.I. Poskacheeva L.P. in a book Ball lightning in a laboratory. Editors Avramenko R.F., Bytchkov V.L. et.al. M.: Khimia. 1994. P.15-55.
15. Ershov A.P., Timofeev I.B., Chuvashev S.N., Shibkov V.M. Ibidem P.112-118.
16. Feder J. Fractals. Plenum Press. New York. 1988. 300 P.
17. Frenkel Ya. I. Kinetic theory of liquids AS USSR Publishers. Moscow-Leningrad. 1959.
18. Grossberg A.Yu.., Khokhlov A.R. Statistical physics of macromolecules M. Nauka. 1989.
19. Physical tables. Editor acad. I.K.Kikoin Atomizdat 1976.
20. Shefer D., Kefer K. In a book: Fractals in physics. Editors. L. Pietronero and E.Tozati. M. Mir. 1988. P.62-71.
21. Smirnov B.M. Ball lightning problem. M. Nauka. 1988.
22. Smirnov B.M. Physics of fractal clusters. M. Nauka. 1988.
23. Landau L. D., Lifshitz E.M. Electrodynamics of continuous media. M. Nauka. 1978.

PROBLEMS OF FLOW STABILIZATION AT SUPERSONIC FLOW DECELERATION IN DUCTS

Guryleva N.V., Ivankin M.A.

Central Aerohydrodynamic Institute (TsAGI) named after Prof. N.E. Zhukovsky
TsAGI, Zhukovsky, Moscow Region, Russia

Methods of flow stabilizing are of important significance for practical use of models and structures of engines with flow deceleration in a pseudoshock. As a rule, it is necessary to carry out control of pseudoshock characteristics, related with decrease of its length/ One of the most effective methods, which permits to decrease the pseudoshock length, to achieve its stabilization, to increase total pressure recovery factor, is the pseudoshock fixing.

The paper considers features of a flow structure and flow parameters under realizing the free and fixed pseudoshocks in flat and axisymmetrical ducts. A number of factors, acting on the pseudoshock fixing in the duct, was defined. A flow pattern in a bow part of the free pseudoshock was defined more exactly in tests. It was shown, that the flow with the pseudoshock cannot be considered within the scope of quasi - steady models.

The pseudoshock fixing was studied at leading edges.

Experiments were run for flat and axisymmetrical ducts.

As shown, pulsations of shocks in the fixed pseudoshock decrease in comparison with the free pseudoshock.

At this regime the flow is close to the quasi-steady flow.

Comparison of the fixation levels for flat and axisymmetrical ducts showed that the fixation level, achieved in the flat duct, is no less than in the axisymmetrical duct.

The fixation in the duct depth was studied. As shown, the pseudoshock fixation at cylindrical struts in the depth of ducts was observed at stable pseudoshock moving, that is in the region of the turbulent boundary layer. The dependence of the pseudoshock fixation extent on the density of the struts placement and the air injection through struts was obtained. As shown, in increasing struts height the level of the pseudoshock fixation increased.

The results obtained can be used for enhancing processes of deceleration, mixing and energy supply in supersonic flows.

The work was performed with the financial support of RFFI (project No 00-01-00158).

EXPERIMENTAL STUDY OF GASDYNAMIC METHODS OF HYDROGEN COMBUSTION STABILIZATION IN SUPERSONIC FLOW

Voloshchenko O.V., Ivankin M.A., Ivanov V.V., Sabelnikov V.A.

Central Aerohydrodynamic Institute (TsAGI) named after Prof. N.E. Zhukovsky
TsAGI, Zhukovsky, Moscow Region, Russia

The paper presents results of an experimental study of gasdynamic methods of hydrogen combustion implementing in a supersonic flow.

For developing a concept of modern multi-mode scramjets using a hydrocarbon fuel it is required to solve a system of complex tasks, one of which is to organize a high effective working process in a combustor at supersonic regimes of the engine operation (at Mach numbers at the combustor entrance M = 2-3). In order to ensure acceptable engine characteristics it is necessary to solve a number of fundamental gasdynamic problems, such as to ensure an intensive mixing of a fuel with a flow, to choose a way for stabilizing the combustion, which can permit to substantially decrease the combustor dimensions and ensure the combustion of a fuel mixture at decreased flow temperatures.

A substantial disadvantage of classical devices for combustion stabilizing is a high-temperature flow action on a combustor wall. It results in a need for creating heat protection systems, considerably increasing the total weight of a construction.

The combustion stabilization by means of gasdynamic methods [1,2] is prospective from this view point. Such study trend, connected with the combustion stabilization in free-hanging local recirculation zones in supersonic flows, arised in the late 80s in TsAGI.

It was suggested to use free-hanging local subsonic zones in a flow as zones, in which the local self-ignition and fuel combustion took place [3].

Tests were run at the TsAGI's test rig T-131V with air heating. The heating was performed by means of kerosene burning in a flow saturated with oxygen. Tests were run in the supersonic flow at the exit of flat expanding ducts at flow parameters: Mach numbers M = 2.5-2.6, stagnation temperature and stagnation pressure in the air heater: T_t =1200-1500 K, P_t = 2.7-3 MPa.

Free-hanging recirculation zones were used as gasdynamic stabilizers. These zones were generated as a result of interference of a gas jet (air with its following replacing by hydrogen) with shock waves of different nature.

The hydrogen self-ignition and stable combustion in the front free-hanging recirculation zone were obtained. The recirculation zone was produced by the interference of a sonic air jet with a strong shock wave. The jet flowed out from the axisymmetrical nozzle, located co-axially at the exit of the flat duct. The shock wave was generated by an unstarted axisymmetrical shaped ducted body, located behind the flat duct. During replacing air, flowing out from the nozzle, by hydrogen the self-ignition and combustion of hydrogen was observed. Boundaries of the stable combustion in the zone ahead of the ducted body were defined.

The self-ignition and stable combustion of hydrogen were obtained in the free-hanging recirculation zone, located in the wake downstream from the axisymmetric

shaped ducted body. The gas jet was blown out through the central nozzle, located in the rear part of the ducted body co-axially to the air jet, passing through the ducted body. The free-hanging recirculation zone arised during destruction of the air jet in a result of the interference with the shock wave in the first barrel of the off-designed air jet, flowing out from the ducted body. During replacing air, flowing out from the nozzle, by hydrogen the hydrogen self-ignition and stable combustion took place.

The analysis for application of various gasdynamic stabilizers was made in tasks of combustion control in the supersonic flow.

The work was performed with the financial support of RFFI (project No 00-00-00158).

REFERENCES

1. G.F. Glotov, N.V.Gurilyova, M.A. Ivankin. Gasthermodynamics of Flows in Model Ducts of Scramjets // ISABE Paper 99-7054, 1999.
2. V.A. Sabelnikov, O.V. Voloshchenko, S.A. Zosimov, M.A. Ivankin, V.V. Ivanov. Gasdynamic methods of combustion stabilization in Supersonic flow. In the collected book: Modern problems of aerospace science. Abstracts of reports of II All-Russian scientific-technical conference of young scientists (Zhukovsky, 26-28 may, 1999), TsAGI, 1999.
3. G.F. Glotov, N.V.Gurilyova, M.A. Ivankin. Aerogasdynamics of Recirculation Areas Created as a Result of Interference of Supersonic Shear Layers and Shock Waves. International Aerospace Congress (IAC'94), Abstracts. - Moscow, 1994.

IGNITION OF CH_4:AIR MIXTURES BY STREAMER DISCHARGE

N.L.Aleksandrov, E.M.Bazelyan, G.A.Novitskii and A.Yu.Starikovskii

Moscow Institute of Physics & Technology, 141700 Dolgoprydny, Moscow region, RUSSIA

1. Introduction

The use of positive streamer corona discharge for the production of active species has become an active area of research in the past decade. Pulsed streamer corona technology is based upon the application of a fast rise time, short duration, repetitive pulsed electric discharge to produce highly reactive free radicals and excited species in a gaseous medium.

It is of interest to study the ignition of combustible gaseous mixtures under the action of streamer corona discharge and to compare its efficiency with that for spark ignition. This is so because corona discharge could provide a more homogeneous and ultra fast ignition in a whole volume.

In the present paper, we simulate the properties of a positive streamer in CH_4-air mixtures in a non-uniform electric field. The production of active species including atoms, radicals and electronically excited molecules is calculated versus initial gas temperature. The results are used to estimate the efficiency of the streamer-corona ignition of the combustion in the considered gaseous mixtures.

2. The simulation model

The 1.5D (axisymmetrical) simulation model and numerical method used in the present calculation are essentially the same as those used by the authors to simulate a long-streamer propagation in atmospheric pressure air [1, 2]. That is, the radius of the streamer channel was assumed to be fixed. The basic dynamic equations for the streamer propagation are the continuity equations for electrons, ions and active species; Poisson's equation for the electric field; and the balance equations for the vibrational energy of N_2 molecules and for the translational energy of neutral species. These equations were solved numerically. The finite-difference method with the adapted mesh was used. The electric field was determined from the condition that the streamer space charge is distributed over the cylindrical channel surface.

Our kinetic model includes around 50 particle species and 240 reactions. Most of the rates of reactions between heavy particles were taken from experiment. The rates of electron—impact reactions and the electron drift velocity were obtained by numerical solution of the Boltzmann equation using the known two-term expansion of the electron velocity distribution function in spherical harmonics.

The vibrational distribution for N_2 was assumed to be an equilibrium one with the temperature T_v. The vibrational temperatures for other molecules and any rotational temperature were assumed to be equal to the gas temperature T. In this case the electron rate and transport coefficients depend on the

gas composition, reduced electric field E/N (N is the gas number density), T_v and T.

3. Simulation results

It is of interest to compare the properties of a streamer in air and in CH_4:air mixtures. We calculated the evolution in time of the streamer velocity and length in humid air and in a N_2:O_2:H_2O:CH_4=71:18:2:9 mixture. The simulation was performed at a pressure of p=10 atm and T=300 and 800 K for a spherical anode of R_a=0.1 cm, an infinitely distant cathode and an applied voltage of U=180 kV (T=300 K) and 100 kV (T=800K). The radius of the streamer channel was assumed to be r_c=0.03 cm. Our calculation shows that the effect of CH_4 admixture on the streamer properties is less pronounced than that of the gas temperature. The temperature effect is due to a change in the composition of positive ions in the streamer channel and as a result due to decelerating electron-ion recombination [3].

Our calculations show that the dominant neutral active species produced in the streamer discharge are O, $N_2(A^3\Sigma_u^+)$, CH_3 and H. The density of O atoms is around $(1\text{-}4)\times10^{16}$ cm^{-3}. The density of $N_2(A^3\Sigma_u^+)$ molecules, CH_3 radicals and H atoms is a few times lower.

4. Initiation of ignition

4.1 Kinetic scheme

The densities of active species in the streamer channel were considered as initial conditions for the numerical modeling of ignition. The kinetic scheme including the following reagents (113 components) was used for the analysis: electronically excited particles ($N(^2D)$, $N(^2P)$, $N_2(a^1\Sigma_u^-)$, $N_2(A^3\Sigma_u^+)$, $N_2(B^3\Pi_g)$, $N_2(C^3\Pi_u)$, $N_2(a'^1\Sigma_u^-)$, $O_2(a^1\Delta_g)$, $O_2(b^1\Sigma_g^+)$, $O(^1D)$), electrons, positive ions (N_2^+, N_3^+, N_4^+, NO^+, N_2O^+, NO_2^+, N_3O^+, $N_2O_2^+$, O^+, O_2^+, O_4^+, H_2O^+, $H_2O_3^+$, H_3O^+, CH_4^+) and neutral species (H, HO_2, H_2O_2, H_2O, OH, O, O_3, NO, CO, CO_2, CH_3, HCHO, HCOOH, CH_3OOH, CH_3O_2, CH_3O).

4.2 Initiation of ignition

We calculated the evolution in time of the mole fraction of (a) electronically excited particles, (b) positive ions and (c) dominant radicals and products of chemical reactions. The results of this calculation show that four characteristic phases of the streamer discharge afterglow may be pointed out. The first one is a plasma decay caused by electron-ion recombination. At the considered high pressures both dissociative recombination to form atoms and radicals and three-body recombination to remove active particles are important. Under studied conditions electronically excited particles are quenched via collisions with neutral molecules in which the internal energy can be used to rise the amount of active particles (see for instance the important reaction $N_2(B^3\Pi_g) + O_2 \rightarrow N_2 + O + O$). This phase lasts fractions of microseconds and is completed when all excited particles (except $O_2(a^1\Delta_g)$) and charged particles are removed.

The second phase corresponds to the induction period of ignition. The possibility of the ignition initiation depends strongly upon the processes in this stage. A necessary condition for the development of ignition is the maintenance of the chain mechanism of oxidation which is determined by the relation between the rates of the chain termination and those of the chain development. Because of a significant difference between the thresholds of these reactions (a few thousand degrees for chain development and zero energy for three-body reactions of the chain termination) the initial value of gas temperature is the main factor which governs the ignition.

Under considered conditions the time of explosion induction is around 70 μs. Thereafter a slow accumulation of radicals and slow increase in gas temperature give way to their explosive rise. This third phase is completed at t=100 μs when the reagents are removed.

The forth phase is characterized by a slow recombination of radicals at high gas temperature. The system reaches an equilibrium for a millisecond.

4.3 The effect of the streamer channel radius on the delay time of ignition

The results of the 1.5D simulation of the streamer process depend on the radius of the streamer channel which is an input parameter. This parameter affects the electric field at the streamer head and the density of electrons and excited particles in the streamer channel. We calculated the induction time at different values of the channel radius r_c. In the range of r_c = 0.01 - 0.03 cm the induction time depends on r_c slightly. At higher and lower values of r_c the effect becomes more pronounced. It seems reasonable to study the ignition by the streamer process experimentally or by using the 2D simulation.

4.4 The effect of initial gas temperature on the delay time of ignition

In order to study the effect of the initial gas temperature T the simulation was performed at different T. The induction time was calculated as a function of T for the thermal ignition (an equilibrium regime) and for ignition which was initiated by the streamer discharge at the applied voltage of 80 kV, the discharge length of 1.4 cm and r_c= 0.03 cm. The difference between the thermal ignition time (an equilibrium regime) and the time of the ignition by streamer process is an order of magnitude at T = 1200 K and exceeds three orders of magnitude at T =800 K. Our calculation shows that the production of active particles by streamer discharge accelerates the chemical reactions in CH_4:air mixtures leading to ignition at the temperatures down to T =700 K for fractions of a millisecond.

In summary, our simulation shows the possibility of the ignition by the streamer process at high pressures of CH_4:air mixtures. The ignition threshold is calculated versus the main parameters of the system.

[1] A.E. Bazelyan and E.M. Bazelyan: High Temp., 31 (1994) 799; 32 (1994) 332.

[2] N.L. Aleksandrov and E.M. Bazelyan: J.Phys.D: Appl.Phys., 29 (1996) 740.

[3] N.L.Aleksandrov and E.M.Bazelyan: J.Phys.D: Appl.Phys., 29 (1996) 2873.